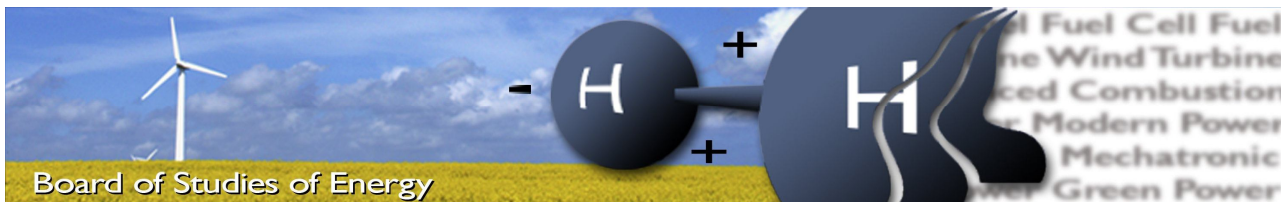


2010-2011

A 3D CAD model of a synchronous generator, shown in a light green color. The model is cut away to reveal the internal stator and rotor components. The generator is mounted on a base with cooling fins and a mounting bracket.

**REACTIVE POWER CONTROL AND FAULT RIDE THROUGH
CAPABILITIES OF SYNCHRONOUS GENERATOR**



Title: Reactive power control and fault ride through capabilities of synchronous generator

Semester: 9/10

Semester theme: Control in converter-fed AC drives

Project period: 01.09.10-30.05.11

ECTS: 60

Supervisors: Kaiyuan Lu, Lars Helle

Project group: PED4-1032

[Aravazhi Anbarasu]

[Catalin Dincan]

Copies: 3

Pages: 144

Appendix: 8

Supplements: 1 CD

SYNOPSIS:

The goal of the project is to investigate a new topology of generator system for wind turbines, consisting of a continuous variable transmission gear box and a synchronous generator with access to the rotor field winding.

Focus is put on reactive power control and fault ride through capabilities of the generator.

The prime mover is an induction motor, supplied from a 3 phase SFC and controlled with FOC. The generator has a constant speed and variable torque. Excitation voltage is supplied from a DC/DC converter.

First, analytical models of the SG and IM are developed. The models are verified and validated through simulation before laboratory implementation.

Principles of operation during grid connection and transient faults are presented. A setup was built in the laboratory. The control was achieved through dSpace. Three phase voltage faults were experimented. Results and conclusions are presented.

By signing this document, each member of the group confirms that all group members have participated in the project work, and thereby all members are collectively liable for the contents of the report. Furthermore, all group members confirm that the report does not include plagiarism.

Contents

Preface	5
Abbreviations	7
Nomenclature	9
List of Figures	13
1 Introduction	17
1.1 Background and Motivation	17
1.2 State of the Art	18
1.3 System description.....	21
1.4 Problem Formulation	22
1.5 Objectives	22
1.6 Limitations.....	23
2 Induction Machine: Theory and Control	25
2.1 Mathematical Model.....	25
2.1.1 Simulation and Validation.....	27
2.2 Induction Motor: Indirect Field Oriented Control Principles.....	28
2.2.1 Slip Estimation.....	29
2.2.2 PI Controllers.....	30
2.3 Lab Implementation.....	39
2.4 Summary.....	44
3 Synchronous Generator: Theory and Control	45
3.1 Synchronous Generator	45
3.1.1 Construction.....	45
3.1.2 Mathematical model –natural reference frame	46
3.1.3 Simulation and Validation.....	51
3.1.4 Lab Implementation	52
3.2 Exciters	53
3.2.1 DC Exciters (Brushed):	53
3.2.2 AC Exciters (Brushless):.....	54
3.2.3 Static Exciters (Brushed):	55
3.2.4 Brushless exciter modeling	55
3.3 Synchronous Generator: Control	57
3.3.1 Synchronization Control	58
3.3.2 Reactive Power Control	60
3.3.3 Static VAR compensators (SCV) and Static Compensators	70
3.3.4 Simulation of SVC and SC.....	71

3.4	Lab Implementation.....	73
3.4.1	Operation Modes – Lead and Lag.....	74
3.4.2	Operation Modes –Unity Power factor	75
3.5	Summary.....	76
4	Excitation converter.....	77
4.1	Thyristor rectifier	77
4.2	Passive rectifier and buck converter	78
4.3	AC/DC –DC/DC with PF control.....	79
4.4	Design specification of the buck converter	83
4.5	PCB Design.....	83
4.6	Summary.....	85
5	Grid Faults.....	87
5.1	Introduction.....	87
5.2	Types of Grid Fault	87
5.3	Simulation of grid fault propagation.....	89
5.4	Simulation of reactive power injection for different grid faults.....	92
5.5	Simulation of reactive power injection for 3~ grid fault	94
5.5.1	No Control/Natural Response.....	94
5.5.2	Control	96
5.5.3	Grid code requirement	98
5.6	Lab Implementation.....	102
5.6.1	Type A.....	103
5.6.2	Type B	105
5.6.3	TYPE C	106
5.6.4	TYPE E	107
5.7	Summary.....	108
6	Conclusion.....	109
7	Future Work.....	111
	Appendix	113
A.	Laboratory Setup	115
B.	Parameters.....	119
	Induction Machine Parameters.....	119
	Synchronous Generator Parameters: 2.15 MW	119
	Synchronous Generator Parameters: 12.5 kW	119
	Buck Parameters: 12.5 kW	120
C.	m-Files.....	121
	Synchronous Machine M-File.....	121
	Induction Machine M-File.....	124

Brushless Exciter M-File.....	124
D. Symmetric Component	125
E. Buck Converter.....	127
F. Terminology of Synchronous Machine Parameters.....	133
G. Simulink & dSpace Blocks.....	139
H. P.U System	141
Bibliography.....	143

Preface

This 9th and 10th semester report is conducted at The Department of Energy Technology. It is written by group PED4-1032 during the period from 1st of September 2010 to 30st of May 2011. The project theme with the title *Reactive power control and fault ride through capabilities* was chosen from the proposals intended for students from PED.

Project authors would like to kindly thank to their supervisors: Kaiyuan Lu and Lars Helle for their support and valuable advices during the project period. We also like to thank Allan Holm Jorgensen for guidance and fruitful discussions

Reading Instructions

The project is documented in a main report and appendixes. Figures, equations and tables are numbered continuously in their respective chapters. For example, Fig. 1.1 is the first figure in chapter 1.

Appendices, source codes and documents are attached on a CD-ROM.

The authors.

Abbreviations

AC/DC	Alternating current/Direct current
AVR	Automatic voltage regulator
BE	Brushless exciter
CVT	Continuous variable transmission
GM	Gain margin
IEEE	Institute of Electrical and Electronic Engineers
IFOC	Indirect Field oriented control
IM	Induction machine
ME	Main exciter
OM	Optimal modulus
PE	Pilot exciter
PF	Power factor
PI	Proportional Integrator
PM	Phase margin
PU	per unit
PWM	Pulse width modulation
SFC	Static frequency converter
SG	Synchronous generator
STATCOM	Static compensator
SVC	Static var compensator
SVM	Space vector modulation
SVPWM	Space vector pulse width modulation
THD	Total harmonic distortion
UPF	Unity power factor
VRT	Voltage response time
ZOH	Zero order holder

Nomenclature

Ψ_d	d axis stator flux	Wb
Ψ_q	q axis stator flux	Wb
Ψ_0	zero component stator flux	Wb
Ψ'_f	magnetizing field flux linkage	Wb
Ψ'_{kd}	d axis damper winding flux linkage	Wb
Ψ'_{kq}	q axis damper winding flux linkage	Wb
Ψ_{md}	d axis mutual flux linkages	Wb
Ψ_{mq}	q axis mutual flux linkages	Wb
E_f	SG induced voltage referred to stator	V
L''_d	d axis subtransient inductance	H
L''_q	q axis transient inductance	H
L'_d	d axis transient inductance	H
L'_{lf}	field leakage inductance	H
L'_{lkd}	d axis damper leakage inductance	H
L'_{lkq}	q axis damper leakage inductance	H
L'_q	q axis transient inductance	H
L_0	zero component inductance	H
L_d	d axis synchronous inductance	H
L_{fd}	Field winding inductance	H
L_{ls}	Stator leakage inductance	H
L_{md}	d axis magnetizing inductance	H
L_{mq}	q axis magnetizing inductance	H
L_q	q axis synchronous inductance	H
T''_{d0}	d axis subtransient open circuit time constant	s
T''_{q0}	q axis subtransient open circuit time constant	s
T'_{d0}	d axis transient open circuit time constant	s
T'_{q0}	q axis transient open circuit time constant	s
T_{em}	electromagnetic torque in the rotor of the synchronous generator	N.m
U_g	Grid voltage	V
V_{rd}	IM rotor d-axis voltage	V
V_{rq}	IM rotor q-axis voltage	V
V_{sd}	IM stator d-axis voltage	V
V_{sq}	IM stator q-axis voltage	V
Z_g	Medium voltage line impedance	Ω
Z_{g2}	High voltage line impedance	Ω
f_g	Grid frequency	Hz
i_0	zero phase stator current	A

i_a	Phase a current	A
i_b	Phase b current	A
i_c	Phase c current	A
i_{d_gen}	generated d axis stator current	A
i_f	SG rotor field winding current	A
i_{fd}	magnetizing field current	A
i_{fo}	BE field winding current	A
i_{md}	d axis magnetizing current	A
i_{mq}	q axis magnetizing current	A
i_{q_gen}	generated q axis stator	A
i_r	SG rotor phase current	A
i_{rd}	IM rotor d-axis current	A
i_{rq}	IM rotor q-axis current	A
i_s	SG stator phase current	A
i_{sd}	IM stator d-axis current	A
i_{sq}	IM stator q-axis current	A
r'_f	Field winding resistance	Ω
r'_{kd}	d axis damper winding resistance	Ω
r'_{kq}	q axis damper winding resistance	Ω
r_s	Stator resistance	Ω
u_0	zero phase stator voltage	V
u_d	d axis stator voltage	V
u_{fd}	exciter field voltage	V
u_q	q axis stator voltage	V
v_f	SG rotor d-axis field winding voltage	V
v_g	SG rotor q-axis field winding voltage	V
v_{kd}	SG rotor d-axis damper winding voltage	V
v_{kq}	SG rotor q-axis damper winding voltage	V
v_r	SG rotor phase voltage	V
v_s	SG stator phase voltage	V
x''_d	d axis subtransient reactance	Ω
x''_q	q axis transient reactance	Ω
x'_d	d axis transient reactance	Ω
x'_{lf}	field leakage reactance	Ω
x'_{lkd}	d axis damper leakage reactance	Ω
x'_{lkq}	q axis damper leakage reactance	Ω
x'_q	q axis transient reactance	Ω
x_d	d axis synchronous reactance	Ω
x_{ls}	Stator leakage reactance	Ω
x_{md}	d axis magnetizing reactance	Ω
x_{mq}	q axis magnetizing reactance	Ω
x_q	q axis synchronous reactance	Ω
Ψ_{rd}	IM rotor d-axis flux	Wb
Ψ_{rq}	IM rotor q-axis flux	Wb
Ψ_{sd}	IM stator d-axis flux	Wb
Ψ_{sq}	IM stator q-axis flux	Wb
θ_e	Synchronous rotating frame angle	rad
θ_{sl}	Slip angle	rad

B	viscous friction coefficient	N.m.s
ω_r	electrical speed of the rotor	rad/s
ω_e	synchronous speed	rad/s
ω_m	mechanical speed of the rotor	rad/s
p	Number of pole pairs	
thetar	rotor angle	rad
J	Moment of inertia of the rotor of the synchronous generator	kg.m ²
L_D	d axis damper winding inductance	H
L_Q	q axis damper winding inductance	H
i_D	d axis damper winding current	A
i_Q	q axis damper winding current	A

List of Figures

Fig 1.1: Share of main components of total number of failures[1].....	17
Fig 1.2:Fixed Speed wind turbine	18
Fig 1.3:Variable Speed wind turbine(Partially Rated Converters).....	19
Fig 1.4:Variable Speed wind turbine(Partially Rated Converters).....	19
Fig 1.5:Topology of variable Speed wind turbine with full rated converters	21
Fig 1.6:Variable Speed wind turbine(CVT)	21
Fig 1.7: Lab setup	21
Fig 2.1:Two-Phase equivalent circuit diagram of induction machine	25
Fig 2.2:Torque/ Slip Characteristics.....	27
Fig 2.3:Nominal operation of induction machine(1455RPM,100Nm).....	28
Fig 2.4:Frame transformations involved in IFOC [6].....	28
Fig 2.5: IFOC Vector Control Implementation[6]	29
Fig 2.6: d-axis current loop with unity feedback.....	32
Fig 2.7: Step response of d-axis current loop.....	33
Fig 2.8: Bode plot of d-axis open loop transfer function.....	33
Fig 2.9: q-axis current loop with unity feedback	34
Fig 2.10: Step response of q-axis current loop.....	35
Fig 2.11: Bode plot of q-axis open loop transfer function	36
Fig 2.12: Block diagram for tuning speed Loop.....	37
Fig 2.13: Block diagram for tuning speed Loop(Step 1).....	37
Fig 2.14: Block diagram for tuning speed Loop(Step 2).....	38
Fig 2.15: Step response of speed loop.....	39
Fig 2.16: Bode plot of speed open loop transfer function.....	39
Fig 2.17:Duty cycles imposed on the inverter(SVM)	40
Fig 2.18:Motor currents.....	40
Fig 2.19: d-axis current – reference and real(a)Lab(b)Simulation.....	41
Fig 2.20: q-axis current – reference and real(Speed Control).....	42
Fig 2.21 :Speed reference and real speed	42
Fig 2.22 :Iq in Torque Control(a)Lab(b)Simulation	43
Fig 2.23:Ripple in Speed.....	44
Fig 2.24:Flux and Phase angle	44
Fig 3.1: Simplified construction of a synchronous machine	45
Fig 3.2: Circuit representation of an idealized machine	46
Fig 3.3: Block diagram of the SG modeling	46
Fig 3.4: Block diagram of the d-axis SG modeling(Flux Based)	47
Fig 3.5: Block diagram of the q-axis SG modeling(Flux Based)	47
Fig 3.6: Block diagram of SG modeling(Voltage Based).....	48
Fig 3.7: Equivalent qd0 circuit	49
Fig 3.8: Te(Electromagnetic torque in pu), Wmec (mechanical speed) and power angle (angle between the induced voltage and grid voltage)	51
Fig 3.9: Current I[pu], Active power P[pu], Reactive power Q[pu] and Induced voltage Ef [pu].Note all quantities referred to the stator side.	52
Fig 3.10: (a)Voltage (b)Current (c)Active Power	53
Fig 3.11: D.C. Exciter	53
Fig 3.12: A.C. Exciter	54
Fig 3.13: Static Exciter.....	55
Fig 3.14:Equivalent circuit of SG without damper windings.....	56
Fig 3.15:Simplified circuit of brushless exciter.....	56

Fig 3.16: Current waveforms at each stage of the exciter.....	57
Fig 3.17: Synchronization controller.....	58
Fig 3.18: Grid and generator phase angles(a) before synchronization (b) after synchronization	59
Fig 3.19(a)Grid and generator voltage before synchronization(b)Locus of the induced and grid voltage.....	59
Fig 3.20: Grid and generator voltage after synchronization.....	60
Fig 3.21: Simplified power flow for generator to grid connection.....	60
Fig 3.22: Phasor diagram of grid connected SG.	61
Fig 3.23: Phasor diagram of operation regions of grid connected generator.....	61
Fig 3.24: Power flow for grid connected generator	62
Fig 3.25: Locus of induced voltage E_f under varying conditions.....	63
Fig 3.26: Current and Power characteristics under constant power operation with variation in induced voltage.....	63
Fig 3.27: Torque ,Speed and Power angle characteristics under constant power operation.....	64
Fig 3.28 : Torque, Speed and Power Angle characteristics for constant excitation.....	65
Fig 3.29: Current, Active and Reactive Power and Power factor variations at constant excitation....	65
Fig 3.30: Torque, Speed and Power angle based on realistic wind data of average wind of 8m/s....	66
Fig 3.31: Current and Power based on realistic wind data of average wind of 8m/s.....	67
Fig 3.32: Constant excitation and Power factor based on realistic wind data of average wind of 8m/s.....	67
Fig 3.33: Variation of induced voltage with variation in input power for unity power factor.....	68
Fig 3.34: Reactive power control Scheme	68
Fig 3.35: Comparison of power angle with implemented control strategy and constant excitation ..	68
Fig 3.36: Comparison of current and reactive power with implemented control strategy and constant excitation.	69
Fig 3.37: Comparison of current and reactive power with implemented control strategy and constant excitation.	69
Fig 3.38 :Different types of compensators	70
Fig 3.39 :Performance capability[17]	71
Fig 3.40:Model of switched capacitor circuit.....	71
Fig 3.41:Simulation of switched capacitors	71
Fig 3.42:Model of STATCOM circuit.....	72
Fig 3.43: Control circuit for STATCOM.....	72
Fig 3.44: Simulation of STATCOM.....	73
Fig 3.45 : (a)Power Factor (b)Active power (c)Reactive power (d)Power angle for constant excitation	73
Fig 3.46 : Voltage and Current (a)Lagging PF (b)Leading PF	74
Fig 3.47 : I_d and I_q for (a)Lagging PF (b)Leading PF.....	74
Fig 3.48 : Three phase currents (a)Lagging (b)Leading.....	74
Fig 3.49 : (a)Power Factor (b)Active power (c)Reactive power (d)Power angle for lagging and leading	75
Fig 3.50: (a)Lagging PF (b)Leading PF	75
Fig 3.51: (a)Power Factor (b)Active power (c)Reactive power (d)Power angle for Unity PF.....	76
Fig 4.1: Converter topologies to supply brushless exciters	77
Fig 4.2:Three Phase Thyristor Rectifier.....	77
Fig 4.3:Three Phase Thyristor Rectifier – Simulation	78
Fig 4.4:Buck converter	78
Fig 4.5:Buck converter simulation.....	79
Fig 4.6:Control and Model of DC/DC H bridge.....	79
Fig 4.7: Voltage Output and Control Signals	80
Fig 4.8: Voltage Output and Control Signals	80

Fig 4.9: Model of AC/DC converter	81
Fig 4.10: Simulation Output	82
Fig 4.11 Gate driver	83
Fig 4.12 Main supply.....	84
Fig 4.13 :PCB layout for buck converter	84
Fig 4.14 : Voltage in buck converter	84
Fig 5.1: Grid Connection of SG with fault location and associated impedances.....	87
Fig 5.2:Type A Propagation	90
Fig 5.3:Type B Propagation	90
Fig 5.4:Type C Propagation	91
Fig 5.5:Type E Propagation	92
Fig 5.6:Type A at node I	93
Fig 5.7:Type D at node I	93
Fig 5.8:Type C at node I	94
Fig 5.9:Type G at node I	94
Fig 5.10 : (a)Voltage dip profile and generator voltage (b) Generator current	95
Fig 5.11 : (a)Voltage dip profile and generator voltage (b) Generator current	96
Fig 5.12 : (a)Active power (b) Reactive power (c)Excitation Voltage	96
Fig 5.13 : (a)Voltage dip profile and generator voltage (b) Generator current	97
Fig 5.14 : (a)Voltage dip profile and generator voltage (b) Generator current	97
Fig 5.15 : (a)Voltage dip profile and generator voltage (b) Generator current	98
Fig 5.16 :Fault ride through requirement[24]	99
Fig 5.17 :Reactive power requirement	100
Fig 5.18 :Power power requirement[24]	100
Fig 5.19 :Voltage profile for simulation of symmetric three-phase faults(Danish Code)	101
Fig 5.20 : (a)Voltage dip profile and generator voltage (b) Reactive power (c)Power angle.....	102
Fig 5.21:Characteristics of 5kW operation.....	102
Fig 5.22:Schematic of grid fault generation.....	103
Fig 5.23:Type A fault to 0.75 [p.u] for 3 [s]	103
Fig 5.24:Type A fault to 0.5 [p.u] for 0.5 [s]	104
Fig 5.25:Type A fault to 0.5 [p.u] for 1 [s] without control.....	104
Fig 5.26:Type A fault to 0.5 [p.u] for 1 [s] with control(TYPO).....	104
Fig 5.27:Type A fault to 0 [p.u] for 1 [s] without control(change name in graph)	105
Fig 5.28:Type B to 0[p.u] for .15 [s] without control	105
Fig 5.29:Type B fault to 0.5 [p.u] for 1 [s] without control	106
Fig 5.30:Type B fault to 0.5 [p.u] for 1 [s] with control	106
Fig 5.31:Type C fault to 0.5 [p.u] for 1 [s] without control	106
Fig 5.32:Type C fault to 0.5 [p.u] for 1 [s] with control	107
Fig 5.33:Type E fault to 0.5 [p.u] for 1 [s] without control	107
Fig 5.34:Type E fault to 0.5 [p.u] for 1 [s] with control.....	107
Fig A.1:Laboratory Setup	115
Fig A.2: (1) Synchronous generator (2) Induction motor (3)VLT FC 302 converter (4)1103 Dspace (5)DC source supply for buck converter (6) Inductor voltage divider (7) Contactors for grid fault (8)Relay to control contactors (9) Buck converter	117
Fig D.3: Symmetrical components.....	125
Fig E.4 Buck converter	127
Fig E.5 Continuous-discontinuous state	129
Fig E.6 Discontinuous mode.....	130
Fig E.7 Characteristic keeping Vd constant.....	130
Fig E.8 Characteristic keeping Vo constant.....	130
Fig E.9 Output voltage ripple	131

Fig F.10: Two axis reactance (a)Synchronous Reactance(b)Transient reactance(c)Sub-transient reactance.	136
Fig F.11: Transient reactance	138
Fig G.12: Main block representing data flow	139
Fig G.13: Data acquisition and protections block.....	139
Fig G.14: Indirect Field Oriented control scheme.....	140
Fig G.15: Reactive power control scheme.....	140

1 Introduction

This chapter presents the background and the motivation of the thesis, continuing with a short overview of state of the art in wind turbine technologies. Furthermore, it describes the system used in the laboratory and continuing with aims of the project and the limitations encountered.

1.1 Background and Motivation

For years now, renewable energy has become the main focus in power production due to depleting fossil resources and environmental concerns surrounding them. Wind energy has been one of the forerunners, which has fostered research in power quality and controllability. This trend is reflected in the grid requirements imposed by various operators.

Hence the wind turbine has become a main area of research across various fields of engineering. This is evident from Fig 1.1 which lists out the various components and the contributions to the failure of the wind turbine. It can be noted that electrical system that includes power converters, transformers etc has the maximum share of 23% in survey of 1500 wind turbines over 15 years.[1]

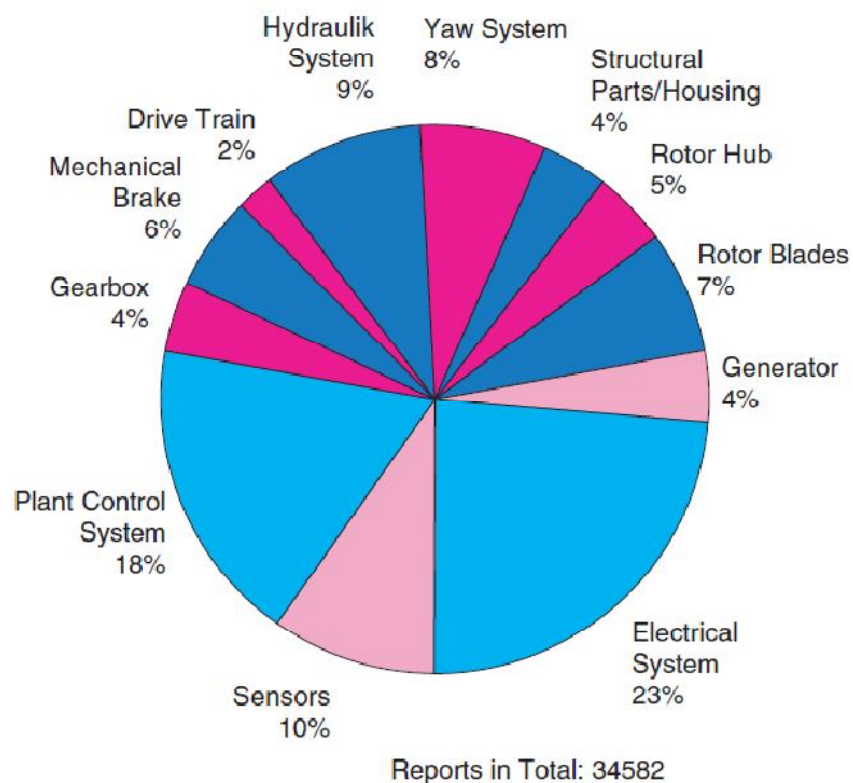


Fig 1.1: Share of main components of total number of failures[1]

A way to approach this problem is to directly connect the generator to the grid. The Synchronous generator is the natural choice as it allows reactive power control for the requirements imposed by the grid operators, who charge high fees for supplying reactive power to the grid. In synchronous generators the power factor " $\cos \Phi$ ", i. e. the reactive power, can be controlled by regulating the voltage at the terminals.

The advantages of this solution are its simplicity and compatibility with today's standard generator technology for feeding the three-phase grid. Moreover, the reactive power can be controlled very easily via the direct current excitation of the rotor.

These advantages, however, are balanced by a series of grave disadvantages. Only very small load angles are possible for compensating for the dynamic loads imposed upon the generator by the wind rotor. Large load surges, for example due to strong gusts, can cause a loss of synchronization. The synchronous generator, in response to even small load peaks tends to produce oscillations which are only poorly damped.

The analysis of the fundamental properties of synchronous generators shows that they can only be used without problems when they are combined with a drive unit which provides a steady driving torque at a fixed speed. But in a wind turbine rotor this, of all things, is not the case. Coupling the generator directly to the fixed-frequency grid forces the generator to run at a constant speed. On the other hand, the wind turbine rotor wants to follow the variations in wind speed. In between there is the mechanical drive train of the wind turbine. High dynamic loads on the mechanical components and severe fluctuations in the electrical power output are the consequences. Successful use of a synchronous generator can, therefore, be achieved only with complex compliance and damping arrangements in the mechanical drive train. Reduction of the dynamic loads can only be achieved by allowing the wind rotor speed a degree of freedom from the grid frequency. In this project it can be achieved by using a continuous variable transmission (CVT) gearbox.[2]

1.2 State of the Art

This section provides a short overview of the available wind turbine topologies. Two types of generators are used: induction generators (squirrel cage, wound rotor, double fed) and synchronous generators (with separate excitation or permanent magnets). The wind turbines can be classified as fixed or variable wind speed.

Fixed speed

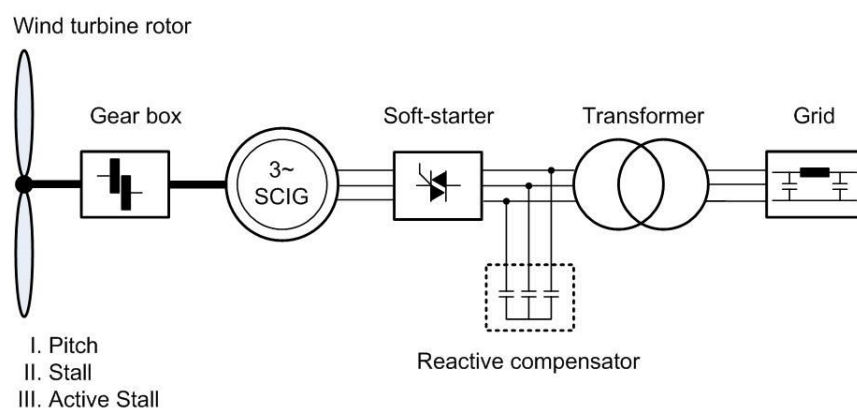


Fig 1.2: Fixed Speed wind turbine

Fixed wind turbines consist of squirrel cage induction generators directly connected to the grid via a transformer. The low speed of the blades is converted to high speed by a gearbox. Frequency of the grid determines the speed of the generator. Power is controlled by the turbine blades with pitch, stall or active control. The generator needs a reactive power compensator to decrease the reactive power demand from the grid. The generator doesn't require synchronization with the grid.

This topology is simple, cheap and robust. On the other hand, it has some drawbacks: the wind turbine is able to operate only at a constant speed, requires expensive mechanical system to absorb high torque stress due to wind gust and it needs thyristor based soft starters to reduce the inrush currents.[3]

Variable speed with partially rated power converters

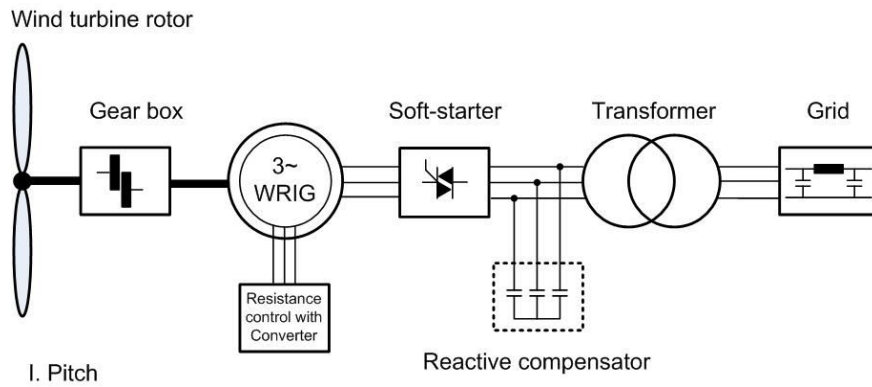


Fig 1.3: Variable Speed wind turbine (Partially Rated Converters)

This wind turbine has a wound rotor induction generator connected to the grid. A power converter is connected to the rotor and changes the rotor resistance, therefore the slip. This is called dynamic slip control. The speed range is limited to 10%. It requires reactive power compensation and a soft starter.

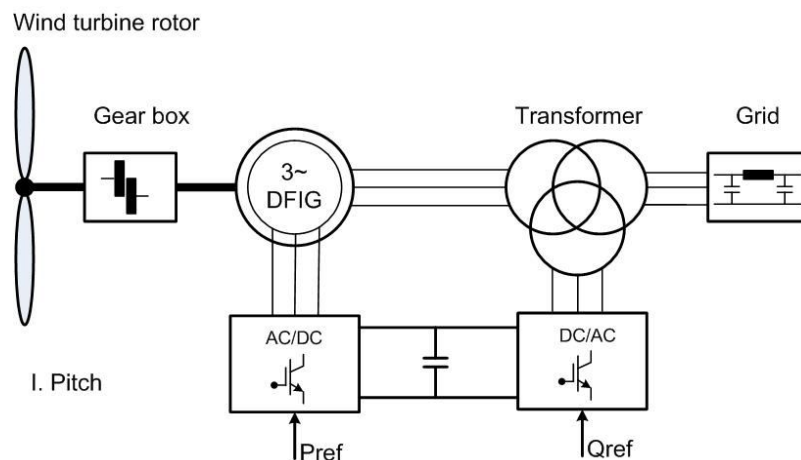


Fig 1.4: Variable Speed wind turbine (Partially Rated Converters)

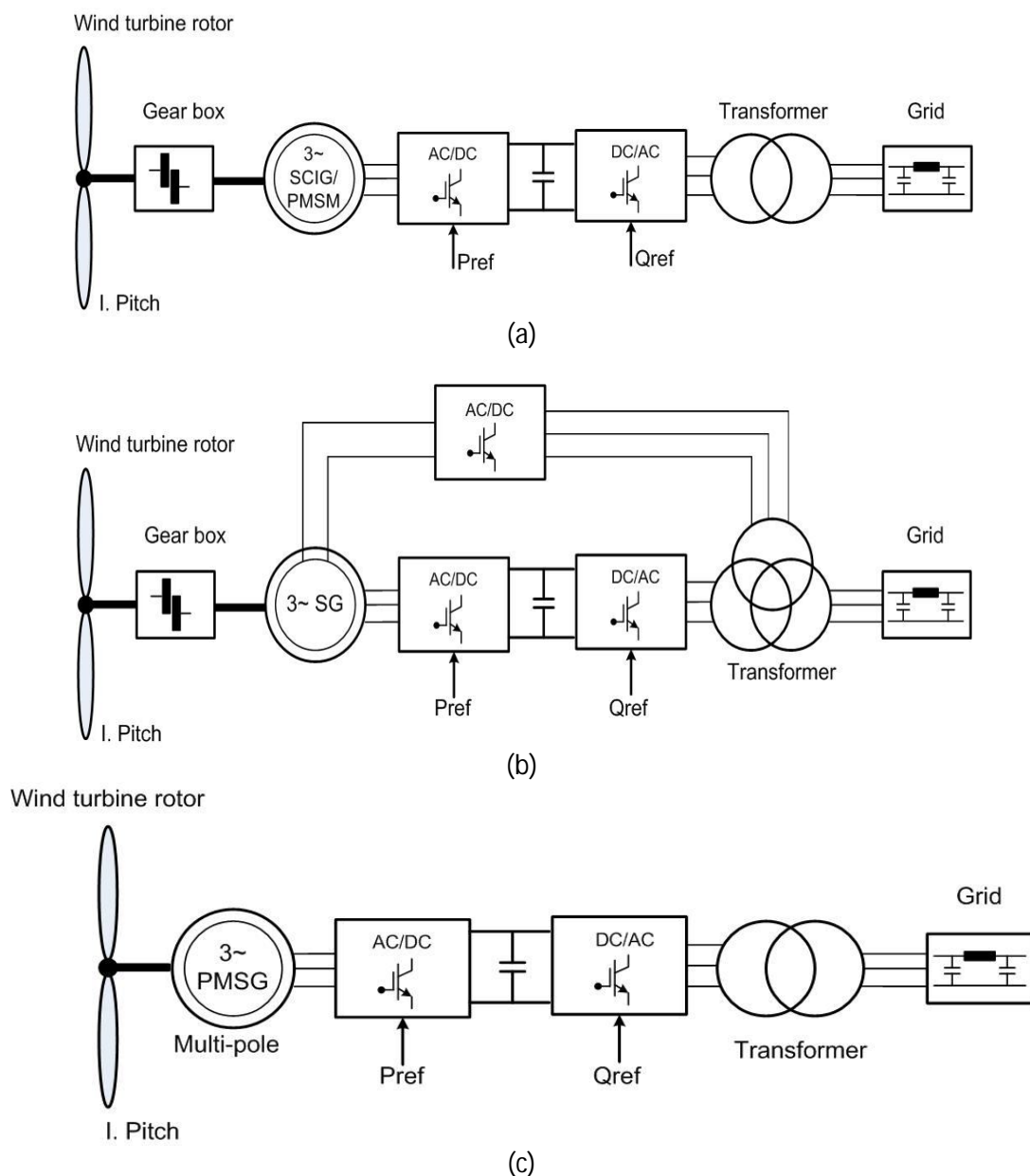
Variable speed wind turbines with double fed induction generators have power converters connected to the rotor windings through slip rings. The stator of the generator is connected directly through the stator. So, only a part of the power produced by the generator passes through the converters and is typically around 30% of the nominal power. It is possible to directly control the active and reactive power. The speed range is increased to around 30% of the nominal speed. A disadvantage is that the generator is sensitive to grid faults, which generates over currents that can damage the rotor windings.[3][4]

Variable speed with full rated power converters

In this type of wind turbines a full rated power converter is connected between the stator and the grid. This will translate into a better technical performance and full range of wind speed. Two types

of subcategories are distinguished: with and without gear boxes. Generators can be squirrel cage induction generator, permanent magnet generator or separately excited synchronous generator. The last one needs an AC/DC converter to supply the rotor windings. A back to back converter is used to control the active and reactive power. For all kind of topologies using full scale converters, the generator is decoupled from the grid through dc link. Wind turbines using multi pole synchronous generator have no need of gear box. Therefore the system cost is decreased and this type of topology seems more attracted.

Variable speed wind turbines with continues variable transmission gearboxes consist of synchronous generator directly connected to the grid. Output speed of the gearbox is constant, while only the torque changes with the wind power. The generator needs a dc excitation converter to supply the rotor windings. A constant speed implies an easier method to synchronize the generator to the grid. Reactive power is controlled through the magnetization circuit.[3]



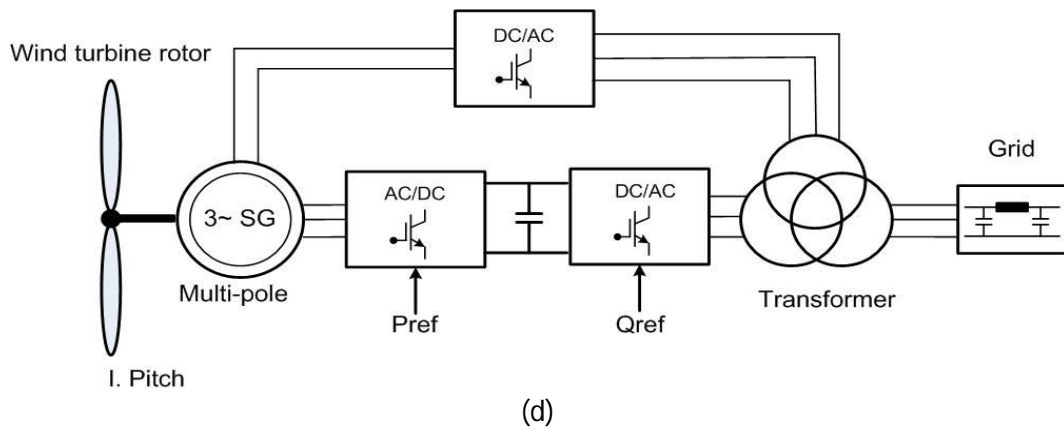


Fig 1.5:Topology of variable Speed wind turbine with full rated converters

Further aspects of this topology such as fault ride through capability and variable power will be investigated in the following chapters.

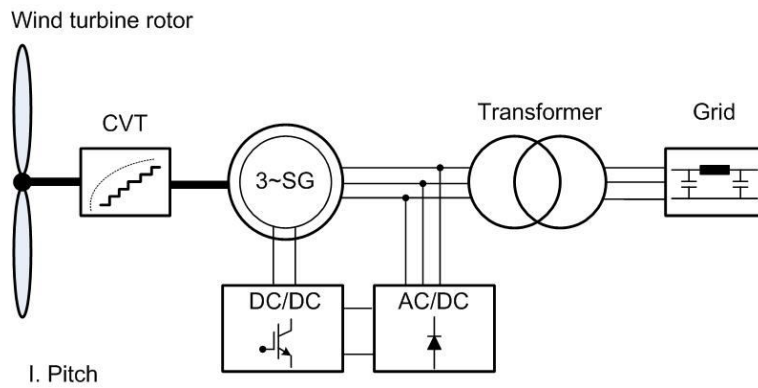


Fig 1.6:Variable Speed wind turbine(CVT)

1.3 System description

The overall wind turbine considered consists of a synchronous generator is driven by a blade and gear system. The Synchronous Generator (SG) is directly connected to the grid.

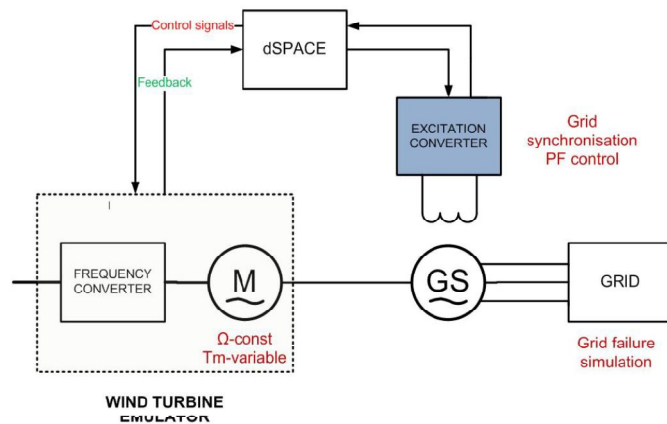


Fig 1.7: Lab setup

Therefore, the speed of the SG shaft is constant while only the torque is variable. The generator is a salient pole type. Brushed exciter machine pose various problems mainly maintenance, hence a generator with brushless excitation is chosen. In the laboratory the wind emulator is an induction motor (15 kW) controlled in torque with a frequency converter. When the generator (12.5 kW) is connected to the grid, it is considered to be in speed control because the grid is stronger and imposes the frequency. Excitation of the generator is obtained from a dc/dc converter. Frequency and excitation converter are controlled with dSpace. Induction machine is controlled with Indirect Field Oriented Control. Following current and voltage measurements are needed:

- Two phase currents and dc link voltage for IFOC
- 3 phase currents and 3 phase voltages of SG to calculate P,Q and power factor
- 3 phase grid voltages for synchronization of the generator

1.4 Problem Formulation

The main aim is to monitor and control the reactive power of the machine to maximize the power (PF=1) supplied to the grid under variable wind conditions (constant speed – variable torque) and also to study the low voltage fault ride through capability of the SG during grid faults to comply with electrical grid codes.

1.5 Objectives

The following objectives can be formulated

- Modeling and simulation
 - Synchronous Generator : Generator and reactive power control
 - Induction Motor : Motor and field oriented control
 - Excitation Converters
 - Grid Faults
- Laboratory Work
 - Setup test bench
 - SG and IM coupled
 - Frequency converters
 - Excitation Converters
 - Measurement modules
 - Build protection panel using fuses and contactors
- Field Oriented Control for IM
 - Build voltage and current sensors
 - Control from dSpace
- Reactive power control for SG
 - Build excitation converters
 - Control from dSpace
 - Test and analysis
- Monitor generator response to grid faults
 - Test in simulation
 - Test and analysis in hardware setup
 - Suggest solutions to arising problems

1.6 Limitations

Some of the limitations are listed below:

1. The synchronous generator, a core part of project, arrived in 2nd part of the project period.
2. Limitation due to inductor based voltage dividers, as Type D faults(see Chapter 5) or change in phase angle couldn't be achieved

2 Induction Machine: Theory and Control

This chapter presents the mathematical model of the induction machine which is used as the prime mover to emulate the wind turbine. Field Oriented control strategy is discussed. The PI controllers used in this strategy are discussed along with the tuning of their parameter. Furthermore, the results of the implementation in both simulation and laboratory are presented

2.1 Mathematical Model

In order to simulate the induction machine a mathematical model is developed which is implemented in MATLAB/Simulink™. Fig 2.1 shows the two-phase equivalent circuit diagram of induction machine.

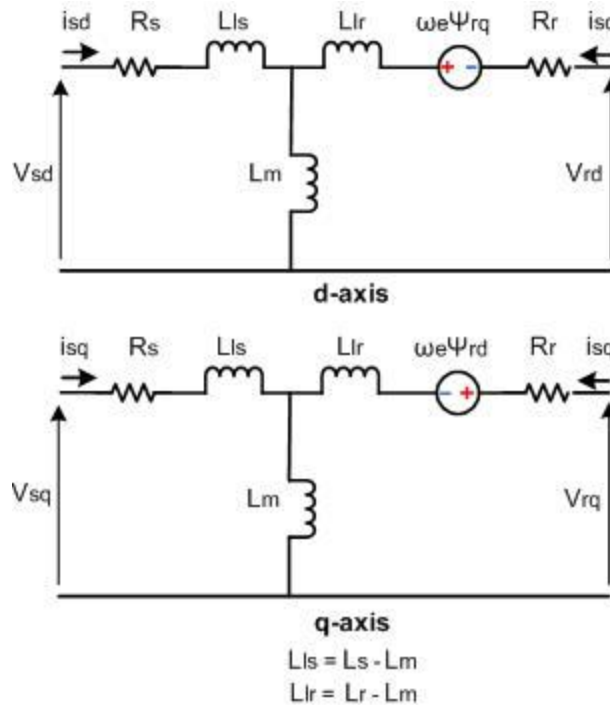


Fig 2.1: Two-Phase equivalent circuit diagram of induction machine

The voltages equations of the dynamic model of induction machine in two-axis stationary frame are given below in Eqn 2.1, 2.2, 2.3 and 2.4

$$V_{sd} = R_s I_{sd} + \frac{d\psi_{sd}}{dt} \quad 2.1$$

$$V_{sq} = R_s I_{sq} + \frac{d\psi_{sq}}{dt} \quad 2.2$$

$$V_{rd} = R_r I_{rd} + \frac{d\psi_{rd}}{dt} + \omega_e \psi_{rq} = 0 \quad 2.3$$

$$V_{rq} = R_r I_{rq} + \frac{d\psi_{rq}}{dt} - \omega_e \psi_{rd} = 0 \quad 2.4$$

But since the machine considered is squirrel cage type. The rotor voltages are (V_{rd} and V_{rb}) zero. The flux equations are given by [5]

The flux equation are given in Eqn 2.5, 2.6, 2.7 and 2.8. The flux consists of two components the product of current along own axis and the self inductance. The second term in each equation represents the product of current along the quadrature axis and the magnetizing inductance.

$$\psi_{sd} = L_s I_{sd} + L_m I_{rd} \quad 2.5$$

$$\psi_{sq} = L_s I_{sq} + L_m I_{rq} \quad 2.6$$

$$\psi_{rd} = L_r I_{rd} + L_m I_{sd} \quad 2.7$$

$$\psi_{rq} = L_r I_{rq} + L_m I_{sq} \quad 2.8$$

The simulation requires the machine parameter namely the inductances and resistances. This can be obtained from the data sheet or nameplate details of the machines (See Appendix B). The matrix/vector representation of modeling is very efficient from a computational standpoint for computer implementation and also has ability to easily handle systems with multiple inputs and outputs. This form of solution is the same as for a single 1st –order differential equation. Hence the equations are re-written by substituting Eqn 2.5, 2.6, 2.7 and 2.8 in Eqn 2.1, 2.2, 2.3 and 2.4.

$$I' = AI + BV \quad 2.9$$

$$I = (I_{sd} \ I_{sq} \ I_{rd} \ I_{rq})^T \quad 2.10$$

$$V = (V_{sd} \ V_{sq} \ V_{rd} \ V_{rq})^T \quad 2.11$$

$$A = \begin{pmatrix} \frac{-1}{\sigma T_s} & \frac{\omega_e(1-\sigma)}{\sigma} & \frac{1}{\sigma(1+\sigma_s)T_r} & \frac{\omega_e}{1+\sigma_s} \\ \frac{-\omega_e(1-\sigma)}{\sigma} & \frac{-1}{\sigma T_s} & \frac{-\omega_e}{1+\sigma_s} & \frac{1}{\sigma(1+\sigma_s)T_r} \\ \frac{1}{\sigma(1+\sigma_r)T_s} & \frac{-\omega_e}{1+\sigma_r} & \frac{-1}{\sigma T_r} & \frac{-\omega_e}{\sigma} \\ \frac{\omega_e}{1+\sigma_r} & \frac{1}{\sigma(1+\sigma_r)T_s} & \frac{\omega_e}{\sigma} & \frac{-1}{\sigma T_r} \end{pmatrix} \quad 2.12$$

$$B = \begin{pmatrix} \frac{1}{\sigma L_s} & 0 & \frac{-1}{\sigma(1+\sigma_r)L_s} & 0 \\ 0 & \frac{1}{\sigma L_s} & 0 & \frac{1}{\sigma(1+\sigma_r)L_s} \\ \frac{-1}{\sigma(1+\sigma_s)L_r} & 0 & \frac{1}{\sigma L_r} & 0 \\ 0 & \frac{-1}{\sigma(1+\sigma_s)L_r} & 0 & \frac{1}{\sigma L_r} \end{pmatrix} \quad 2.13$$

Where

$$\sigma = 1 - \frac{L_m^2}{L_s L_r}, \text{leakage factor}$$

$$\sigma_s = \frac{L_s}{L_m} - 1$$

$$\sigma_r = \frac{L_r}{L_m} - 1$$

ω_e is the electrical speed of the rotor.

The electromagnetic torque developed is related to the speed:

$$J \frac{d\omega_r}{dt} = T_e - T_l - B\omega_r \quad 2.14$$

$$p \cdot \omega_r = \omega_e \quad 2.15$$

2.1.1 Simulation and Validation

The validity of the model is verified by comparing to the nameplate details (see Appendix B) The slip - torque characteristics for the 15kW motor is plotted in Fig 2.2.

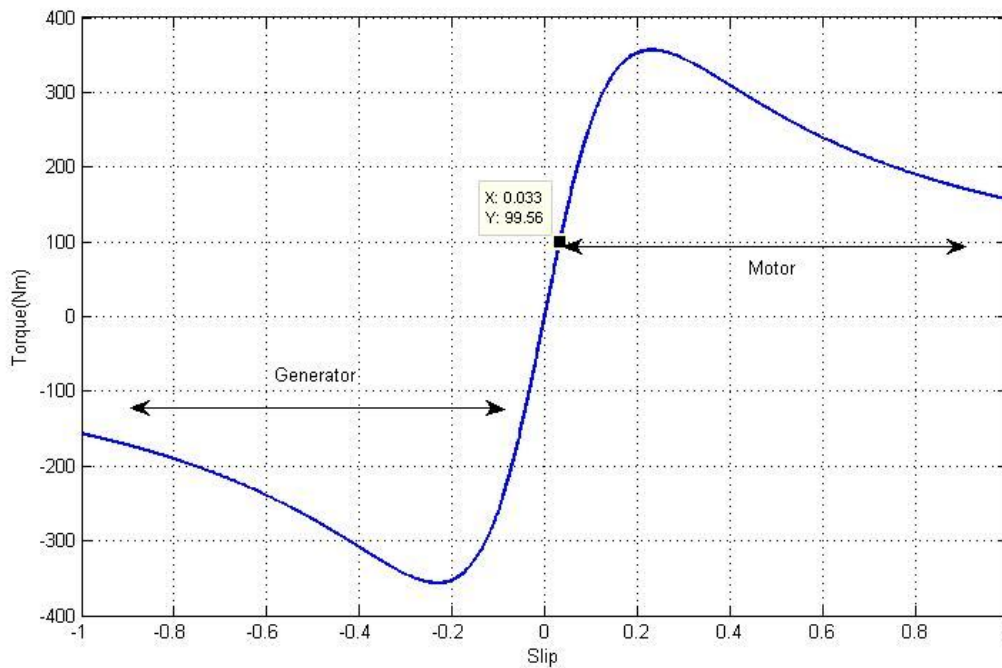


Fig 2.2: Torque/ Slip Characteristics

It can be noted that for a slip of 0.033 corresponds to a speed of 1455[rpm] and torque generated is about 100Nm as stated in nameplate details. Hence the model is verified for nominal operation.

Fig 2.3 shows the nominal operation for V/f control where the operation speed is 1455 rpm for a load of 100Nm.

This is illustrated by the step in torque from 0 to 100[Nm] at 5[s].

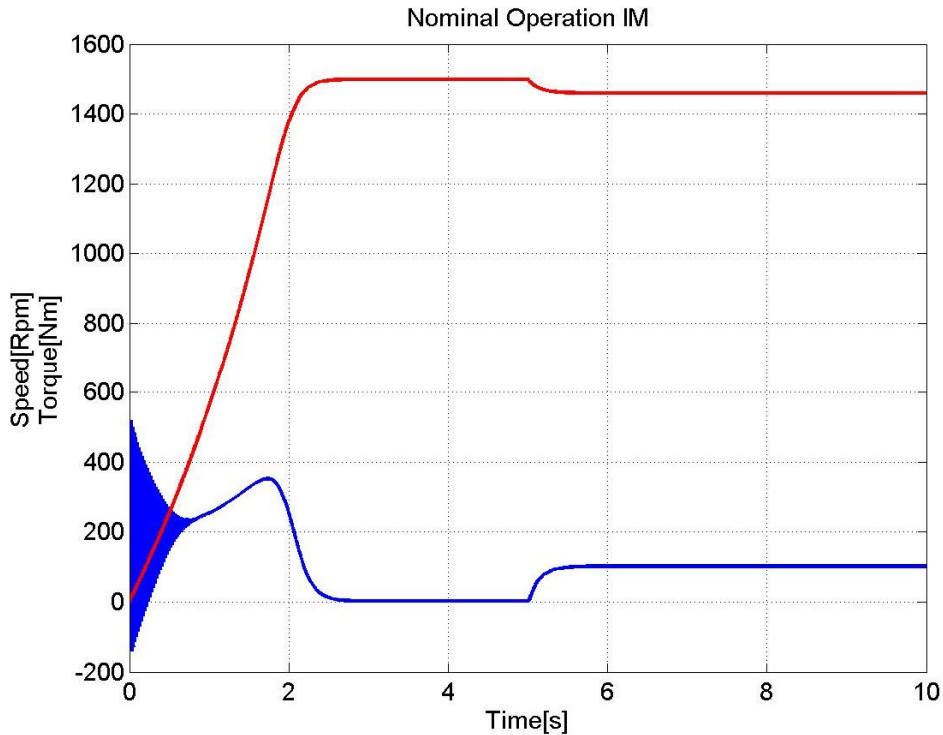


Fig 2.3:Nominal operation of induction machine(1455RPM,100Nm)

2.2 Induction Motor: Indirect Field Oriented Control Principles

In this project, the prime mover is controlled to emulate constant speed and varying torque operation of wind rotor blade. Apart from which the synchronization of the grid is also achieved by controlling the speed of the prime mover. So the control is operated in speed mode till synchronization and then in torque control mode. In order to achieve high dynamic performance in both modes – torque control and speed control, Indirect Field Oriented Control is implemented, which is a type of vector control.

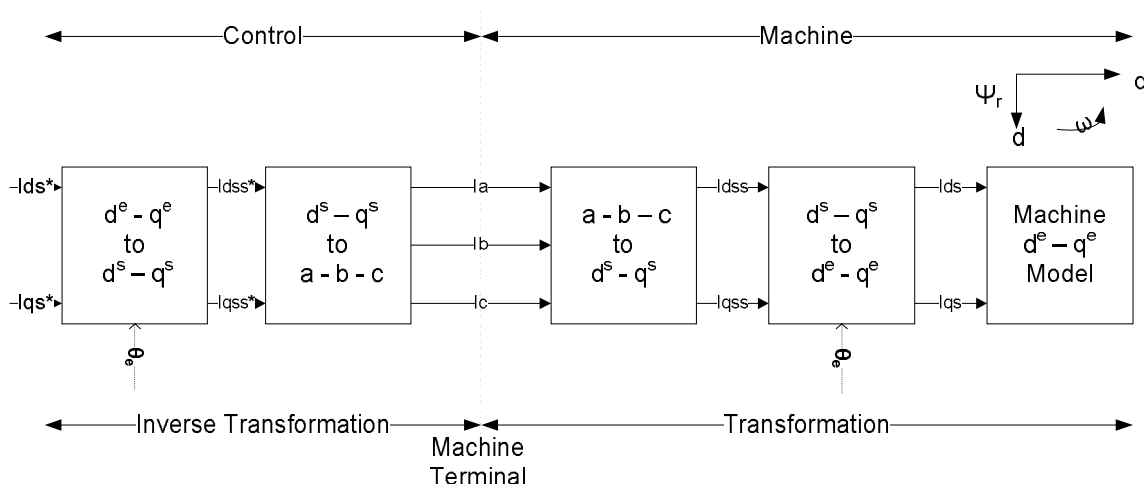


Fig 2.4:Frame transformations involved in IFOC [6]

The fundamentals of vector control can be explained using Fig 2.4 where the machine model is represented in a synchronously rotating frame .The inverter is omitted, assuming it has unity current gain. It should be noted the vector angle (θ_e) of the synchronously rotating frame is used to

transform from one frame to another. The vector angle ensures I_{ds} component of current is aligned to the rotor flux along the d -axis of the synchronous frame. Hence the calculation of the rotor angle is essential for the implementation of vector control. In IFOC this is obtained by method of slip estimation, which is explained in the subsequent section.

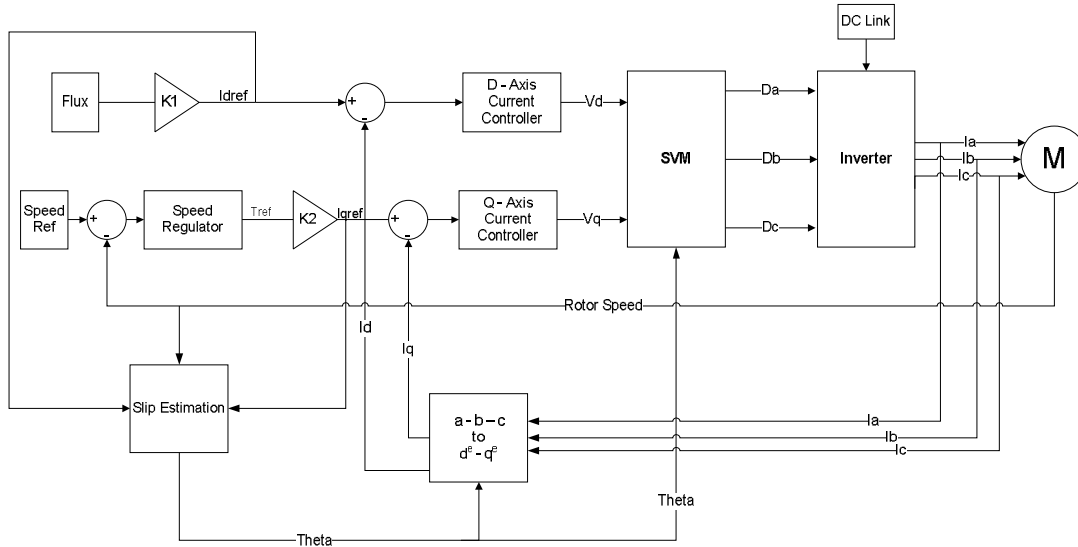


Fig 2.5: IFOC Vector Control Implementation[6]

The advantage of FOC is the independent control of torque and flux. This done by aligning the rotor flux to the d -axis of the rotating frame. Hence the control is decoupled and I_d is used to control flux and I_q is used to control torque.

The control flow is shown in Fig 2.5. The q -axis of the control scheme has a cascaded controller arrangement- q -axis current controller as the inner loop and speed regulator as the outer loop. The output of the speed loop is the torque reference which corresponds to a reference q -axis current.

$$T_{ref} = \frac{3}{2} p \Psi_r I_{q} \quad 2.16$$

It is desirable to have constant flux operation as it enables high torque sensitivity per ampere of stator current. [6]. Hence the d -axis of the control scheme consists of only a current controller.

2.2.1 Slip Estimation

The Indirect or feed-forward method is based on the simple principle of measuring the rotor angle (θ_r) and predicting the slip angle (θ_{sl}) which are related to synchronous angle (θ_e) as expressed in 2.17.

$$\theta_e = \int \omega_e = \int \omega_r + \omega_{sl} = \theta_r + \theta_{sl} \quad 2.17$$

The rotor equations of the induction machine are :

$$\frac{d\Psi_{dr}}{dt} + R_r I_{dr} - (\omega_e - \omega_r) \Psi_{qr} = 0 \quad 2.18$$

$$\frac{d\Psi_{qr}}{dt} + R_r I_{qr} + (\omega_e - \omega_r) \Psi_{dr} = 0 \quad 2.19$$

And the flux linkages are

$$\Psi_{dr} = L_r I_{dr} + L_m I_{ds} \quad 2.20$$

$$\Psi_{qr} = L_r I_{qr} + L_m I_{qs} \quad 2.21$$

Re-arranging Eqn 2.20 and 2.21 to obtain the rotor currents, as they cannot be measured physically. The following equations are obtained.

$$I_{dr} = \frac{1}{L_r} \Psi_{dr} - \frac{L_m}{L_r} I_{ds} \quad 2.22$$

$$I_{qr} = \frac{1}{L_r} \Psi_{qr} - \frac{L_m}{L_r} I_{qs} \quad 2.23$$

Substituting in Eqn 2.18 and 2.19

$$\frac{d\Psi_{dr}}{dt} + \frac{R_r}{L_r} \Psi_{dr} - \frac{L_m}{L_r} R_r I_{ds} - \omega_{sl} \Psi_{qr} = 0 \quad 2.24$$

$$\frac{d\Psi_{qr}}{dt} + \frac{R_r}{L_r} \Psi_{qr} - \frac{L_m}{L_r} R_r I_{qs} + \omega_{sl} \Psi_{dr} = 0 \quad 2.25$$

To decouple the control, the d-axis of the rotating frame is aligned with the rotor flux

Hence
$$\Psi_{qr} = 0 \quad 2.26$$

$$\frac{d\Psi_{qr}}{dt} = 0 \quad 2.27$$

Substituting Eqn 2.26 and Eqn 2.27 in Eqn 2.24 and 2.25, it is obtained that:

$$\frac{R_r}{L_r} \frac{d\Psi_{dr}}{dt} + \Psi_{dr} = L_m I_{ds} \quad 2.28$$

$$\omega_{sl} = \frac{R_r I_{qs}}{L_r I_{ds}} \quad 2.29$$

Hence θ_e is calculated by substituting Eqn 2.29 in Eqn 2.17 to provide the rotor angle and the control is implemented as mentioned in section 2.2. [6]

2.2.2 PI Controllers

In synchronously rotating frame the fundamental components of the machine variables namely currents and voltage are DC quantities in steady state. PI controllers are used to regulate these

variables. The tuning of the PI is crucial to obtain desired dynamic performance of the machine. In the following section the tuning of each is discussed in detail. The parameters are calculated based on certain criteria such as [7]:

1. In case of cascaded loops the outer loop is slower than the inner loop (Bandwidth of inner loop larger than the outer loop).
2. Overshoot is no more than 5% ($M_p < 5\%$).

A generic PI controller can be expressed as:

$$C(s) = K_p + \frac{K_i}{s} = K_p \left(\frac{1 + s\tau}{s\tau} \right) \quad 2.30$$

Where,

C(s)=Controller in Laplace domain

K_p= Proportional Gain

K_i= Integral Gain

τ= Integral Time Constant

2.2.2.1 D-axis current loop

The d-axis voltage equation is

$$V_{sd} = I_{sd}R_s + \frac{d\psi_{sd}}{dt} \quad 2.31$$

$$\psi_{sd} = L_s I_{sd} + L_m I_{rd} \quad 2.32$$

$$\psi_{rd} = L_r I_{rd} + L_m I_{sd} \quad 2.33$$

$$I_{rd} = \frac{\psi_{rd} - L_m I_{sd}}{L_r} \quad 2.34$$

Substituting Eqn 2.32,2.33 and 2.34 in Eqn 2.31

$$V_{sd} = I_{sd}(R_s + sL'_s) + \left(s \frac{L_m}{L_r} \psi_{rd} \right)_2 \quad 2.35$$

$$L'_s = L_s - \frac{L_m^2}{L_r} \quad 2.36$$

The component of Eqn 2.35 termed 2 is neglected in further analysis to simplify the tuning process. Nevertheless, its presence in the real system is not avoidable, unless it is compensated. The PI parameters will be slightly different in laboratory implementation.

Hence Eqn 2.35 is reduced to the transfer function represented in Eqn 2.37:

$$G_{id}(s) = \frac{I_{sd}}{V_{sd}} = \frac{1}{R_s + sL'_s} = \frac{1}{R_s(1 + sT'_s)} \quad 2.37$$

The dynamics of the system is modeled by taking into account various delay in the system. In order to represent better the real system, certain delays are introduced with respective times:[7]

- Control algorithm - Delays introduced by calculation time(T_s)
- Zero-order-hold (ZOH) – Sample and hold delay($0.5T_s$)
- Inverter - Delay due to pulse width modulation in Inverter($0.5T_{pwm}$)
- Sensor – Sample and hold delay introduced by the current sensor($0.5T_s$)

Where $T_s = \frac{1}{F_s}$, $T_{pwm} = \frac{1}{F_{pwm}}$ and F_{pwm} , F_s are the switching and sampling frequencies respectively (5 kHz).

The switching frequency is chosen as 5 kHz to satisfy the Nyquist sampling theorem, which states that for lossless digitization, the sampling rate should be *at least twice* the maximum frequency responses.

Each of these delays can be approximated as Pade Approximant of the form [7]

$$e^{-T_d s} \cong \frac{1}{T_d s + 1} \quad 2.38$$

Hence the control loop is modeled as shown in Fig 2.6. The sensor delay which would appear on the feedback loop has been re-arranged to obtain unity feedback.

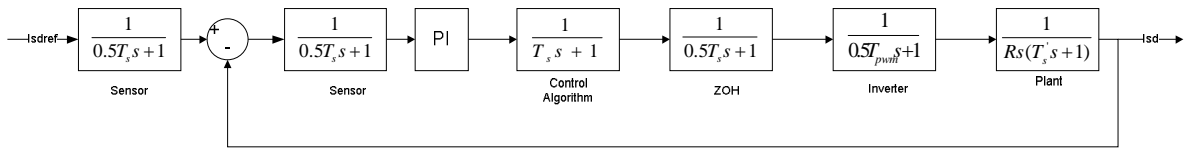


Fig 2.6: d-axis current loop with unity feedback

From Fig 2.6 the open loop transfer function is given by

$$G_{isd}(s) = \left(K_p + \frac{K_i}{s}\right) \frac{1}{T_s s + 1} \frac{1}{0.5T_s s + 1} \frac{1}{0.5T_s s + 1} \frac{1}{0.5T_{pwm} s + 1} \frac{1}{R_s (1 + sT'_s)} \quad 2.39$$

Now, coefficients of the PI regulator can be determined. The zero of the controller is chosen to neutralize the effect of the slowest pole, to improve dynamics in the controlled system. Slowest pole is that of the plant. Afterwards, proportional gain is found on the basis of magnitude optimum criterion. [7][8]. Finally, parameters are tuned to the following values.

$$K_p = 1$$

$$K_i = 6.1$$

The step response is shown in Fig 2.7 indicates the following characteristics

Peak Overshoot(M_p)=0% < 5%(Design Criteria)

Rise Time(T_r , 10%-90%)=418ms

Settling Time(T_s , 2%) =573ms

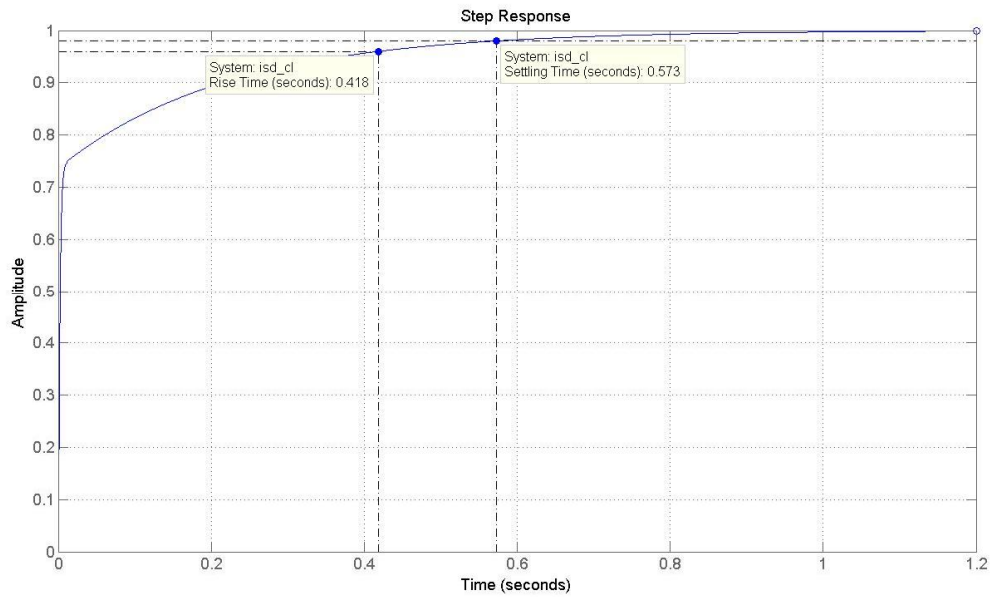


Fig 2.7: Step response of d-axis current loop.

The stability of the system is analyzed based on Bode plot shown in Fig 2.8. The gain margin (GM) is 23.4 [dB] and the phase margin (PM) is 101[deg]. Hence, the system for closed loop is also stable. The bandwidth for this controller in closed loop is 168.1 [Hz].

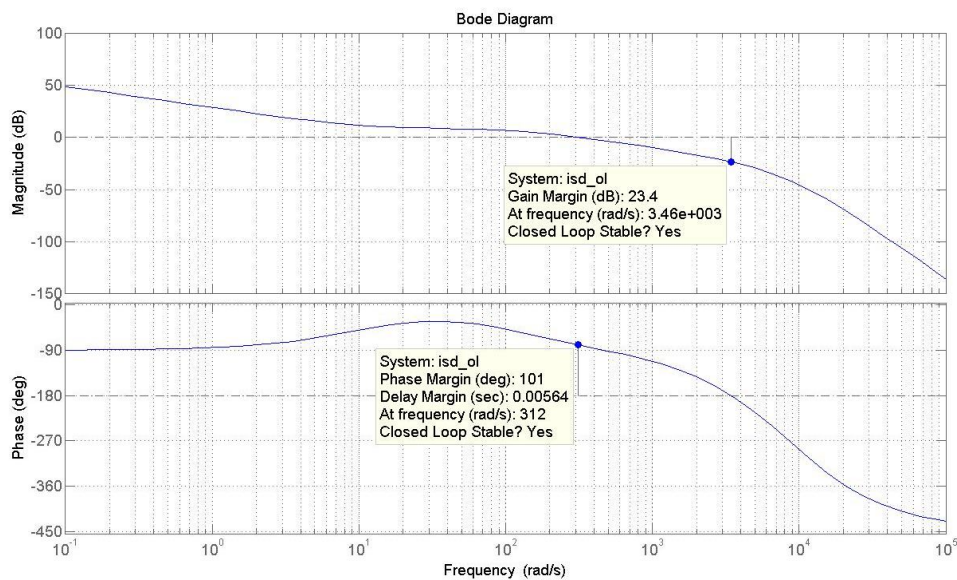


Fig 2.8: Bode plot of d-axis open loop transfer function

2.2.2.2 Q-axis current loop

The q-axis voltage equation is

$$V_{sq} = I_{sq}R_s + \frac{d\psi_{sq}}{dt} + \omega_e\psi_{sd} \quad 2.40$$

$$\psi_{sq} = L_s I_{sq} + L_m I_{rq} \quad 2.41$$

Substituting Eqn 2.41 in Eqn 2.40

$$V_{sq} = I_{sq} R_s + \frac{d(L_s I_{sq} + L_m I_{rq})}{dt} + \omega_e \psi_{sd} \quad 2.42$$

$$I_{rq} = -(\omega_e - \omega_r) \psi_{rd} - \frac{d\psi_{rq}}{dt} \quad 2.43$$

Rotor flux q-component, can be determined by q-component of stator

$$\psi_{rq} = I_{sq} \left(L_m - \frac{L_r L_s}{L_m} \right) \quad 2.44$$

Substituting Eqn 2.43 and 2.44 in Eqn 2.42

$$V_{sq} = \left((R_s + sL_s) I_{sq} - s^2 \frac{L_m}{R_r} \left(L_m - \frac{L_r L_s}{L_m} \right) I_{sq} \right)_1 - \left(s \frac{L_m}{R_r} (\omega_e - \omega_r) \psi_{rd} + \omega_e \psi_{sd} \right)_2 \quad 2.45$$

Term (2) is considered as a disturbance, and is omitted in the analysis. However, the coupling exists in the real system. [7] Hence the plant can be modeled as after some mathematical manipulation:

$$G_{iq}(s) = \frac{I_{sq}}{V_{sq}} = \left(\frac{1}{\sigma T_{st} T_r s^2 + T_{st} s + 1} \right) \frac{1}{R_s} \quad 2.46$$

Where

$$T_{st} = \frac{L_s}{R_s}$$

$$\sigma = \frac{L_s}{L_m} - 1$$

The dynamics of the system is modeled by taking into account various delay in the system as in d-axis current loop.

The open loop transfer function is given by

$$G_{isd}(s) = \left(K_p + \frac{K_i}{s} \right) \frac{1}{T_s s + 1} \frac{1}{0.5 T_s s + 1} \frac{1}{0.5 T_s s + 1} \frac{1}{0.5 T_{pwm} s + 1} \left(\frac{1}{\sigma T_{st} T_r s^2 + T_{st} s + 1} \right) \frac{1}{R_s} \quad 2.47$$

The block diagram is shown below:

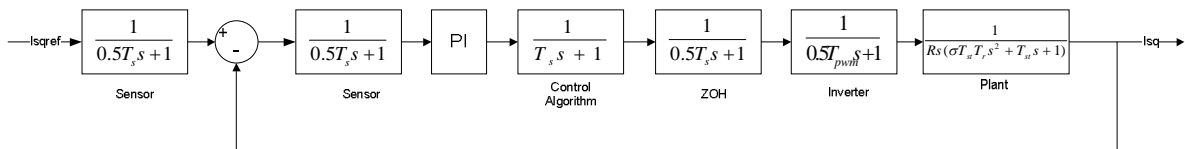


Fig 2.9: q-axis current loop with unity feedback

Solving Eqn 2.46 we have the two time constants of the plant are

$$T_{iq(1)} = 14.07ms$$

$$T_{iq(2)} = 163.42ms$$

Now, coefficients of the PI regulator can be determined. The zero of the controller is chosen to neutralize the effect of the slowest pole which is $T_{iq(2)}$ in this case. K_p and K_i is used to calculated using magnitude optimum criterion.[8] Finally, parameters are tuned to the following values.

$$K_p = 1$$

$$K_i = \frac{K_p}{T_{isq(2)}} = 6.1$$

The step response is shown in Fig 2.10.

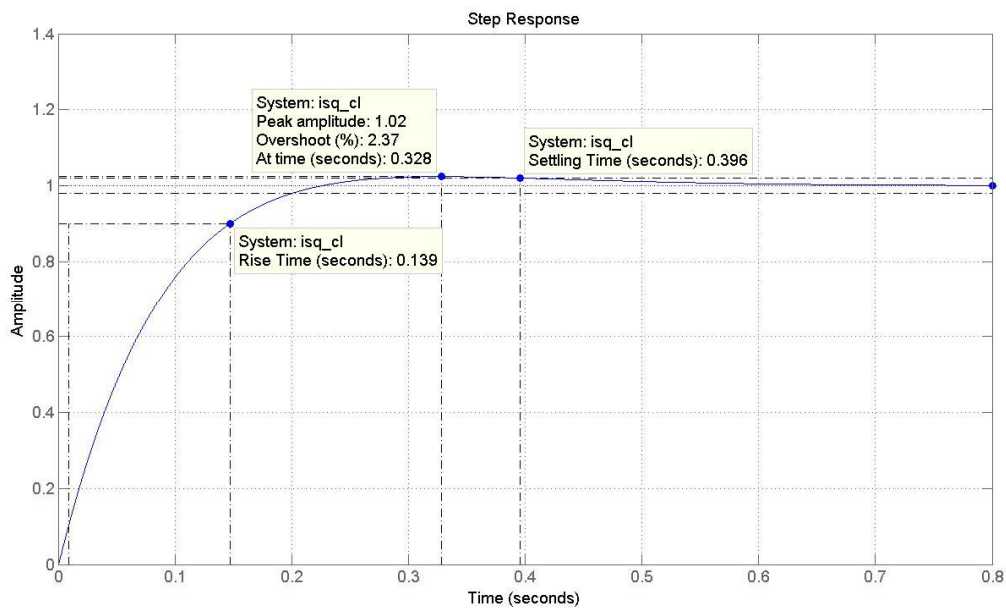


Fig 2.10: Step response of q-axis current loop.

The step response indicates as the characteristics

Peak Overshoot (M_p) = 2.37% < 5% (Design Criteria)

Rise Time (T_r , 10%-90%) = 139ms

Settling Time (T_s , 2%) = 396ms

The stability of the system is analyzed based on Bode plot shown in Fig 2.11. The gain margin (GM) is 51.7 [dB] and the phase margin (PM) is 82.8[deg]. Hence, the system for closed loop is also stable. The bandwidth for this controller in closed loop is 168.1 [Hz].

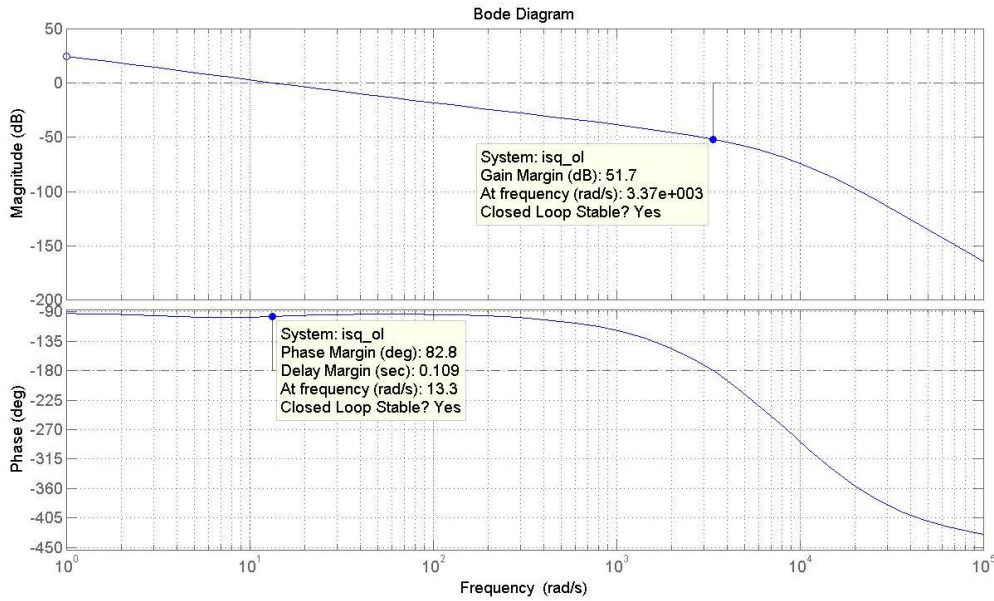


Fig 2.11: Bode plot of q-axis open loop transfer function

2.2.2.3 Speed Loop

The speed loop on the q-axis is part of a cascade controller whose inner loop consists of the q-axis current controller. Hence, the transfer function of the inner current loop has to be formulated. As, only the slowest pole of the plant of q-current loop is cancelled by its regulator, the other one is included in equivalent time constant computation [7]. It is calculated based on Fig 2.9

$$T_{iq(ol)}^{eq} = T_{iq(1)} + 0.5T_{pwm} + 0.5T_s + T_s + 0.5T_s = 15.2ms \quad 2.48$$

The closed loop transfer function can be expressed as:

$$G_{iq(cl)}^{eq}(s) = \frac{1}{2(T_{iq(ol)}^{eq}s)^2 + 2T_{iq(ol)}^{eq}s + 1} \quad 2.49$$

The sensor delay occurring in the input to the current controller as a consequence of obtaining a unity feedback system the transfer function is included in the transfer function.

$$G_{iq}^{eq}(s) = (0.5T_s s + 1) \frac{1}{2(T_{iq(ol)}^{eq}s)^2 + 2T_{iq(ol)}^{eq}s + 1} \quad 2.50$$

But

$$\frac{(1 + 0.5T_s s)(1 - 0.5T_s s)}{(1 - 0.5T_s s)} = \frac{1 - (0.25T_s s)^2}{(1 - 0.5T_s s)} \approx \frac{1}{(1 - 0.5T_s s)} \quad 2.51$$

Hence

$$G_{iq}^{eq}(s) = \frac{1}{(1 - 0.5T_s s)} \frac{1}{\left(2(T_{iq(ol)}^{eq}s)^2\right)_1 + 2T_{iq(ol)}^{eq}s + 1} \quad 2.52$$

Term 1 in Eqn 2.52 is negligible in lines with Eqn 2.51. The equivalent time constant of q-axis current loop can be computed as

$$T_{iq}^{eq} = 2T_{iq(ol)}^{eq} - 0.5T_s = 30.3ms \quad 2.53$$

Hence the simplified transfer function of the q-axis current loop is

$$G_{iq}^s(s) = \frac{1}{1 + T_{iq}^{eq}s} \quad 2.54$$

The mechanical equation is given by

$$J \frac{d\omega_r}{dt} = T_e - T_l - B\omega_r \quad 2.55$$

Hence the transfer function is calculated as:

$$\frac{\omega_r(s)}{\Delta T(s)} = \frac{1}{Js + B} \quad 2.56$$

The resulting speed depends also on the load torque, which is treated as the disturbance. Hence the total control is modeled as shown in Fig 2.12

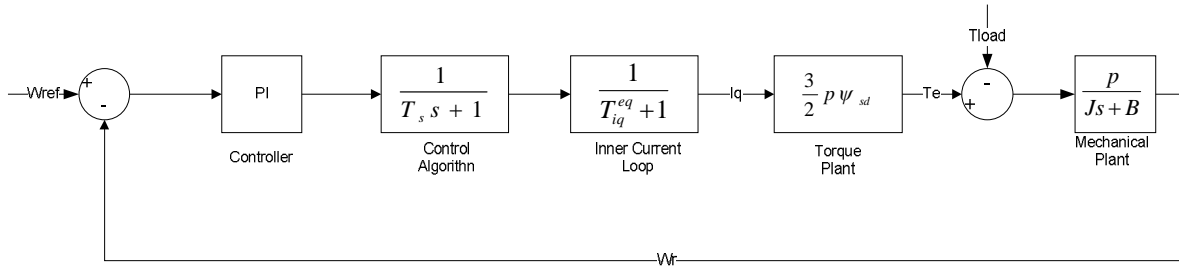


Fig 2.12: Block diagram for tuning speed Loop

The system is considered linear, thus it can be resolved by principle of superposition.[7]The tuning is done in a two step process.

Step 1: Speed is treated as an input of the system, and torque is set to zero. In this case, only proportional part of the regulator is utilized as shown in Fig 2.13

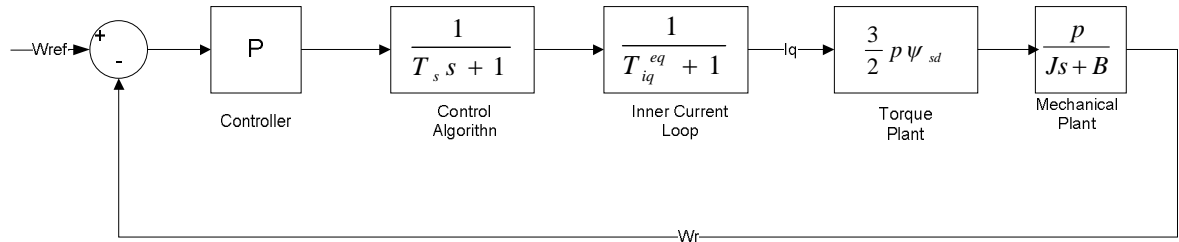


Fig 2.13: Block diagram for tuning speed Loop(Step 1)

Hence the open loop transfer function of the system is

$$G_{\omega}(s) = K_p \frac{1}{T_s s + 1} \frac{1}{T_{iq}^{eq} s + 1} \frac{3p\psi_{sd}}{2} \frac{p}{Js + B} \quad 2.57$$

Further simplifications include calculating a equivalent time constant and neglecting the effects of viscous friction co-efficient

$$G_{\omega}(s) = K_p \frac{1}{T_{\omega}^{eq} s + 1} \frac{3p^2 \psi_{sd}}{2Js} \quad 2.58$$

Where
$$T_{\omega}^{eq} = T_{iq}^{eq} + T_s = 30.5ms \quad 2.59$$

In order to find optimal solution, magnitude optimum criterion is used. [8]

$$K_p = 0.1586$$

Step2: Input torque is examined, while the speed is kept zero.

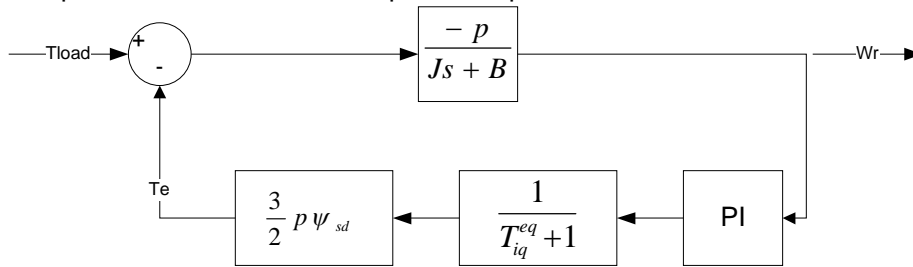


Fig 2.14: Block diagram for tuning speed Loop(Step 2)

Mathematically the function can be expressed as:

$$G_{\Delta T}(s) = K_p + \frac{K_i}{s} \frac{1}{T_{iq}^{eq} s + 1} \frac{3p\psi_{sd}}{2} \frac{-p}{Js + B} \quad 2.60$$

Eqn 2.60 is manipulated to resemble the standard form for use with symmetric optimum criterion method.

$$G_{\Delta T}(s) = \frac{-p}{J} \frac{(2T_{iq}^{eq} T_{\omega} s (T_{iq}^{eq} + 1))}{2(T_{iq}^{eq})^2 T_{\omega} s^3 + 2T_{iq}^{eq} T_{\omega} s^2 + T_{\omega} s + 1} \quad 2.61$$

The integral time constant is computed by comparison to be

$$T_{\omega} = 4T_{iq}^{eq} = 122ms \quad 2.62$$

Hence

$$K_p = 0.57$$

$$K_i = 4.67$$

The step response is shown in Fig 2.15 indicates the following characteristics

Peak Overshoot (M_p)=49.7%

Rise Time (T_r , 10%-90%)=125ms

Settling Time (T_s , 2%)=1.42s

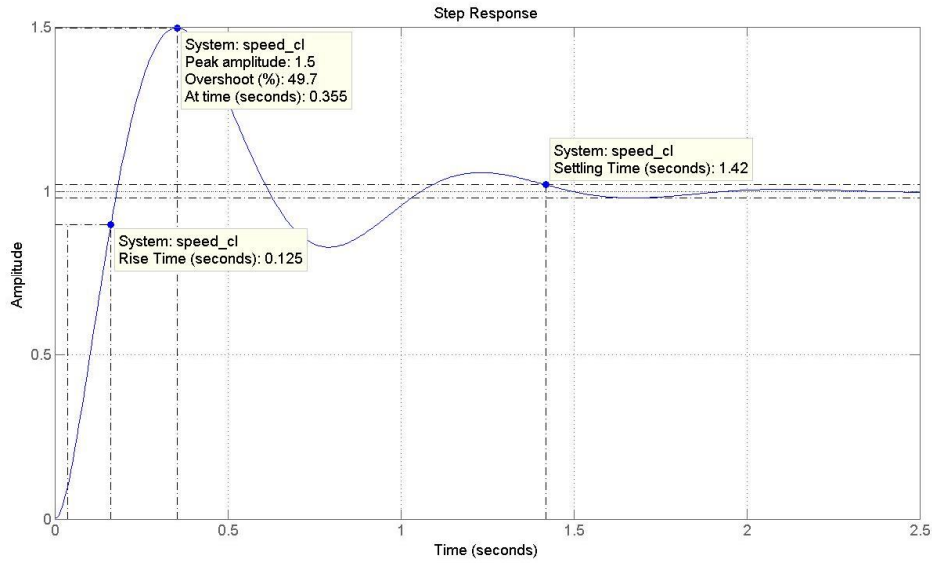


Fig 2.15: Step response of speed loop.

The stability of the system is analyzed based on Bode plot shown in Fig 2.11. The gain margin (GM) is 56.1 [dB] and the phase margin (PM) is 30.8[deg]. Hence, the system for closed loop is also stable. The bandwidth for this controller in closed loop is 13.4 [Hz] which is significantly lower than q-axis current loop hence the control is slower, which is one of the design requirements.

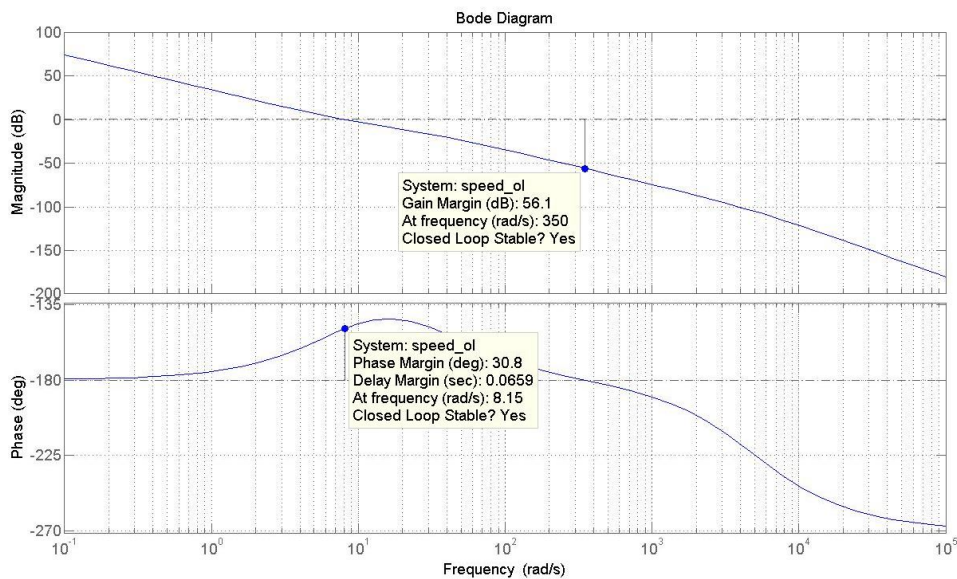


Fig 2.16: Bode plot of speed open loop transfer function

2.3 Lab Implementation

The prime mover is controlled through dSpace via a VLT frequency converter. The following graphs present the validity of the implementation. Space vector modulation is employed to control the switches of the inverter. Fig 2.17 show the duty cycles for all three phases of the controller at 50[Hz] operation. The characteristic third harmonic component is observed. This is because space vector modulation is used to control the inverter.

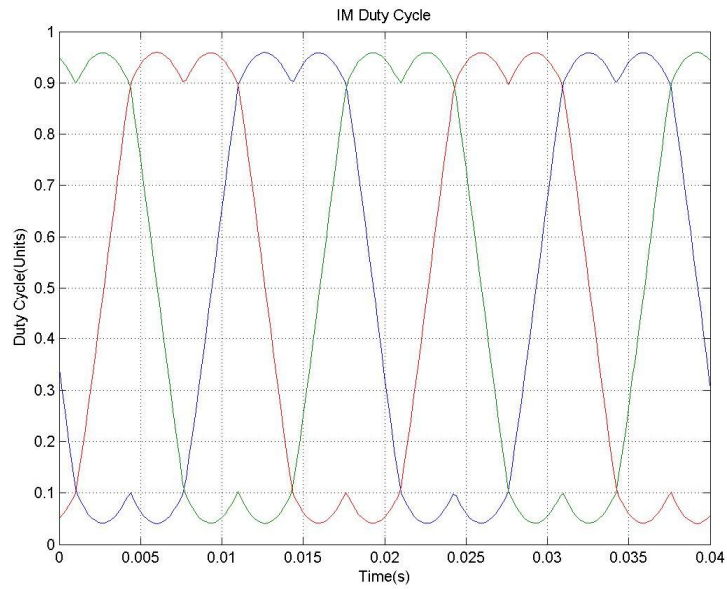


Fig 2.17:Duty cycles imposed on the inverter(SVM)

The duty cycle varies from 0 to 1 in conformance with operation specifications of dSpace. The resulting current is shown in Fig 2.18 which doesn't contain the third harmonic component.

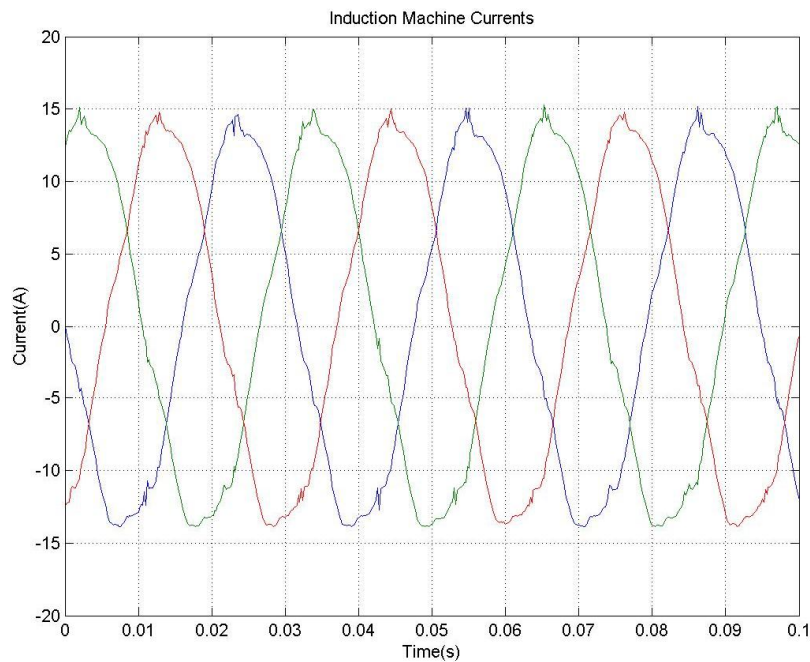
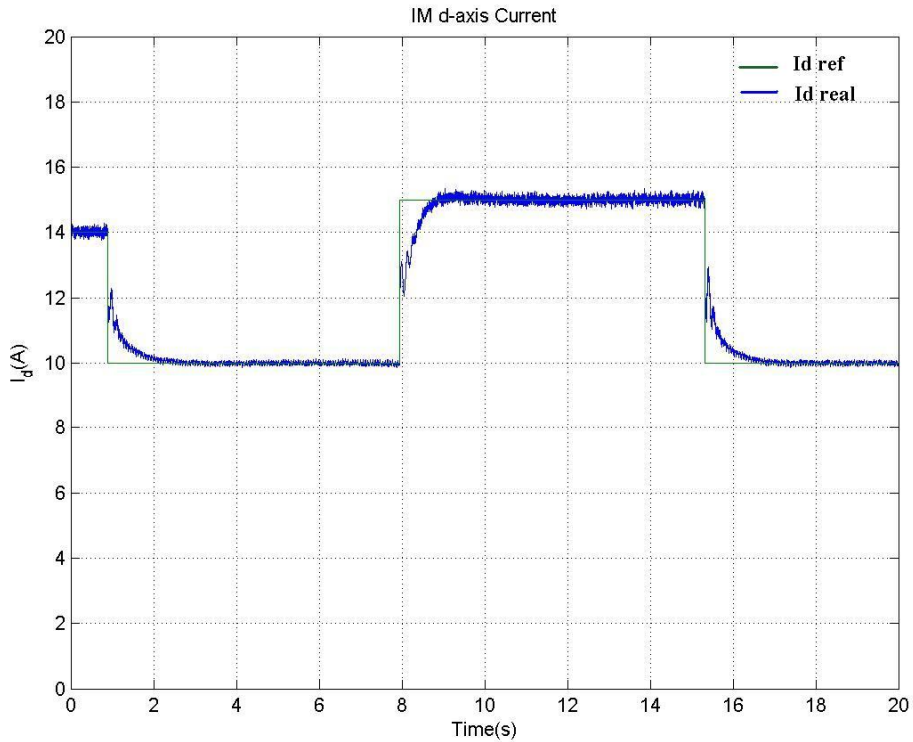


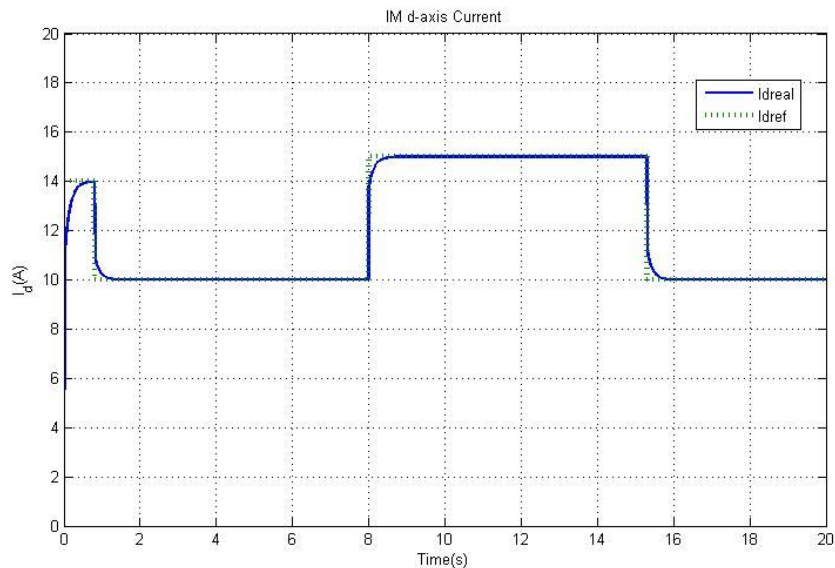
Fig 2.18:Motor currents

Fig 2.19 and Fig 2.20 show the performance of the current controllers used in the scheme at rated speed. The reference of I_d is varied from a starting value of 14[A] to 10[A] at $t=1[s]$, stepped up from 10[A] to 15[A] at $t=8[s]$ and stepped down from 15[A] to 10[A] at $t=15[s]$. The measured current is seen to follow the reference confirming the satisfactory operation of the controller. The nominal value of I_d is 14[A](calculated from rated values) for a flux value of 0.9 Wb seen in Fig 2.24 which also shows the stable flux component which is obtained by a modified flux estimator. The estimated

angle in accordance with equation 2.29 is shown in Fig 2.24 . The reference of I_q is stepped up from starting value of 5.8[A] to 13[A] at around 1[s] and it is stepped down from 13[A] to 5.8[A] at around 9.5[s].



(a)



(b)

Fig 2.19: d-axis current – reference and real(a)Lab(b)Simulation

I_q is responsible for the torque generated in the machine . The response consists of a low frequency ripple this could be caused by:

- Torsional vibration due to coupling.
- Improper tuning of current loop
 - In torque control the current is more stable as seen in Fig 2.22
 - This is not the case because the speed shown in Fig 2.23 is stable has a max ripple of 1.5 [rpm].

The overall speed loop verification is presented in Fig 2.21 where the speed is stepped down from 1000[rpm] starting point to 800[rpm]. The measure speed is seen to follow the reference.

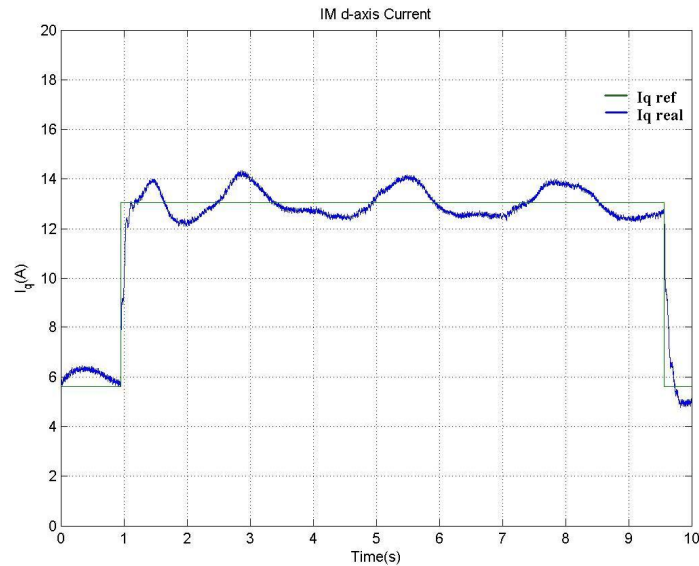


Fig 2.20: q-axis current – reference and real(Speed Control)

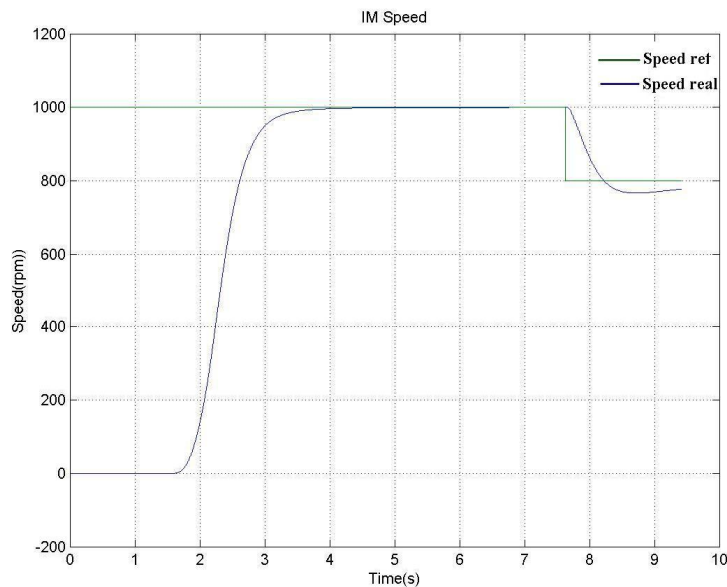


Fig 2.21 :Speed reference and real speed

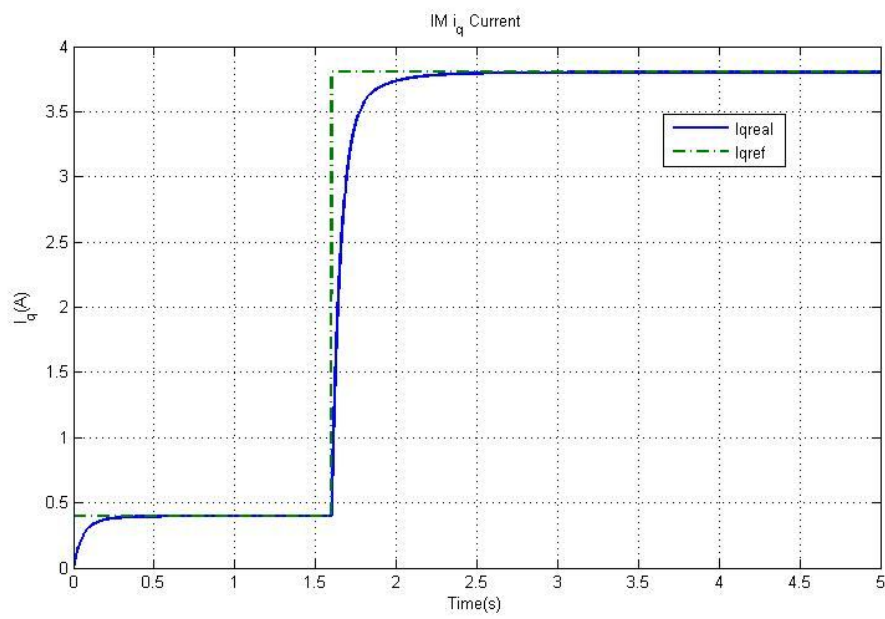
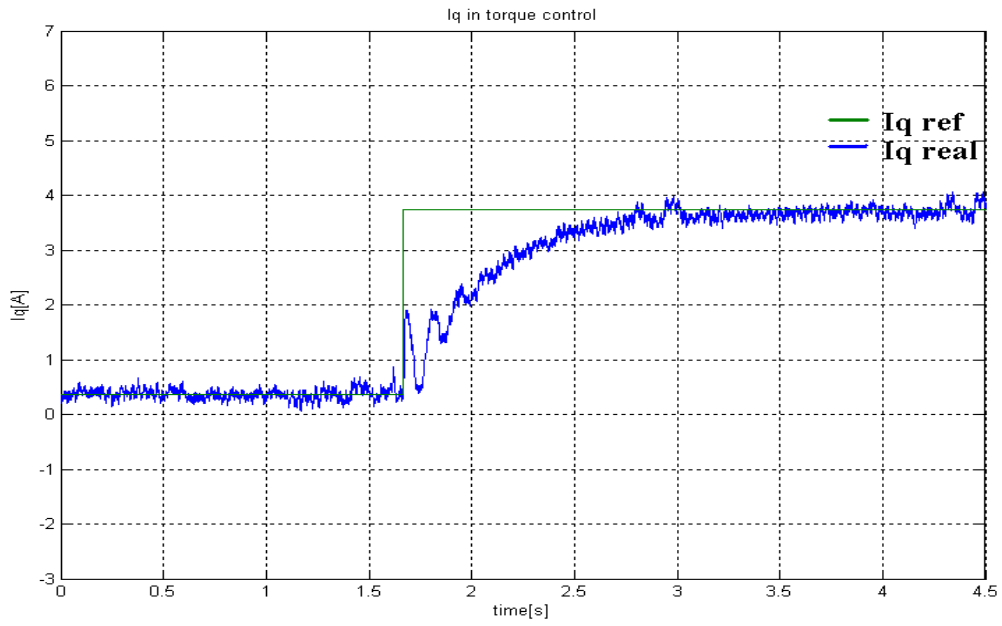


Fig 2.22 :Iq in Torque Control(a)Lab(b)Simulation

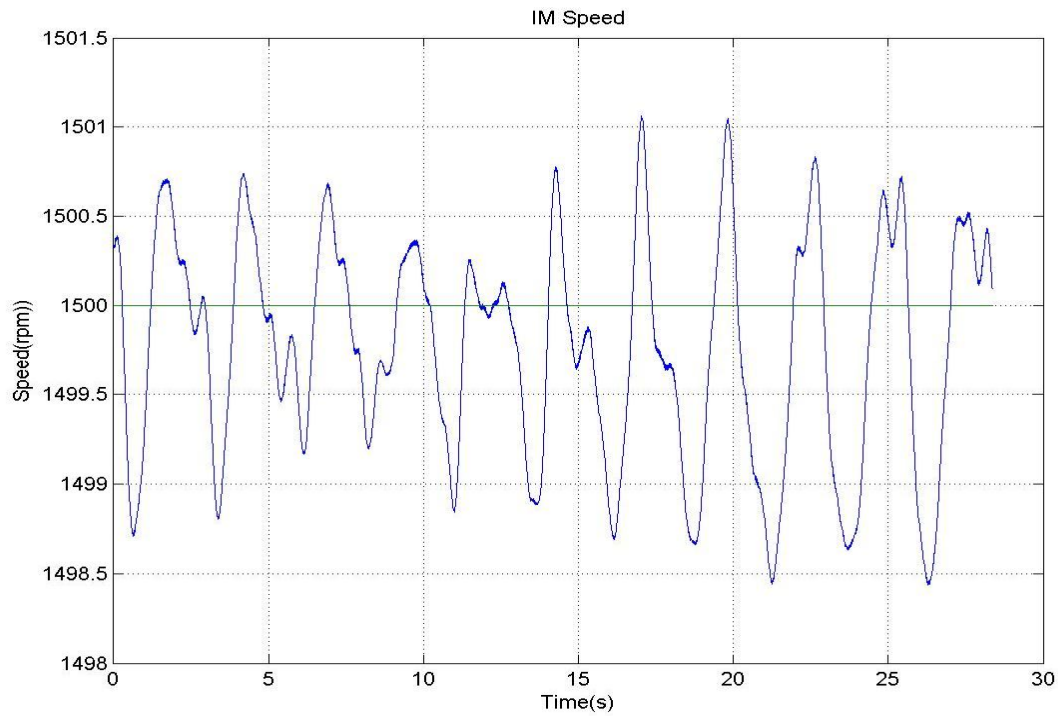


Fig 2.23:Ripple in Speed

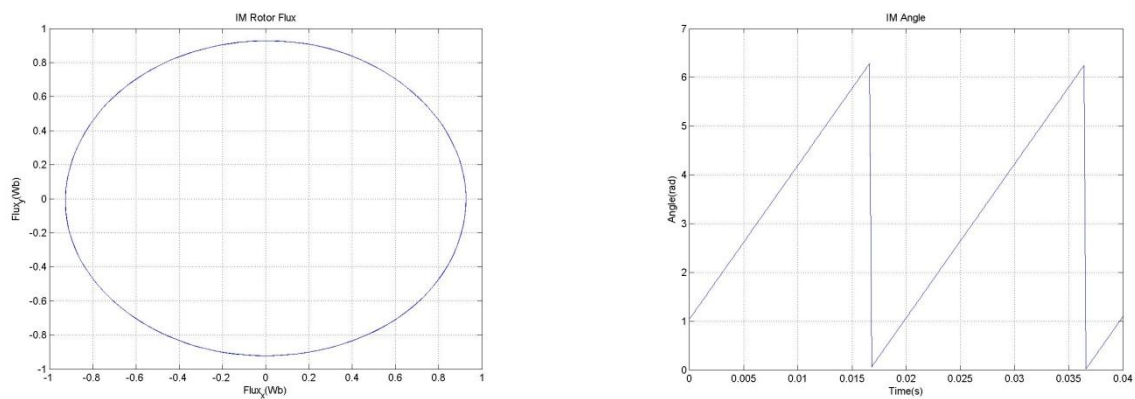


Fig 2.24:Flux and Phase angle

2.4 Summary

The mathematical model of the induction machine along with the indirect field oriented control was implemented in simulation. The control scheme was also realized in physical setup. Indirect field oriented control was discussed in details. The systematic method of tuning the PI controllers employed in the control was discussed. The results of the lab were validated by comparing to those produced from simulation.

3 Synchronous Generator: Theory and Control

This chapter discusses the theory and general behavior of the classical synchronous generators used in wind turbine application. A mathematical model of the generator is presented and implemented in simulation. It is compared with rated values of a 2.15 MW machine parameters. Exciters which form an integral part of the generator are discussed. Brushless exciter which is used in this project is implemented in simulation. The scheme used to control the reactive power is discussed in detail for various operation points. A short description of alternate solution to compensate reactive power is also presented. Laboratory results for the different operation points namely lead, lag and unity power factor are presented and discussed.

3.1 Synchronous Generator

A synchronous machine is one in which the average speed is directly proportional to the frequency of the electrical system to which it is connected. Three-phase synchronous generators are the primary source of all the electrical energy the society consumes.

The induction motor is the workhorse when it comes to converting electrical energy to mechanical energy; the synchronous machine is the principal means of converting energy from mechanical to electrical. [9]

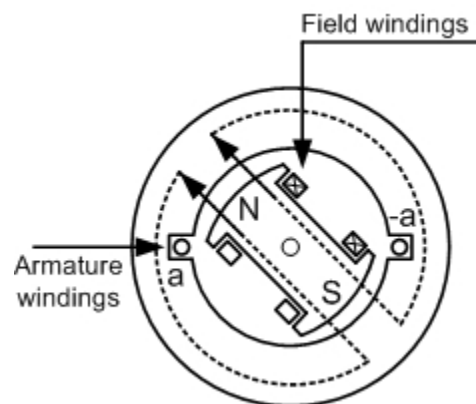


Fig 3.1: Simplified construction of a synchronous machine

3.1.1 Construction

The stator of a synchronous machine consists of a stack of laminated ferromagnetic core with internal slots, a set of three-phase distributed stator windings placed in the core slots. The turns of the stator windings are equally distributed over pole-pairs, and the phase axes are spaced $2\pi/3$ electrical radians apart. The cross sectional shape of the rotor can be salient or cylindrical. Salient pole construction is mainly used in hydro-generators to match the low speed of the hydraulic turbines, while the cylindrical one is used in steam generators.[9]

Direct current excitation to the field winding can be supplied through a pair of insulated slip rings mounted on the rotor shaft. The second excitation method dispenses of the slip rings and is called brushless excitation.

In the two pole representation of a synchronous machine, the axis of the north-pole is called the direct or the d-axis. The quadrature or the q-axis is 90 electrical degrees ahead of the direct axis. The excitation field will be along the d-axis, and the stator induced voltage E_f will be along the q-axis. The rotor may have additional windings. The salient-pole rotor machine has one or two damping windings, one on the d-axis and the other one on the q-axis. Damper windings in the equivalent machine model can be used to represent physical amortisseur winding. An idealized machine model of the synchronous machine is shown in Fig 3.2.

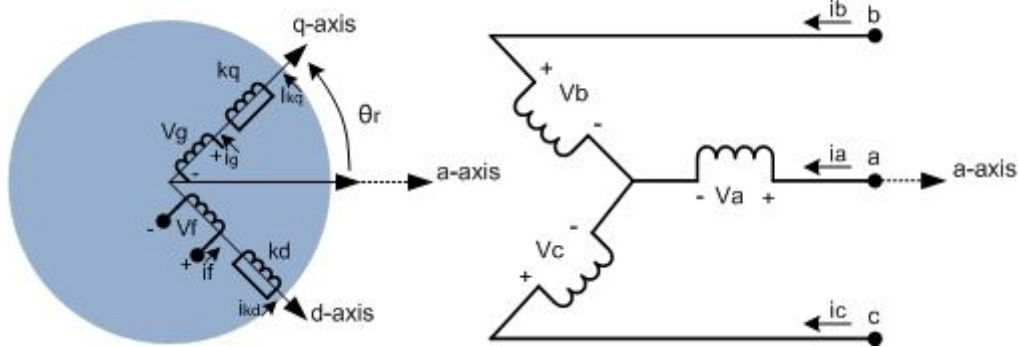


Fig 3.2: Circuit representation of an idealized machine

Behavior of the machine can be predicted with the 3-phase salient pole equations. Stator variables can be transformed to a reference frame fixed in the rotor frame (Parks' equations). However, they can still be transformed to an arbitrary reference frame. In this chapter, the voltage and electromagnetic torque equations are established. Equations which describe the steady state behavior are derived from Park's equations. The first analysis are valid for a linear magnetic system, therefore saturation is not taken into account.[9]

3.1.2 Mathematical model –natural reference frame

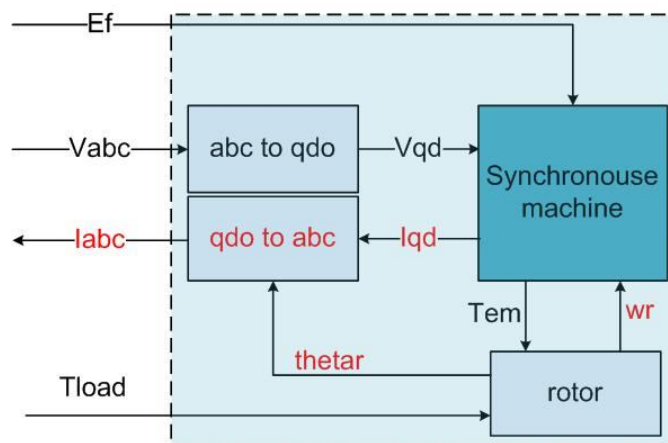


Fig 3.3: Block diagram of the SG modeling

Three phase voltages are the input along with excitation voltage referred to the stator and load torque. The model outputs currents, speed and electromagnetic torque.

The operating conditions of a synchronous machine can be subdivided into two basic categories:

1. Steady state operating conditions, where there are no changes in the kinetic energy of the system or, more accurately, where the changes in this energy are theoretically infinitely slow
2. Transient operating conditions, characterized by a periodic changes in the kinetic energy of the system during the post-fault process[10]

Hence the modeling of SG can be done to incorporate the desired characteristics. In this project two models are used – Voltage based and Flux based as seen below

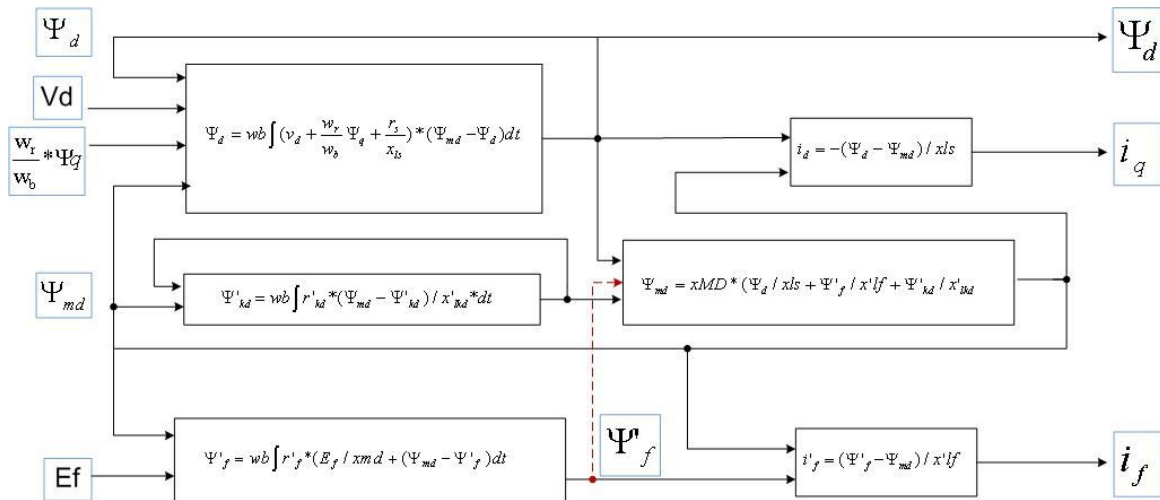


Fig 3.4: Block diagram of the d-axis SG modeling(Flux Based)

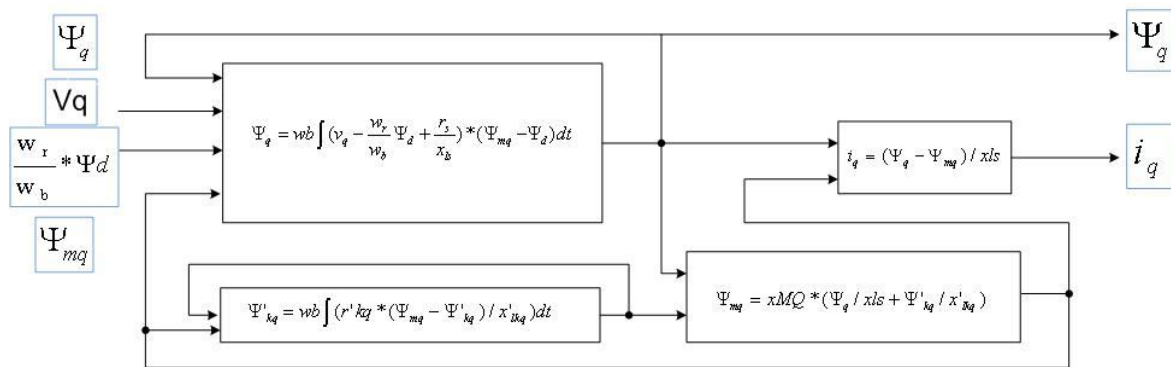


Fig 3.5: Block diagram of the q-axis SG modeling(Flux Based)

Transients arise from a sudden change in a control value (step change in load, voltage, frequency of the power supply, field excitation) are characterized by participation of the inertial masses in the transient process, by changes in the total kinetic energy. During sub transient time the damper winding limit the stator flux penetrating the rotor. The damper winding current start to decay, transient period starts. Changes in the field winding react the same, but slower. In steady state, stator induced flux penetrates stator and rotor. The voltage based model uses more machine parameters (reactance's and time constants). It is possible to see the voltage at the generator terminal before and after synchronization.

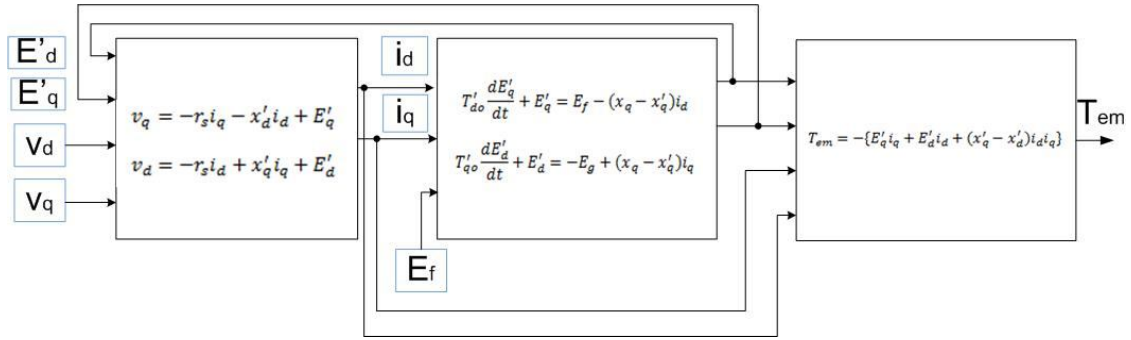


Fig 3.6: Block diagram of SG modeling(Voltage Based)

Using the sign conventions, the electrical equations are obtained by using Kirchhoff's voltage law for stator, rotor and excitation winding, by equating the voltage at the winding's terminal to the sum of resistive drop and $\frac{d}{dt}\Psi$ term. Damper windings are always short circuited. Their terminal voltage is zero. Therefore, the equations are arranged in the following form:

$$\begin{bmatrix} v_s \\ v_r \end{bmatrix} = \begin{bmatrix} r_s & 0 \\ 0 & r_r \end{bmatrix} \begin{bmatrix} i_s \\ i_r \end{bmatrix} + \frac{d}{dt} \begin{bmatrix} \Psi_s \\ \Psi_r \end{bmatrix} \quad 3.1$$

$$v_s = [v_a, v_b, v_c]^t \quad 3.2$$

$$v_r = [v_f, v_{kd}, v_g, v_{kq}]^t \quad 3.3$$

$$i_s = [i_a, i_b, i_c]^t \quad 3.4$$

$$i_r = [i_f, i_{kd}, i_g, i_{kq}]^t \quad 3.5$$

$$r_s = \text{diag}[r_a, r_b, r_c]^t \quad 3.6$$

$$r_r = \text{diag}[r_f, r_{kd}, r_g, r_{kq}]^t \quad 3.7$$

$$\Psi_s = [\Psi_a, \Psi_b, \Psi_c]^t \quad 3.8$$

$$\Psi_r = [\Psi_f, \Psi_{kd}, \Psi_g, \Psi_{kq}]^t \quad 3.9$$

Transformation to qd0 – rotating reference frame:

In natural reference frame, the total flux in a winding is dependent on the matrix of inductances. Being a salient pole machine, the matrix is dependent on the position of the rotor. This represents a big difficulty in modeling the machine. The solution is to change the reference from stationary abc to qd0 rotating with the rotor.

Direct transformations from stationary to rotating reference frame and inverse are given by the following matrices: [11]

$$T_{qd}(\theta_r) = \frac{2}{3} \begin{bmatrix} \cos\theta_r & \cos(\theta_r - \frac{2\pi}{3}) & \cos(\theta_r + \frac{2\pi}{3}) \\ \sin\theta_r & \sin(\theta_r - \frac{2\pi}{3}) & \sin(\theta_r + \frac{2\pi}{3}) \end{bmatrix} \quad 3.10$$

$$T_{qd}^{-1}(\theta_r) = \frac{2}{3} \begin{bmatrix} -\sin\theta_r & \cos\theta_r \\ -\sin(\theta_r - \frac{2\pi}{3}) & \cos(\theta_r - \frac{2\pi}{3}) \\ \sin(\theta_r + \frac{2\pi}{3}) & \cos(\theta_r + \frac{2\pi}{3}) \end{bmatrix} \quad 3.11$$

Where, θ from is 3.12 calculated :

$$\theta_r(t) = \int_0^t \omega(t) dt + \theta_0 \quad 3.12$$

and ω is the electrical speed of the rotor.

Hence any three set of variables in abc reference frame expressed in a $qd0$ rotating frame and it's inverse with the help of the matrices:

$$\begin{bmatrix} f_q \\ f_d \end{bmatrix} = T_{qd} \begin{bmatrix} f_a \\ f_b \\ f_c \end{bmatrix} \quad 3.13$$

$$\begin{bmatrix} f_a \\ f_b \\ f_c \end{bmatrix} = T_{qd}^{-1} \begin{bmatrix} f_q \\ f_d \end{bmatrix} \quad 3.14$$

The equivalent circuit representation of the SG based on the above voltage and flux equations is shown in Fig 3.7. All rotor parameters are referred to the stator. During the simulation, if actual values of the rotor are known, then the turn ratio between stator and rotor has to be known.[11]

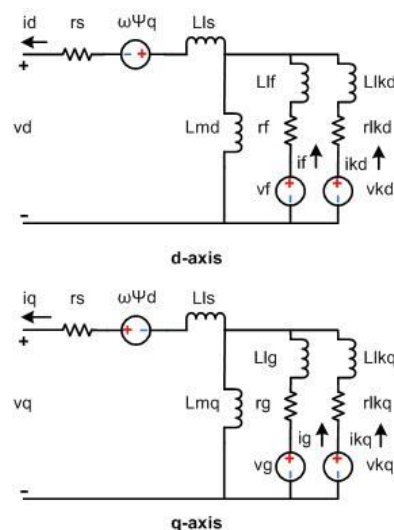


Fig 3.7: Equivalent $qd0$ circuit

The voltage equations in the rotor's $qd0$ reference frame with rotor quantities referred to the stator are given below for a synchronous generator:

$$-v_d = r_s i_d - \Psi_q \omega_r + \frac{d}{dt} \Psi_d \quad 3.15$$

$$-v_q = r_s i_q + \Psi_d \omega_r + \frac{d}{dt} \Psi_q \quad 3.16$$

$$v_f = r_f i_f + \frac{d}{dt} \Psi_f \quad 3.17$$

$$v_g = r_g i_g + \frac{d}{dt} \Psi_g \quad 3.18$$

$$v_{kd} = r_{kd} i_{kd} + \frac{d}{dt} \Psi_{kd} \quad 3.19$$

$$v_{kq} = r_{kq} i_{kq} + \frac{d}{dt} \Psi_{kq} \quad 3.20$$

$$-v_d = r_s i_d + \Psi_q \omega_r + \frac{d}{dt} \Psi_d \quad 3.21$$

The armature windings are magnetically coupled because of cross-coupling terms in d and q axis equations. The terms represent speed voltages, the product between rotor speed and flux linkage of the other axis.

Flux linkage equations for every winding are shown below:

$$\Psi_d = L_d i_d + L_{md} i_f + L_{md} i_{kd} \quad 3.22$$

$$\Psi_q = L_q i_q + L_{mq} i_g + L_{mq} i_{kq} \quad 3.23$$

$$\Psi_f = (L_{md} + L_f) i_f + L_{md} i_{kd} - L_{md} i_d \quad 3.24$$

$$\Psi_g = (L_{mg} + L_g) i_g + L_{mg} i_{kg} - L_{mg} i_q \quad 3.25$$

$$\Psi_{kd} = L_{md} i_f + (L_{kd} + L_{md}) i_{kd} - L_{md} i_d \quad 3.26$$

$$\Psi_{kq} = (L_{kq} + L_{mq}) i_{kq} - L_{mq} i_q \quad 3.27$$

$$\Psi_{mq} = L_{mq} (i_q + i_g + i_{kq}) \quad 3.28$$

$$\Psi_{md} = L_{md} (i_d + i_f + i_{kd}) \quad 3.29$$

To complete the model of the generator, the mechanical equation is needed. The equation relates the load torque to the electromagnetic torque. Electromagnetic torque is obtained from the input power that is transferred through the air-gap. When referred to rotor reference frame, power is:

$$P_{em} = \frac{3}{2} \omega_r (\Psi_d i_q - \Psi_q i_d) \quad 3.30$$

$$P_{em} = \frac{3}{2} \frac{P}{2} \omega_{rm} (\Psi_d i_q - \Psi_q i_d) \quad 3.31$$

$$T_{em} = \frac{3}{2} (\Psi_d i_q - \Psi_q i_d) \quad 3.32$$

Expression of electromagnetic torque is in 3.32. The currents in terms of flux linkages are expressed as:

$$i_q = \frac{1}{L_{ls}} (\Psi_q - \Psi_{mq}) \quad 3.33$$

$$i_d = \frac{1}{L_{ls}} (\Psi_d - \Psi_{md}) \quad 3.34$$

$$i_g = \frac{1}{L_{lg}} (\Psi_g - \Psi_{mq}) \quad 3.35$$

$$i_f = \frac{1}{L_{lf}} (\Psi_f - \Psi_{md}) \quad 3.36$$

$$i_{kq} = \frac{1}{L_{lkq}} (\Psi_{kq} - \Psi_{mq}) \quad 3.37$$

$$i_{kd} = \frac{1}{L_{lkd}} (\Psi_{kd} - \Psi_{md}) \quad 3.38$$

3.1.3 Simulation and Validation

The model is validated for a 2.125 MW (parameters in APPENDIX B) machine. The values of the outputs are normalized to the P.U system (See Appendix H).

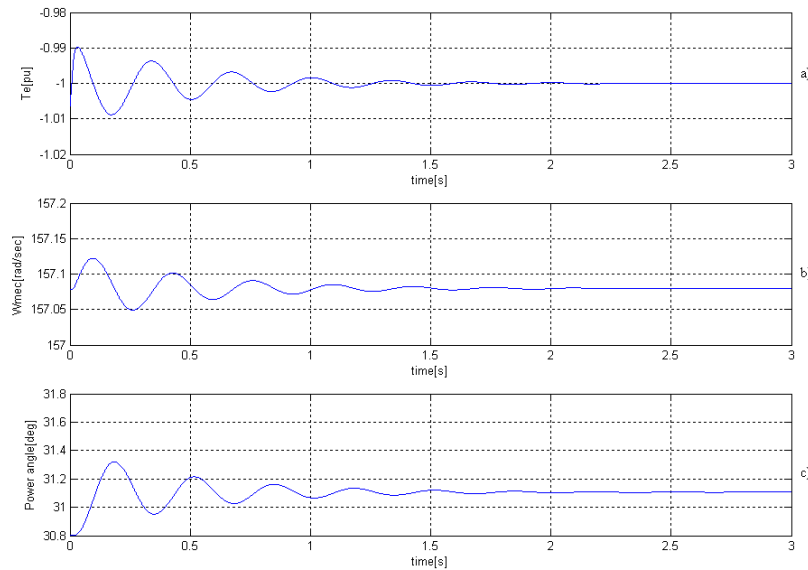


Fig 3.8: T_e (Electromagnetic torque in pu), W_{mec} (mechanical speed) and power angle (angle between the induced voltage and grid voltage)

As per the sign convention the electromagnetic torque produced by the machine is negative to signify generator operation as seen in Fig 3.8. Small decaying transients are seen in the torque waveform. Damping windings (R_{pkd} -dampers resistance, L_{pkd} -damper inductance) influence the peak of the transients and the time to reach steady state. The model is tested for steady state operation hence the initial condition of the rotor speed was set to around 157 rad/sec(2 –pole pairs/50hz)

assuming the SG is grid connected at start of operation. The use of initial conditions results in reduction of high transients which would appear until the system has reached steady state.

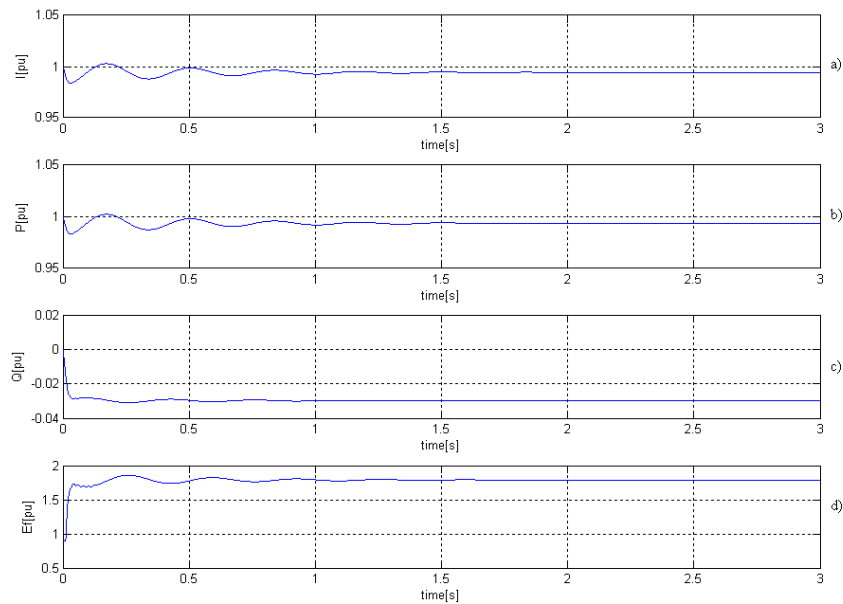


Fig 3.9: Current I [pu], Active power P [pu], Reactive power Q [pu] and Induced voltage E_f [pu]. Note all quantities referred to the stator side.

Comparing Fig 3.8 and Fig 3.9 it is seen that current is proportional to the torque developed in the machine and also the active power output of the machine. As per sign convention power delivered to the grid is positive and power consumed is negative. In case of reactive the sign convention holds good. Hence when consuming power the grid is seen as a capacitor and when injecting reactive power the grid is seen as an inductor. At nominal operation at steady state the reactive power in the system is kept close to zero. Fig 3.9 shows that $\frac{Q(\text{reactive power})}{S(\text{apparent power})} = 1.02\%$, ie reactive power is only a small amount of total power conversion in the system. Hence the active power conversion efficiency is very high.

3.1.4 Lab Implementation

The machine is tested in island mode by dissipating the power on a variable resistive load as shown in Fig 3.10. It ascertains the generator's ability to supply a load of up to 5kW. It demonstrates the ability of the safety contactors.

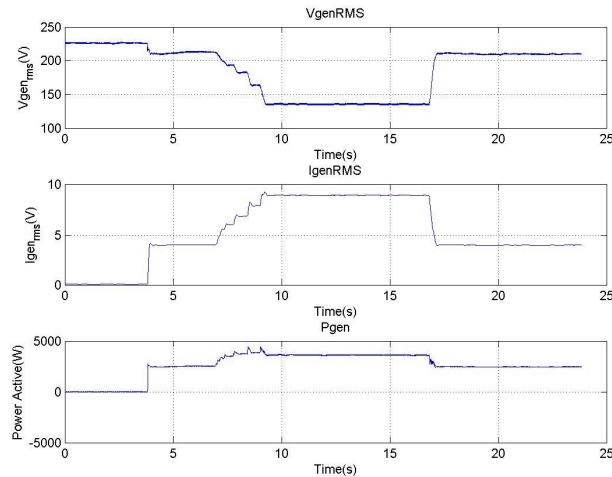


Fig 3.10: (a)Voltage (b)Current (c)Active Power

3.2 Exciters

Another important component of the synchronous machine is the excitation system. There are three types of exciters, each with numerous adaptations in the industry:

3.2.1 DC Exciters (Brushed):

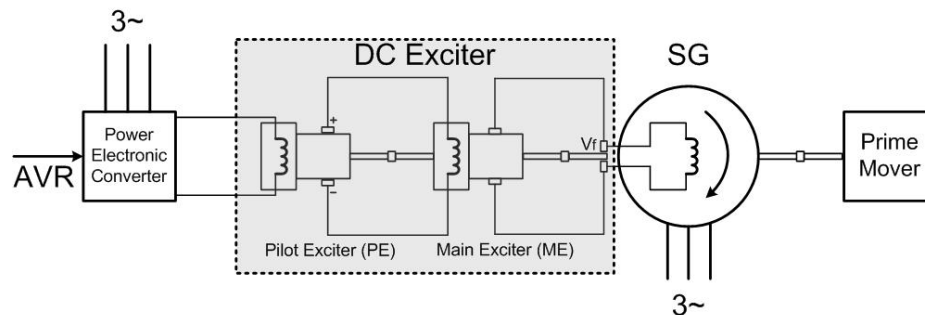


Fig 3.11: D.C. Exciter

The dc field excitation of a generator is an important part of its design. This is because the field must ensure a stable ac terminal voltage and also respond to sudden load changes in order to maintain system stability.

In order to attain it, two dc generators are used: main exciter and a pilot exciter. Both are placed on the SG main shaft. The ME supplies the SG field winding (V_f), by way of brushes and slip-rings, while the PE supplies the ME field winding.

Under normal conditions the exciter voltage lies between 125 V and 600 V. It is regulated manually or automatically by control signals that vary the I_c current, produced by the pilot exciter. The power electronic source required to supply the PE field winding is of very low power ratings. The two DC generators supply a total power amplification around 600/1. Typically, a 25 kW exciter is needed to excite a 1000 kVA generator (2.5% of its rating) whereas a 2500 kW suffices for an alternator of 500 MW (0.5% of its rating).

Under normal conditions the excitation is varied automatically by an AVR. It responds to the load changes so to maintain a constant ac line voltage or to control the reactive power delivered to the electric utility system. A serious disturbance on the system may produce a sudden voltage drop across the terminals of the alternator. The exciter must then react very quickly to keep the ac voltage from falling. For example, the exciter voltage may have to rise to twice the nominal value in as little as 300 to 400 milliseconds. [4]

A low power electronics external supply for the exciter is considered an advantage. The following are considered drawbacks:

- Slow time response due to the large field winding time constants of the two excitation circuits plus the time constants of the two armature windings
- Problems with brush wearing
- Transmission of all excitation power (up to 5% of rated SG power) of the SG has to be through the slip-ring brush mechanism
- Flexibility of the exciter shafts and mechanical couplings adds at least one additional shaft torsion frequency for the turbine-generator shaft.[12]

3.2.2 AC Exciters (Brushless):

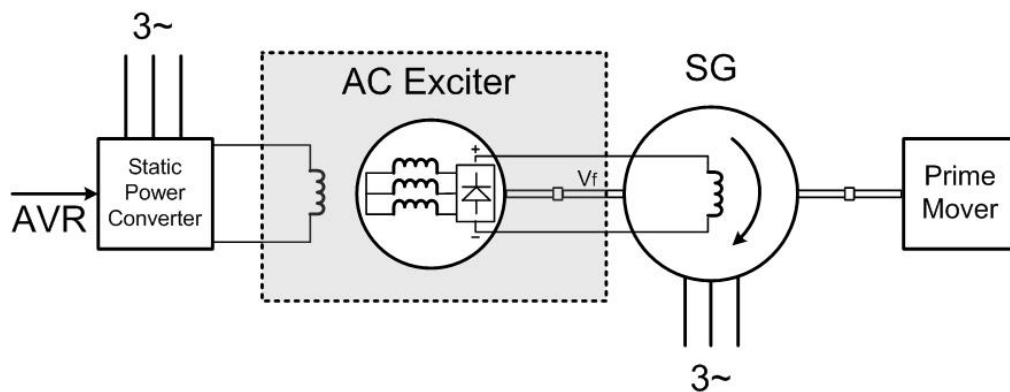


Fig 3.12: A.C. Exciter

Maintenance and operation cost of brushed exciter are high due to brush wear and carbon dust which require cleaning, repairing and replacement of brushes/slip rings and commutators on conventional dc excitation systems. In order to eliminate this problem, *brushless excitation systems have been developed.*

AC exciters are basically 3 phase inside-out synchronous generators, consisting of a rotating armature and stationary field. The output is rectified by solid-state rectifier elements mounted on the rotating structure and fed directly to the machine's field winding.

So, compared with the dc exciter, the 3 phase rectifier replaces the commutator, slip-rings, and brushes. In other word, the commutator (mechanical rectifier) is replaced by an electronic rectifier. Hence the brushes and slip-rings are no longer needed.

The stator-based field winding of the AC exciter is controlled from the AVR. The static power converter now has a rating about 1/20(30)of the SG excitation winding power ratings, as only one step of power amplification is performed through the AC exciter.

Thus, the AC exciter is characterized by the following:

- Absence of electric brushes in the exciter and in the SG
- Addition of a single machine on the main SG-turbine shaft
- Moderate time response in V_f (SG field winding voltage), as only one (transient) time constant (T_{d0}) (SEE APPENDIX F) delays the response; the static power converter delay is small in comparison
- Addition of one torsion shaft frequency due to the flexibility of the AC exciter machine shaft and mechanical coupling
- Small controlled power in the static power converter (1/20[30] of the field-winding power rating) [12]

3.2.3 Static Exciters (Brushed):

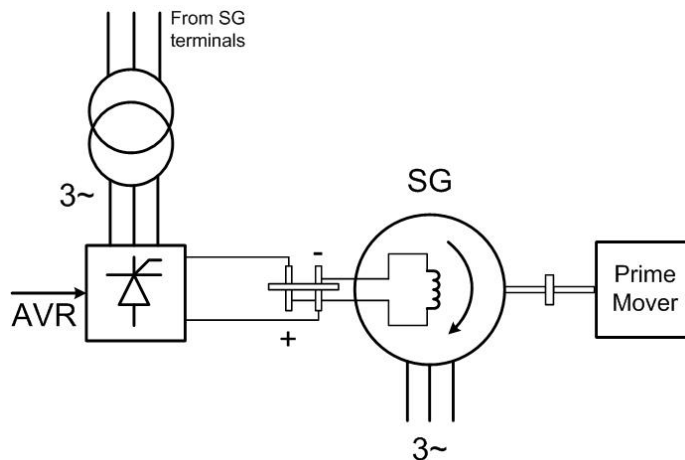


Fig 3.13: Static Exciter

These types of exciters are controlled rectifiers directly supplying the field winding of the SG through slip-rings and brushes. The controlled rectifier is supplied from a combined voltage transformer and current transformer connected in parallel and in series with the SG stator windings. Static power electronics exciters are characterized by fast voltage response, but still the T_{d0} time constant of the SG delays the field current response.

3.2.4 Brushless exciter modeling

Usually the rotor in a SG is directly supplied with DC voltage through brushes. Wind turbine synchronous generators are subjects of weather conditions and if they have brushes or slip rings they are severely influenced. Alternative solutions such as brushless exciters were developed, which is basically an inverted synchronous machine with a rectifier. The inverted synchronous machine has a fixed winding and rotating windings, where AC current is generated if field winding is excited. The current is after rectified and fed to the rotating rectifier. [13]

Since the exciter is in fact a synchronous machine with rectifier, the same principles can be applied when modeling it. The following assumption are made while modeling the brushless exciter

1. Damper windings are neglected [13]
2. Commutation in rectifier is simple, no more than 3 diodes conduct in the same time.

Also the exciter is modeled in p.u. and parameters of the brushless exciter gathered from different manufacturers. Simulation is not checked with laboratory machine as the rotor is physically inaccessible.

Brushless exciter can be seen as linear current transformers. According to manufacturers, they will not operate in saturated conditions. The ripple of the rectified current is reduced if the exciter machine has considerably more poles than the main machine.

The exciter machine model equations are:

$$V_d = R_a i_d + \frac{d\Psi_d}{dt} + p\omega\Psi_q \tag{3.39}$$

$$V_q = R_a i_q + \frac{d\Psi_q}{dt} - p\omega\Psi_d \tag{3.40}$$

$$V_f = R_f i_f + \frac{d\Psi_f}{dt} \tag{3.41}$$

$$\Psi_d = L_d i_d + L_{md} i_f \tag{3.42}$$

$$\Psi_q = L_q i_q + L_{mq} i_f \tag{3.43}$$

$$\Psi_f = (L_{md} + L'_f) i_f - L_{md} i_d \tag{3.44}$$

Models for the direct and quadrature axis of the exciter are shown in figure below:

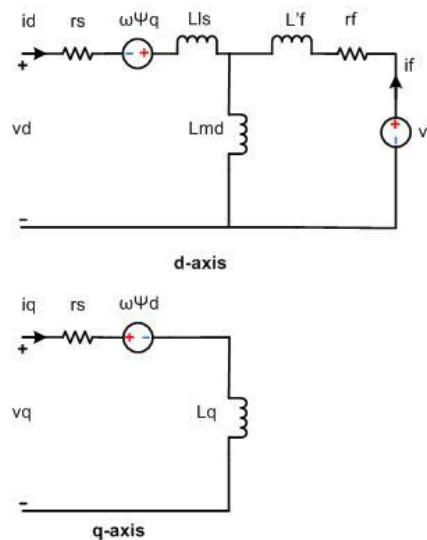


Fig 3.14:Equivalent circuit of SG without damper windings

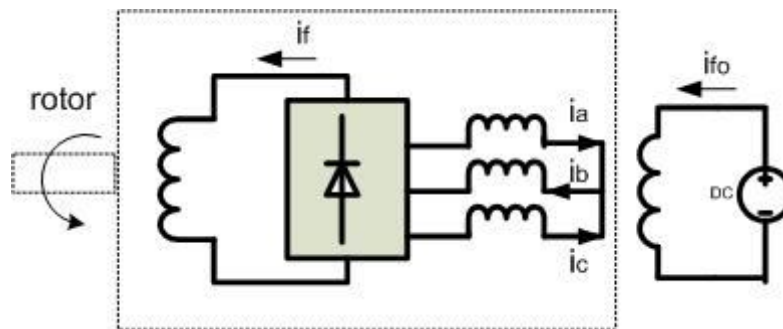


Fig 3.15:Simplified circuit of brushless exciter

The design of the exciter is based on IEEE standards 421. The main factors in deciding the exciter are:

1. *Transient gain*: Influences small signal and dynamic stability. Small values fail to give desired performance, too high values produce faster response but give dynamic instability during faults.

2. *Ceiling voltage*: Usually set to 160 to 200 percent of rated field voltage to preserve stability after the clearance of a three phase fault on the higher voltage side of the SG set up transformer. Lower values translate to better efficiencies, increasing it may result in better transient stability. Practical limits of ceiling voltage are about $500 V_{dc}$.

Exciters are usually designed for frequencies in the range of 180 to 450 Hz to cut the rectified output voltage pulsations. They also have a large number of poles. Voltage regulation of the diode rectifier in SG excitation circuit is neglected.

The AC exciter rating is given by nominal voltage and current for steady state, and maximum voltage and current for transients.

The voltage response time (VRT) is the time in seconds for the excitation voltage to travel 95% of the difference between maximum and nominal voltage.[12]

If a reduced voltage time response is needed, this will lead to severe limitations in the AC exciter sub transient reactance. Star connection of AC exciter armature phases is preferred in order to reduce the third harmonic current.

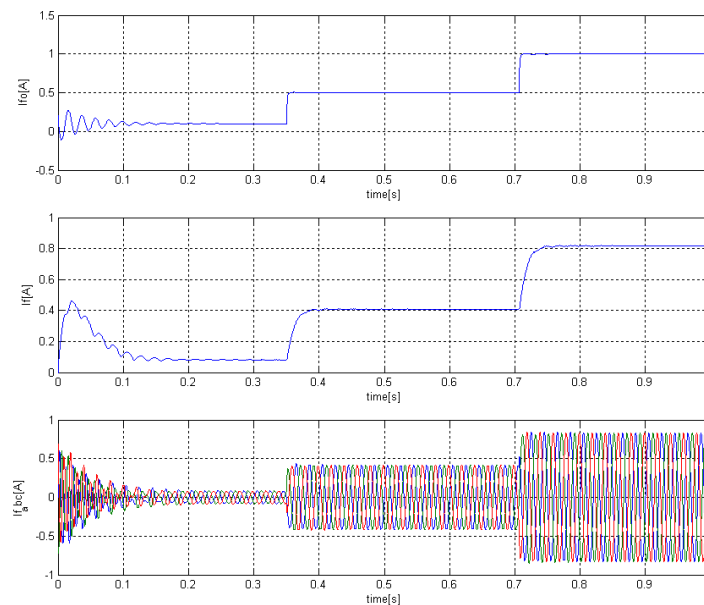


Fig 3.16: Current waveforms at each stage of the exciter

Fig 3.16(a) shows the input current from the DC source. The response on the AC side is however slower as seen in Fig 3.16(b) this affects the response time of the reactive power controller. A drawback of using solid-state diode rectifiers is the voltage must naturally decay when the reference is stepped down.

3.3 Synchronous Generator: Control

The operation of (AC) power systems is evaluated based on its response when subjected to variations in active and reactive load. It is desirable to have nearly constant or limited variations in frequency and voltage during steady state.

Active power flow is related to a prime mover's energy input and, thus, to the speed of the synchronous generator (SG). On the other hand, reactive power control is related to terminal voltage. Large active power load would lead to collapse in speed, while large reactive power loads cause voltage to collapse.[12]

The project requires control of synchronous machine under different scenario namely

1. Synchronization Control
This control is implemented on SG, at no-load, to achieve synchronization with the grid.
2. Reactive Power Control
This control is implemented when the SG is directly connected to the grid (load).
 - i. to maintain unity power factor under steady state operation
 - ii. to fulfill reactive power requirements of the grid during low-voltage grid faults

3.3.1 Synchronization Control

The synchronization of the SG is based on the following criteria

1. Voltage level (amplitude) of generation should match the voltage level of the external network.
2. Frequency of generation should match the frequency of the external network.
3. The point of cycle (or phase angle) for each phase of generation should equal the point of cycle for each corresponding phase of the external network. [14]

The synchronization scheme is implemented as a two step process where the amplitude of the output voltage in open-circuit is controller via excitation circuit and the frequency/phase is controlled through PI, which regulates the speed of the prime mover to match with the network.

$$\frac{d\theta_r}{dt} = \omega_r \quad 3.45$$

Using difference
$$\frac{\Delta\omega_r(s)}{\Delta\theta_r(s)} = s \quad 3.46$$

The PI structure is shown in Fig 3.17. The plant is expressed in Eqn 3.46.

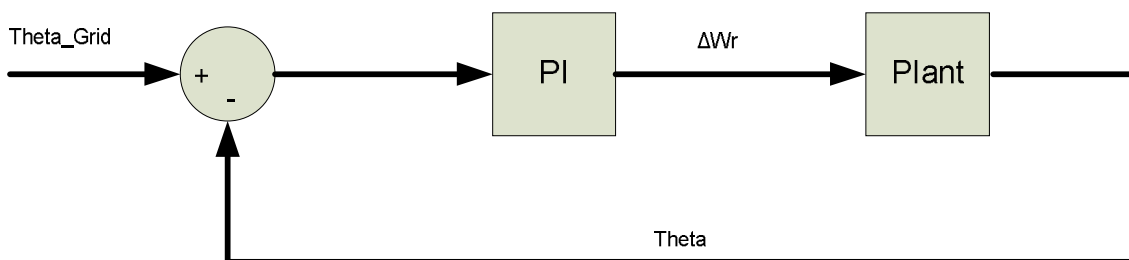


Fig 3.17: Synchronization controller

The synchronization controller outputs the speed correction that is needed to synchronize with the grid angle. Fig 3.18 shows the grid and generator angle pre- and post-synchronization. A phase difference of 18[deg] is seen in Fig 3.18(b). Experimentally this is proved to be satisfactory for synchronization. This can be justified from the fact that synchronization is semi-automatic in nature. However for automatic control would operate at a smaller error tolerance.

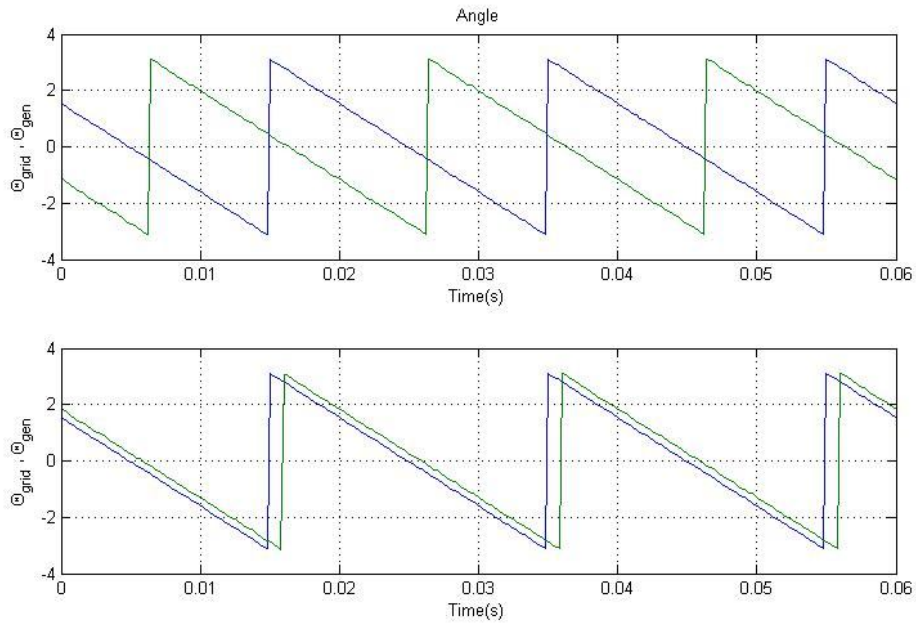


Fig 3.18: Grid and generator phase angles(a) before synchronization (b) after synchronization

The voltages to validate the synchronization controller are shown in Fig 3.19(a) and Fig 3.20. The corresponding phases are color coded/matched. It can be noted that the generator voltages represent as dotted line is not purely sinusoidal because of the non-sinusoidal windings in the machine. This is acceptable for synchronization as the error is below the tolerance limit of 5%. Fig 3.20 shows that the phase difference when synchronized is about 0.001[s] which translates to 18[deg]. This is the power angle for the power transfer.

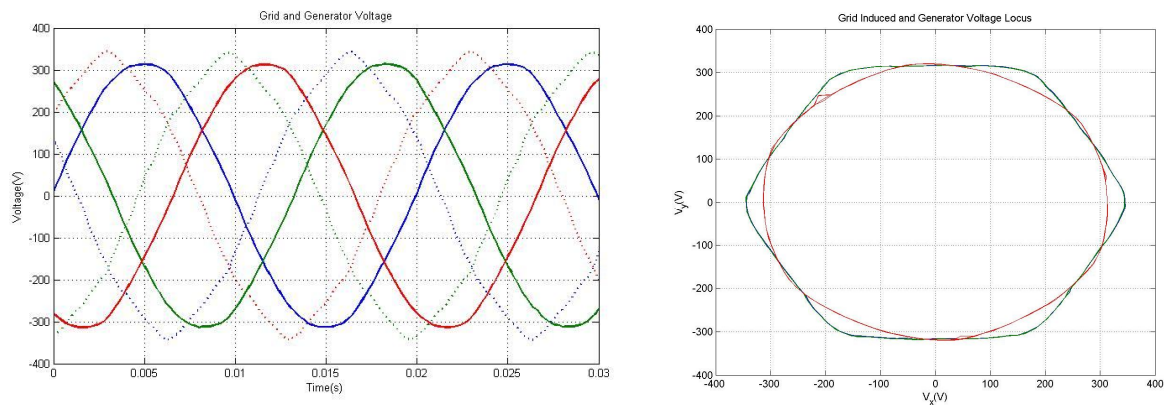


Fig 3.19(a)Grid and generator voltage before synchronization(b)Locus of the induced and grid voltage

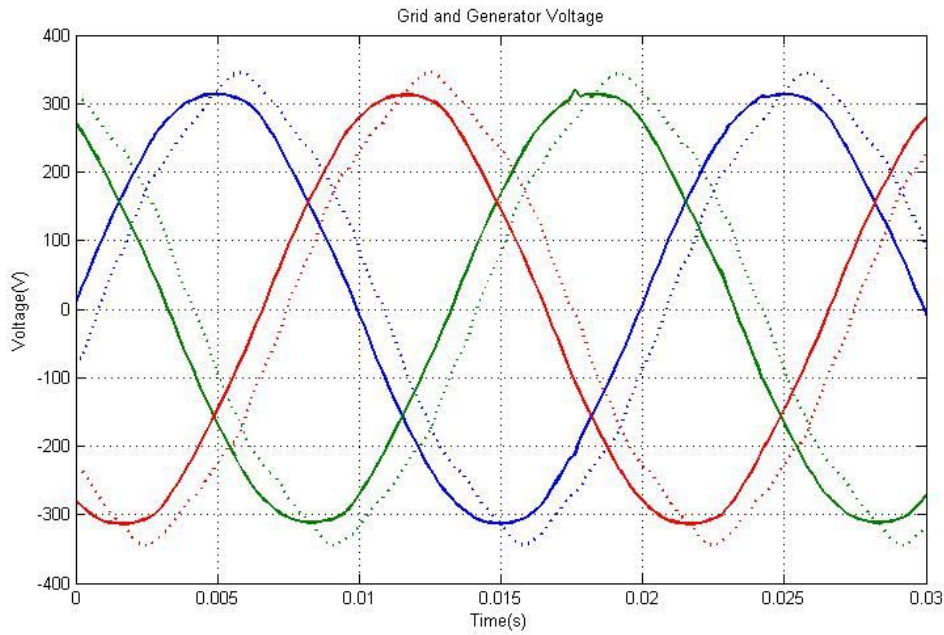


Fig 3.20: Grid and generator voltage after synchronization

3.3.2 Reactive Power Control

This section presents the theory behind the reactive power control of the synchronous machine. Fig 3.21 is relevant because it is encountered in the study of generators, synchronous motors and transmission lines. Applying Kirchhoff's voltage law to this circuit:

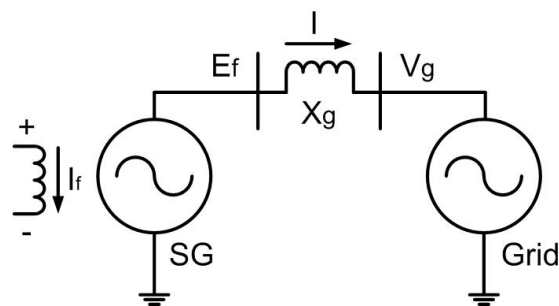


Fig 3.21: Simplified power flow for generator to grid connection

$$E_f = V_g + jIX \quad 3.47$$

From Fig 3.22 it can be seen that, assuming current (I) lags grid voltage (V_g) with an angle θ and induced voltage (E_f) leads V_g by a power angle (δ). Phasor (IX) leads (I) by 90° . The active power transferred is:

$$P = V_g I \cos \theta \quad 3.48$$

$$\frac{IX}{\sin \delta} = \frac{E_f}{\sin \Psi} \quad 3.49$$

$$= \frac{E_f}{\sin(90^\circ + \theta)} \quad 3.50$$

$$= \frac{E_f}{\cos\theta} \quad 3.51$$

$$P = \frac{E_f V_g}{X} \sin\delta \quad 3.52$$

The magnitude of P is determined by the phase angle between E_f and V_g . The active power always flows from the leading to the lagging voltage. [4]

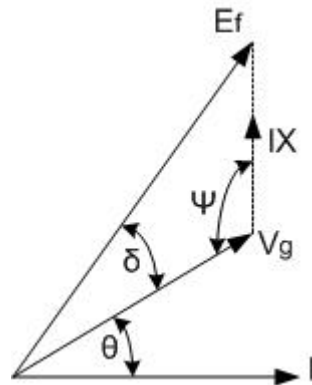


Fig 3.22: Phasor diagram of grid connected SG.

The reactive power flow of an SG can be controlled through output voltage which is performed through excitation (current or voltage) control. The quality of voltage control quality depends on the machine parameters and excitation power source dynamics. The knowledge of load reactive power dependency on voltage is essential to voltage control system design. [12]

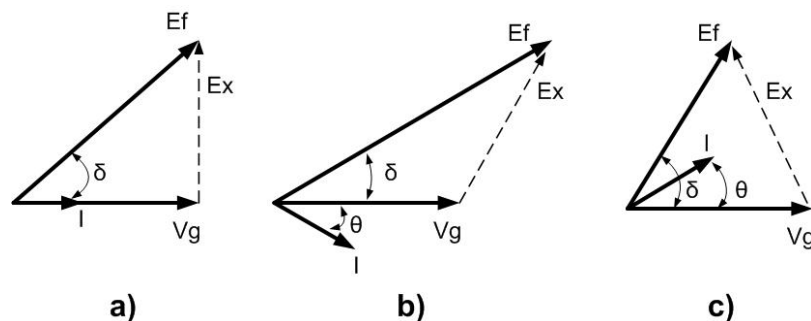


Fig 3.23: Phasor diagram of operation regions of grid connected generator

In Fig 3.23 the various operating region of the SG are shown assuming that the machine is connected to an infinite bus. Hence V_g is constant and only the response of the current to varying excitation is shown. By rule of thumb lagging power factor supplies reactive power to the grid and leading power factor consumes reactive power. A simple induction generator, with no additional capacitors attached, will during normal operation consume reactive power. This reactive power has to be produced somewhere in the grid. It is preferred that the wind farm power station is reactive power neutral, since the distribution of reactive power is relatively cost intensive [15]

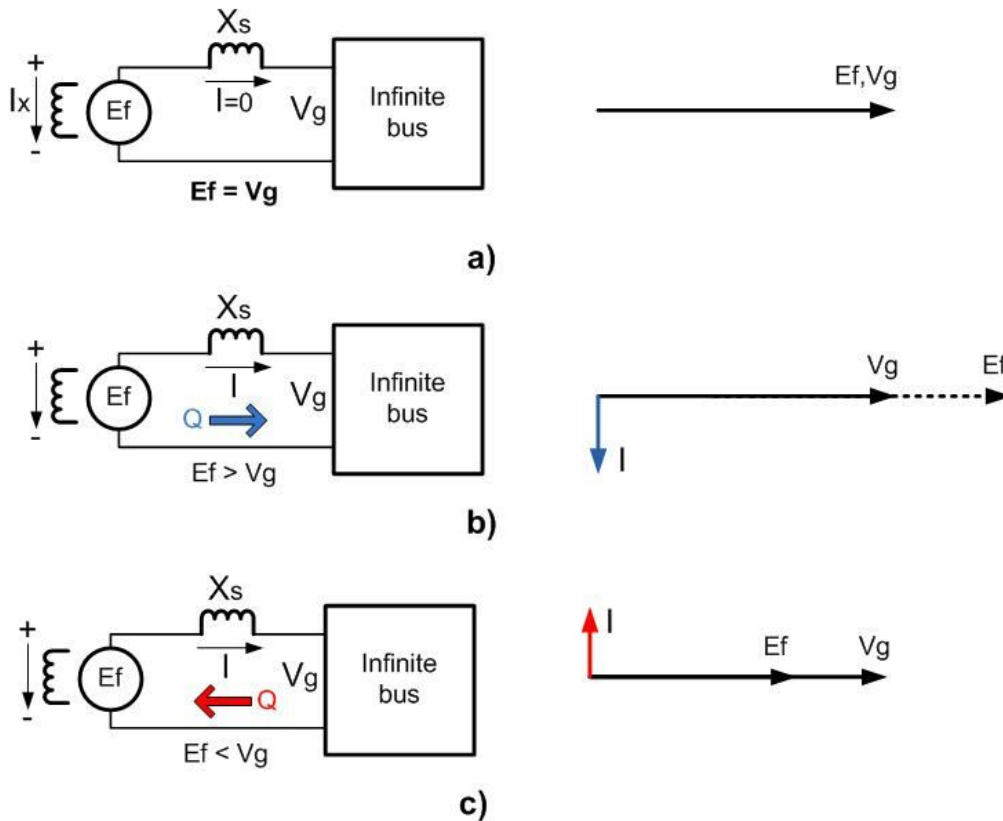


Fig 3.24: Power flow for grid connected generator

Immediately after the synchronization of the SG to the grid, the induced voltage E_f is equal and in phase with the terminal voltage V_g of the system. There is no difference of potential across the synchronous reactance and, the load current I , is zero. The generator delivers no power.

If the excitation voltage is increased, the induced voltage E_f will increase and voltage drop will occur across X_s , and a current I will flow as seen in Eqn 3.54.

$$E_x = E_f - V_g \quad 3.53$$

$$I = (E_f - V_g) / X_s \quad 3.54$$

The current will lag the voltage with 90° , due to the inductive reactance. Therefore, the generator sees the grid as an inductive load. So, at over-excitation of the SG, reactive power is supplied to the infinite bus. A decrease of excitation current will lead to a decrease of E_f . As a result, E_x becomes negative. Therefore, I leads V_g , which means the generator sees the systems as a capacitor. Under excitation of the SG will lead to a draw of reactive power from the grid.

If the induced voltage E_f is again equal and in phase with V_g , and the prime movers increases the mechanical torque, then the rotor will accelerate. Therefore, E_f will slip ahead of the phasor V_g , leading it by an angle δ . Even it the same voltages have the some amplitude, the phase difference will create a potential difference across X_s . A current I will start to flow (lagging 90° behind E_f). The generator starts to give active power to the grid. This is illustrated in Fig 3.25.

In order to achieve unity power factor of the SG it is worthwhile to understand the behavior of the machine under various permutations of field excitation and input power. In this section the response of SG under constant power-varying excitation and constant excitation-varying power are discussed.

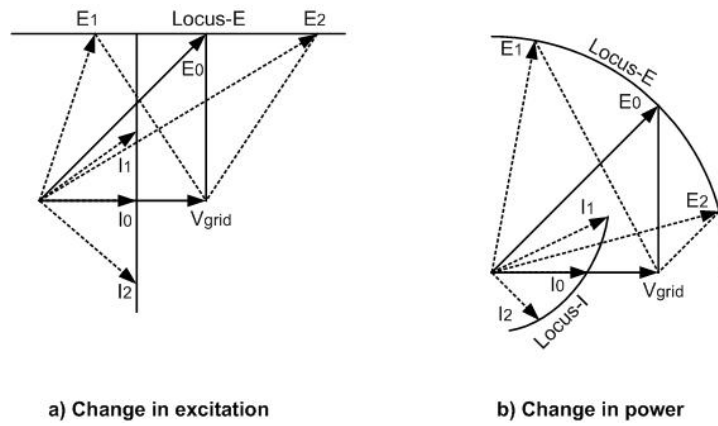


Fig 3.25: Locus of induced voltage E_f under varying conditions

Fig 3.25(a) shows the locus of E_f for constant power input under lead, lag and unity power factor

3.3.2.1 Case I: Constant power-Varying excitation

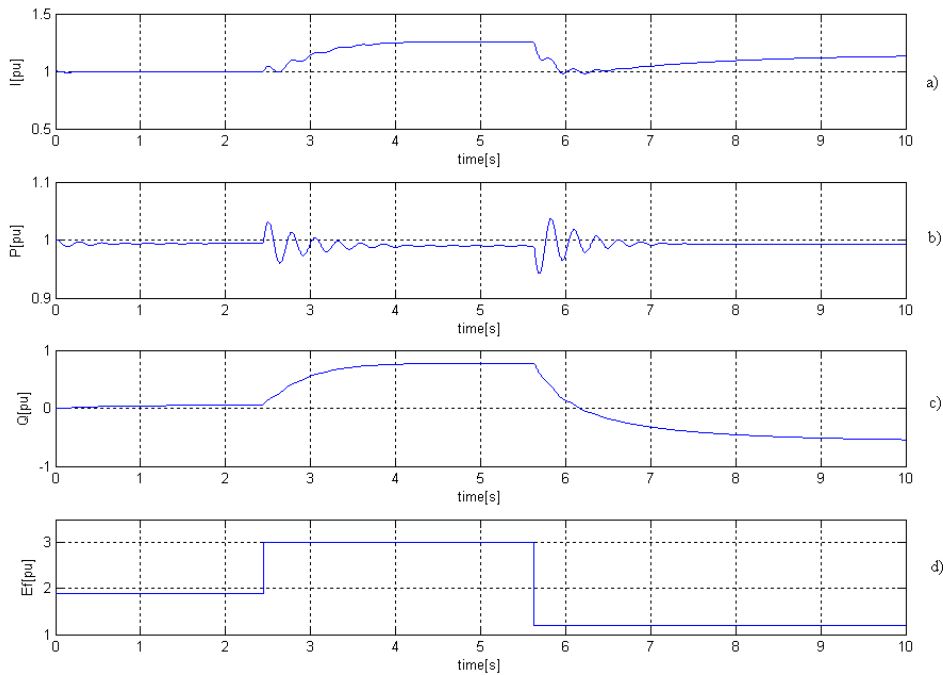


Fig 3.26: Current and Power characteristics under constant power operation with variation in induced voltage.

Fig 3.26 and Fig 3.27 exemplify the behavior during a constant power-varying excitation operation.

The excitation is varied at $t=2.5$ as seen in Fig 3.26 E_f is increased to 3[p.u.] from nominal value of 1.98 [p.u.].(see Appendix H) This translates to over-excitation of the SG. In confirmation with the theory presented in the preceding section, the reactive power (seen in Fig 3.26) is positive (power injected into the grid) and power angle is decreased to 22° (see Fig 3.27) because a stronger field is setup in the stator winding and the induced voltage slips less compared nominal operation.

Conversely at $t=5.6$, E_f is reduced to 1.3 p.u. Therefore, SG is under-excited, consuming reactive power as expected and working with a power angle of 42° . (see Fig 3.27). Since the input power is constant the torque developed in the machine is constant as seen in Fig 3.27 except during the step in induced voltage where transients are observed due to change in power angle. Speed perturbations are also observed during step change in excitation voltage.

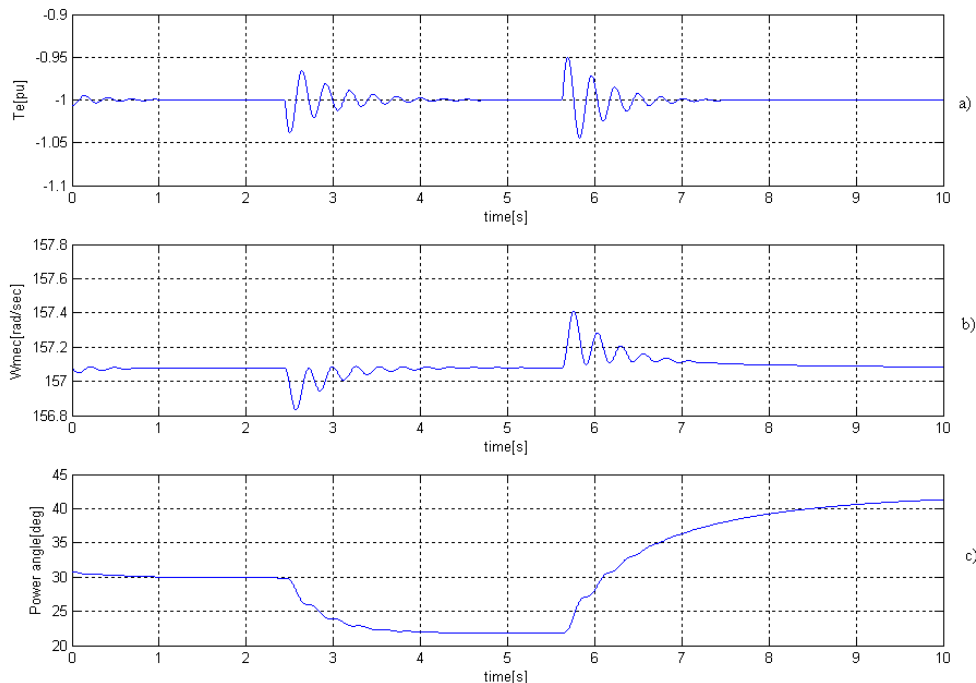


Fig 3.27: Torque ,Speed and Power angle characteristics under constant power operation.

Fig 3.25(b) shows the locus of E_f for constant excitation under lead, lag and unity power factor.

3.3.2.2 Case II: Constant excitation-Varying power

In Fig 3.28 T_e is varied at $t=3.5$ dropping to 0.5 [p.u]. The excitation voltage is constant in this case. Power angle has decreases to around 17° . This is a result of over excitation of the machine for a given input power as a result the SG injects reactive power (see Fig 3.29). The current and active power are directly proportional to the input power or torque at around 0.5 [p.u]

At $t=6.4$ the load is increased to 1.5 [p.u]. High transients are seen in electromagnetic torque and rotor speed (see Fig 3.28). As the excitation voltage is constant, the SG is under excited. It starts to consume reactive power (see Fig 3.29). Power angle is steadily increases; If excitation voltage is not increased, the SG loses synchronization as power angle approaches values above 90° . It should be noted that the power factor is below unity in both cases. Hence it confirms that the power factor is load dependent and the excitation voltage has to be changed accordingly to maintain a constant power angle corresponding to unity power factor.

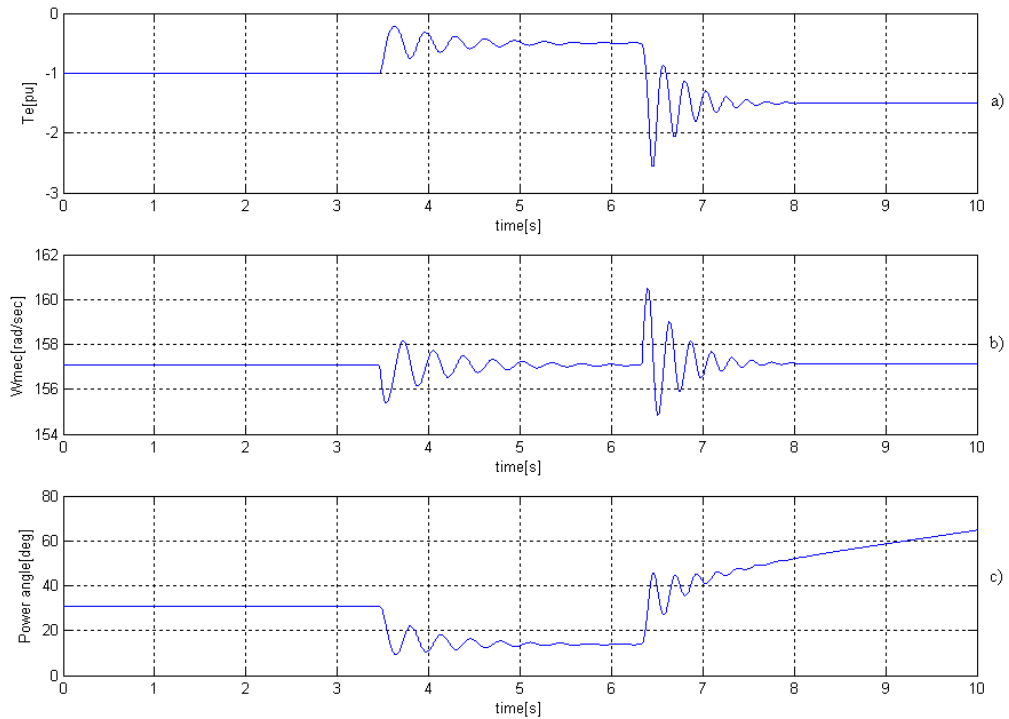


Fig 3.28 : Torque, Speed and Power Angle characteristics for constant excitation

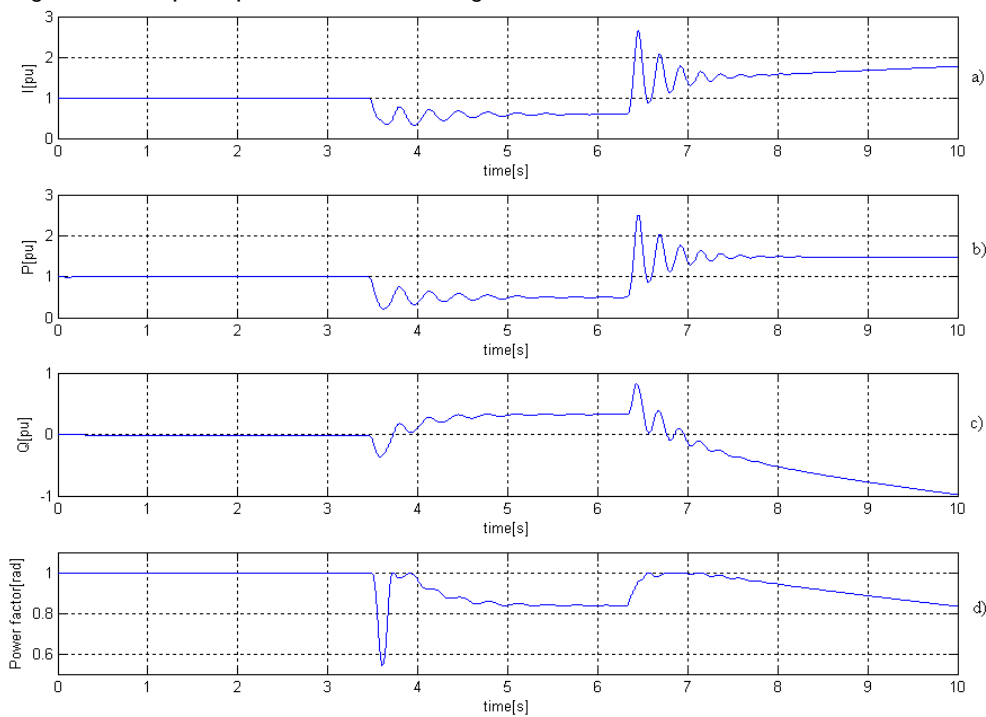


Fig 3.29: Current, Active and Reactive Power and Power factor variations at constant excitation

In real wind turbines, the torque deviations are fairly smooth and owing to mechanical filtering and also the wind characteristics. Nevertheless, changing load so abruptly will lead to high transients in currents (see Fig 3.29) up to 2.5 [p.u.]. Usually at these values, SG protections are triggered.

A more realistic condition pertaining to actually wind turbine operation is shown in Fig 3.30, Fig 3.31 and Fig 3.32. During 50[s] the real wind data is used and actual power from wind (translated into torque) is applied to the SG model.

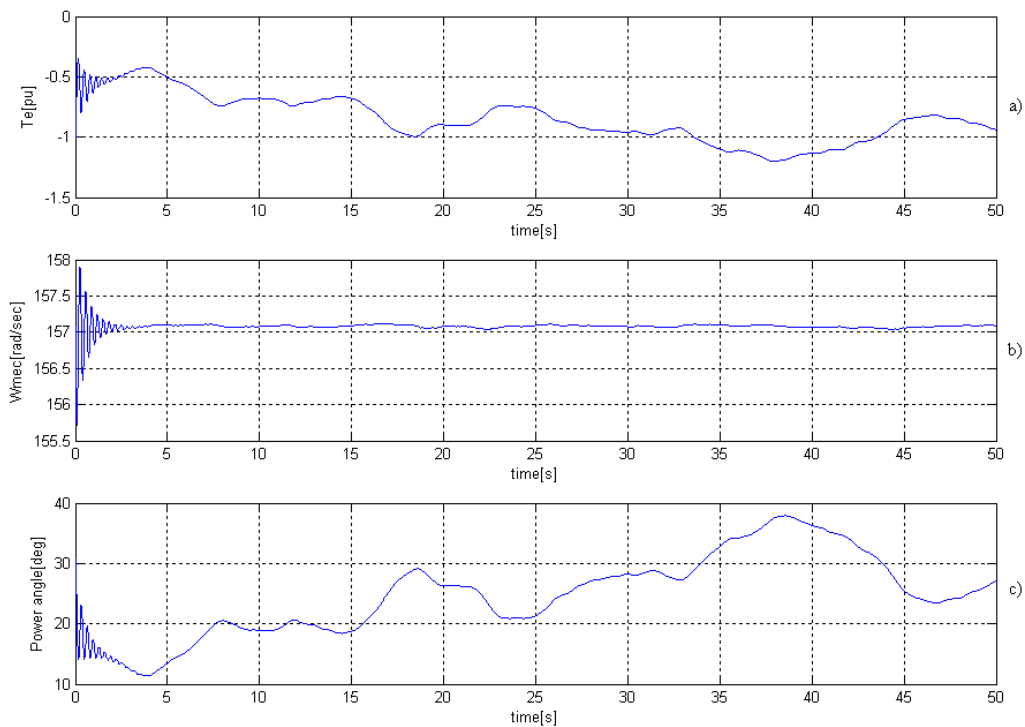


Fig 3.30: Torque, Speed and Power angle based on realistic wind data of average wind of 8m/s.

The output electromagnetic torque is equal to input load torque but with negative sign (see Fig 3.30). This system has a constant excitation voltage at nominal value. As expected the load angle is directly proportional to the load torque and can be seen in Fig 3.30 as is the current (see Fig 3.31).

In Fig 3.31 the following characteristics can be seen with respect to the reactive power. Initially the induced voltage E_f is at 1.89 p.u. nominal value as the average torque is around the nominal value. During the first 20 seconds, load torque is smaller than nominal torque. Therefore, SG is over excited. Reactive power is negative between 35 and 43 sec implying under-excitation since the absolute value of torque is greater than 1[p.u]. The power factor in Fig 3.32 varies with the torque.

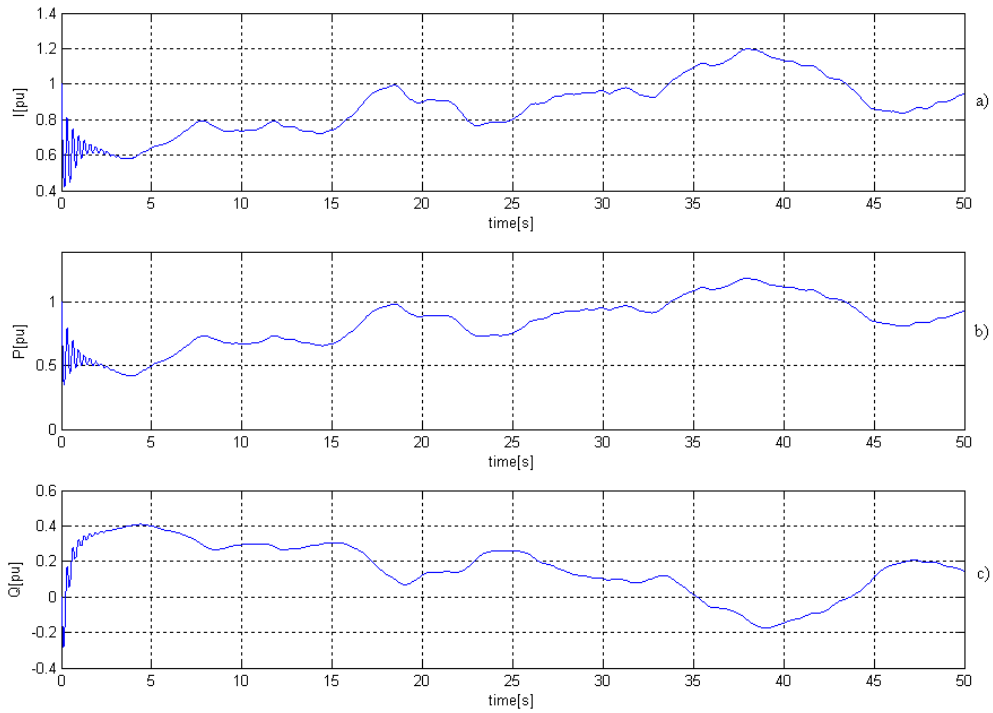


Fig 3.31: Current and Power based on realistic wind data of average wind of 8m/s.

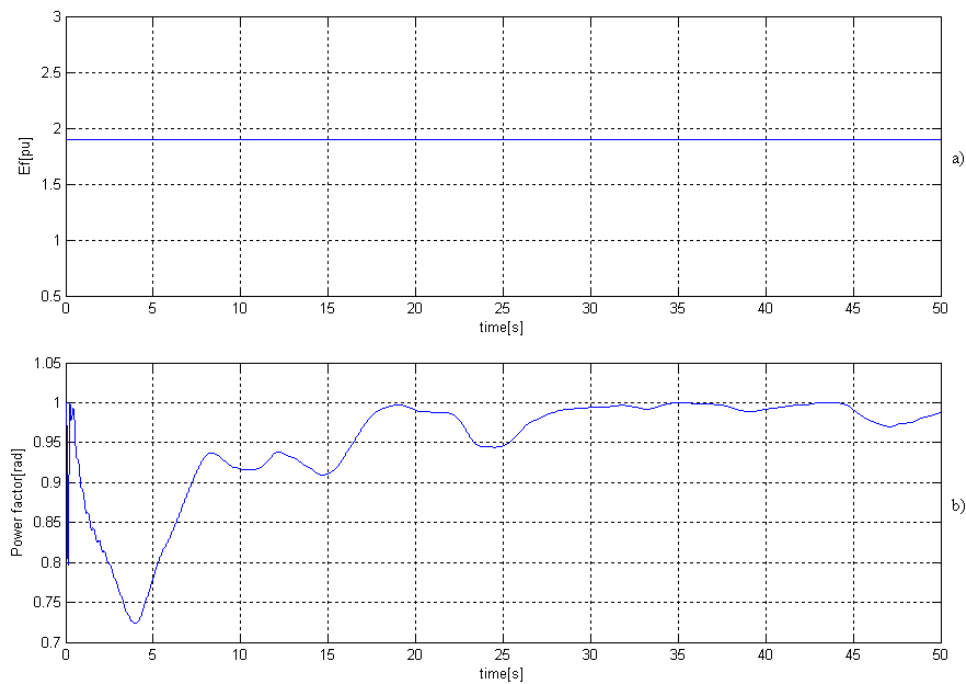


Fig 3.32: Constant excitation and Power factor based on realistic wind data of average wind of 8m/s.

Fig 3.33 shows that the locus of E_f that must be followed in order to maintain unity power factor.

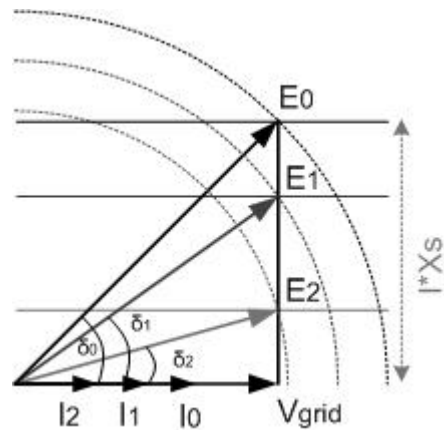


Fig 3.33: Variation of induced voltage with variation in input power for unity power factor.

With the understanding of the behavior of the synchronous machine, the reactive power control is implemented as Var Controller Type II model as recommended in [16]. For unity power factor operation an empirical formula is used:

$$Q_{ref} = Q_0 + K \cdot \Delta V \tag{3.55}$$

Hence a PI controller as shown is used to regulate the power factor

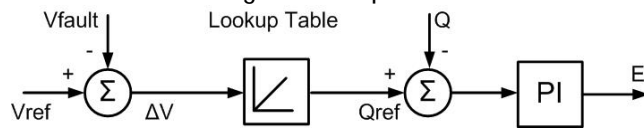


Fig 3.34: Reactive power control Scheme

Fig 3.35, Fig 3.36 and Fig 3.37 present power angle, current, reactive power, excitation voltage and power factor with and without control on the excitation voltage.

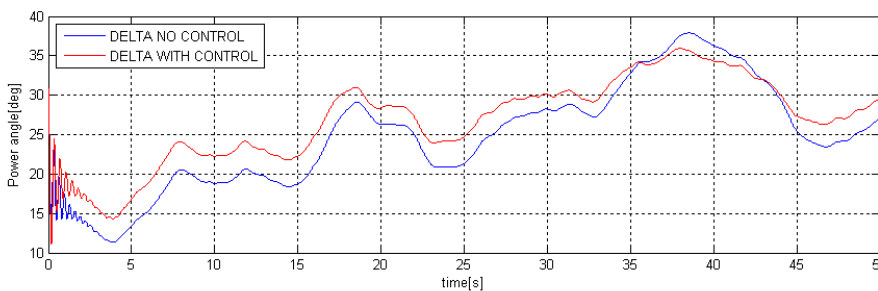


Fig 3.35: Comparison of power angle with implemented control strategy and constant excitation

As it has been already established the power angle is a reflection of the load in the machine hence a closer examination of Fig 3.35 shows that for sub nominal torque at nominal excitation the power angle is smaller as compared to the power angle at unity power factor operation. This is a result of over excitation. Conversely are super-nominal torque values for nominal excitation the power angle is greater than the power angle at unity power factor operation.

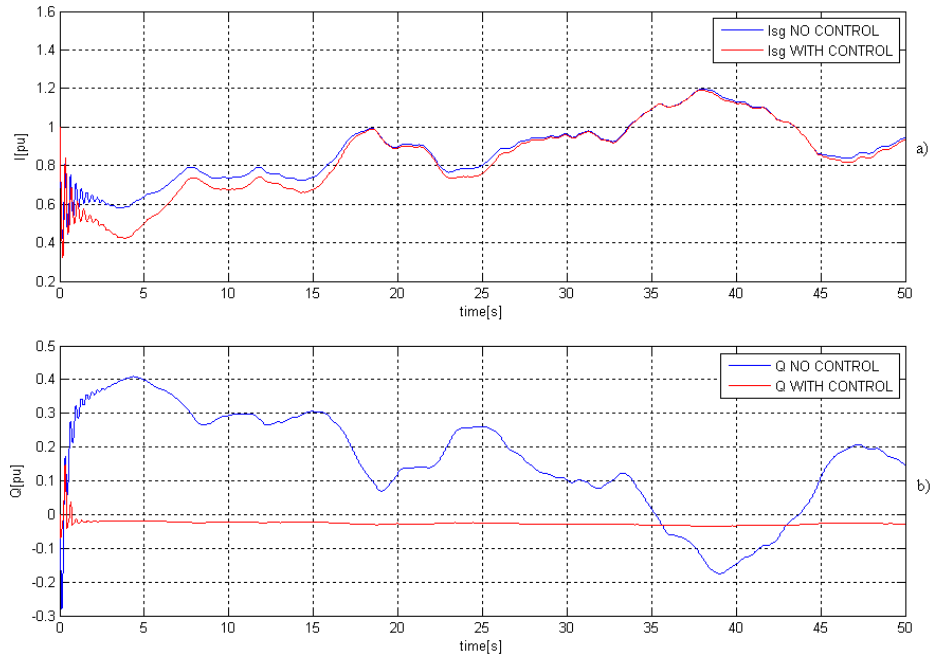


Fig 3.36: Comparison of current and reactive power with implemented control strategy and constant excitation.

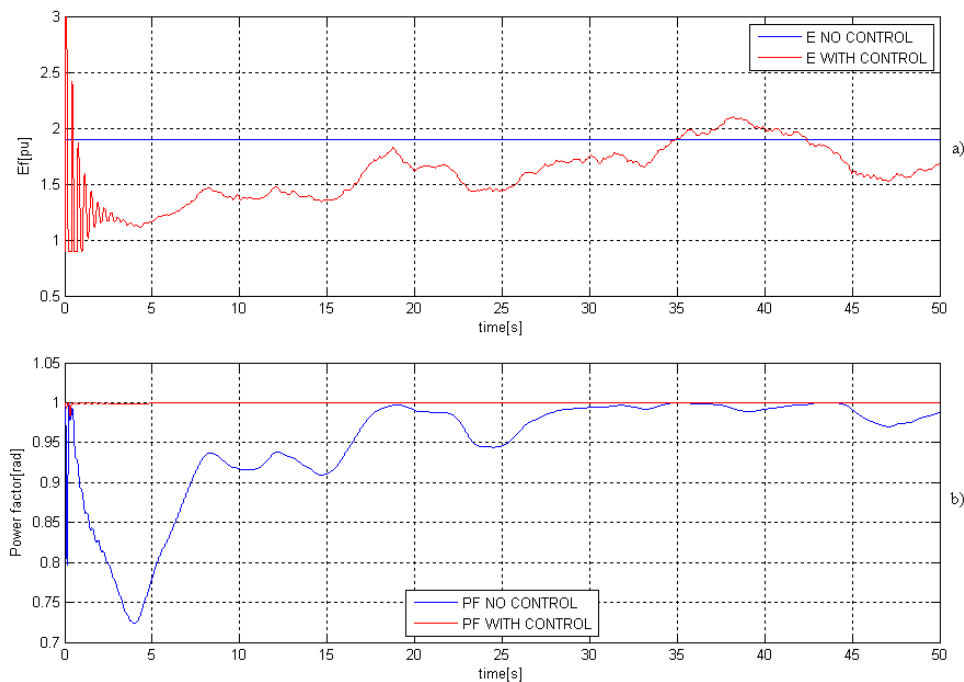


Fig 3.37: Comparison of current and reactive power with implemented control strategy and constant excitation.

The current in the Fig 3.36 shows the average or magnitude to the current is independent of the reactive power in the system and is only related with the load and the power angle. However the power factor in Fig 3.37 represents the ratio of active current (useful) to reactive current. Hence maintaining unity power factor ensures maximum efficiency of the system. Fig 3.36 show the reactive power in the system under influence of controller and without a control which conforms with the discussion above.

The variation of E_f to maintain unity power factor is plotted in Fig 3.37 which validates the controller design and performance for the given parameters of the machine. It is worthwhile to note that saturation limit of rotor and stator inductance will limit the upper value of induced voltage. Hence limit the reactive power capability of the SG. Auxiliary systems such as STATCOMS, capacitors switched capacitors etc. may have to be employed to comply with grid codes. This is discussed in the subsequent section.

3.3.3 Static VAR compensators (SCV) and Static Compensators

Static VAR compensators (SCV) and Static Compensators can supply reactive power far away from synchronous generators by controlling reactive power injected in to the PCC it is possible to regulate the ac voltage of the connection bus. Required reactive power is approximately one third of the nominal active power of a wind park. The various options are presented below along with their merits and demerits.

- Switched capacitors
 - The reactive current can be controlled only in discrete steps depending on the amount of switched components.
 - Poor dynamics due to limited switching time.
 - Regular maintenance of the breakers.
- Static VAR compensators
 - SVC can deliver or drain controlled reactive power according to the power system needs.
 - The presence of SVC close to the terminals of the SG influences the excitation control. A co-ordination between this two is required.
 - Combines thyristor switches with capacitor banks.
 - It is possible to obtain a smooth variation of reactive power over the complete installed power
 - Switching time is relatively fast.
- Static synchronous compensation
 - Static version of a synchronous machine VAR compensators.
 - An advanced SVC using a PWM converter supplying a capacitor.
 - Ability to perform smooth variation of reactive current.
 - Current injection depends on the grid voltage.
 - Operates according a linear Q/V characteristic.[17]

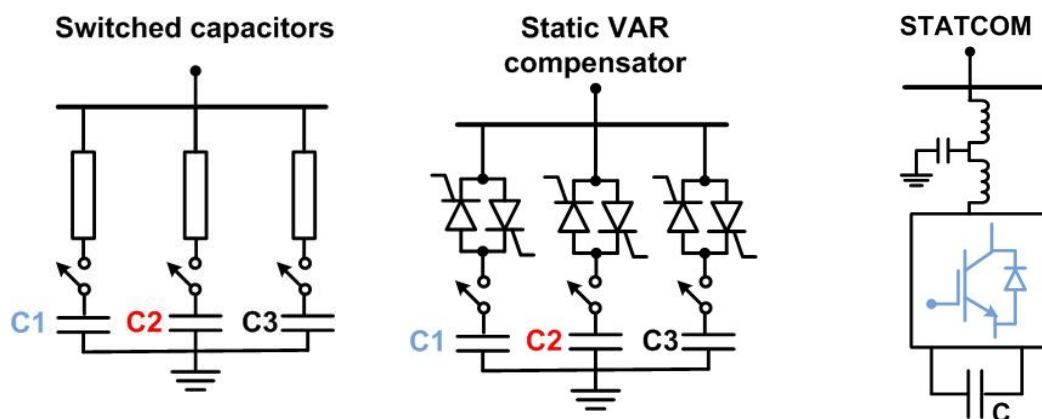


Fig 3.38 :Different types of compensators

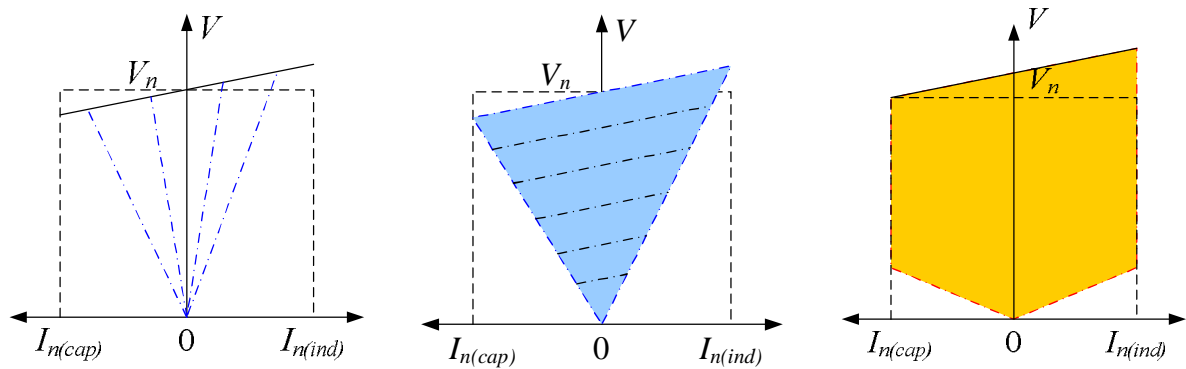


Fig 3.39 :Performance capability[17]

Fig 3.38 and Fig 3.39 show the various compensators and their reactive current injection capability.

3.3.4 Simulation of SVC and SC

The performance of the SCV and SC was tested in simulation. It was implemented in PLECS™ as seen in Fig 3.40.

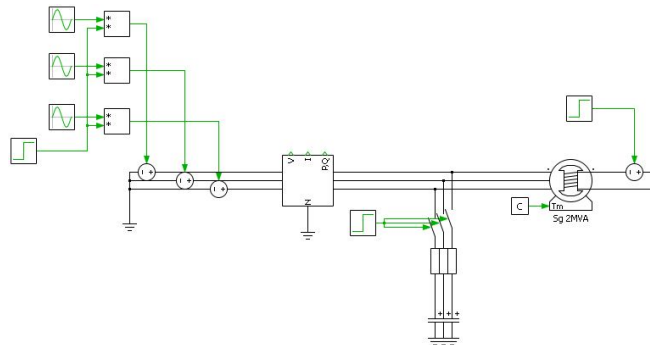


Fig 3.40:Model of switched capacitor circuit

The simulation result is shown below:

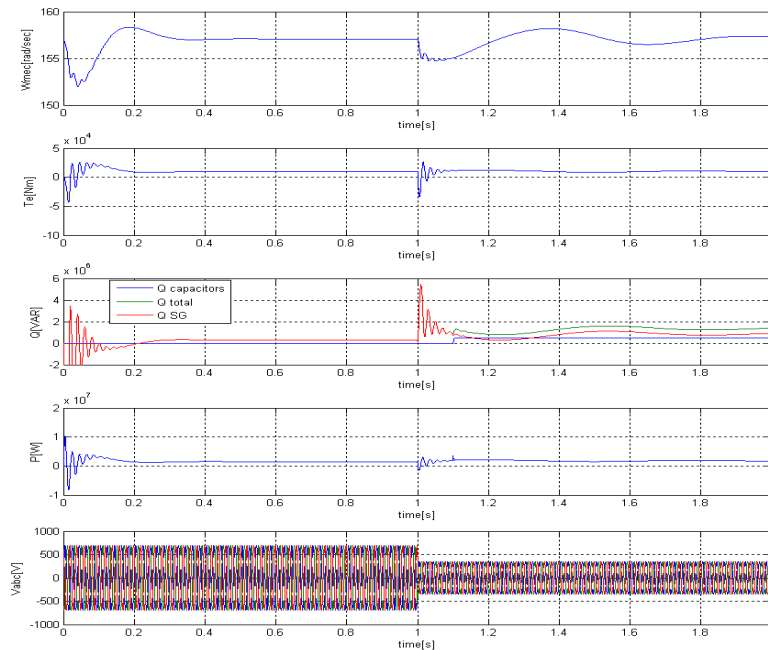


Fig 3.41:Simulation of switched capacitors

- At $t=1$ sec, a three phase fault is applied. Total injected reactive power is given by SG and capacitor banks. In order not to lose synchronization with the grid, the power angle of the SG has to be less than 90° . During the fault, the generator is over excited, in order to supply grid with reactive power. Reactive power capabilities of a SG indicate the amount of power the generator can deliver at a certain active power. There are limitations due to field and stator windings. Their temperature will increase above the limit, if the capabilities limits are not considered and damage to the machine may occur.
- Therefore, in order to help the machine give the required amount of Q , demanded by grid codes operators, the bank of capacitors are switched on. The technology is simple and robust. Q can be delivered in discrete steps.

The other solution is with the STATCOM, which is modeled as shown below

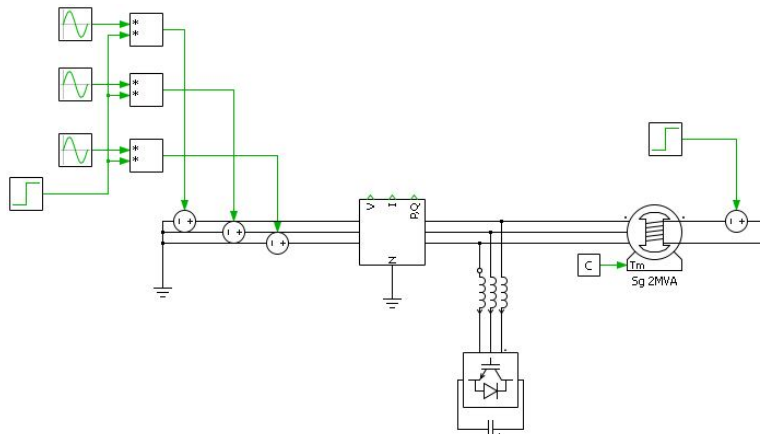


Fig 3.42: Model of STATCOM circuit

The control circuit for the STATCOM is shown below

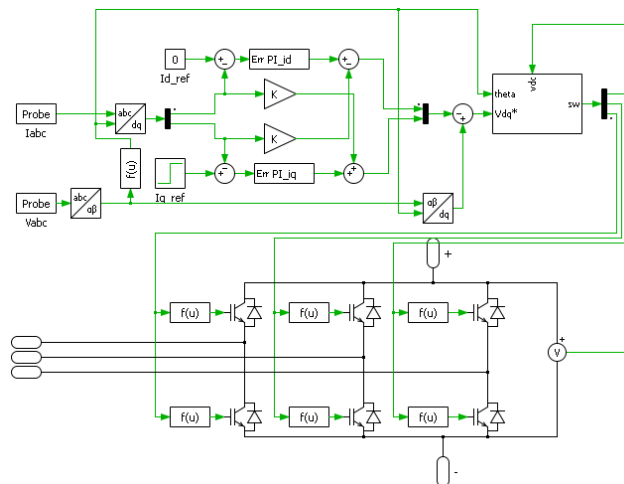


Fig 3.43: Control circuit for STATCOM.

The simulation result is shown below:

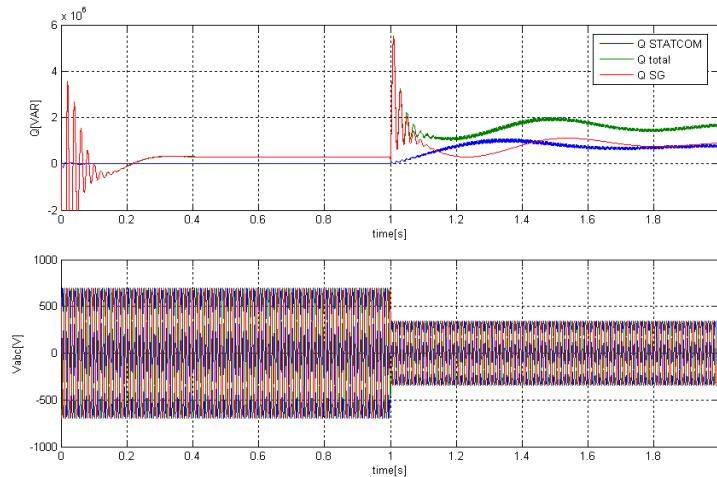


Fig 3.44: Simulation of STATCOM

- Better dynamics than capacitors with classic switches
- Reactive power is controlled in smooth steps.
- Size of STATCOM is dependent on the size of SG. For example, if the generator is able to give 90% of the necessary reactive power, then the STATCOM should be designed in order to withstand current of 10% of nominal reactive currents.

3.4 Lab Implementation

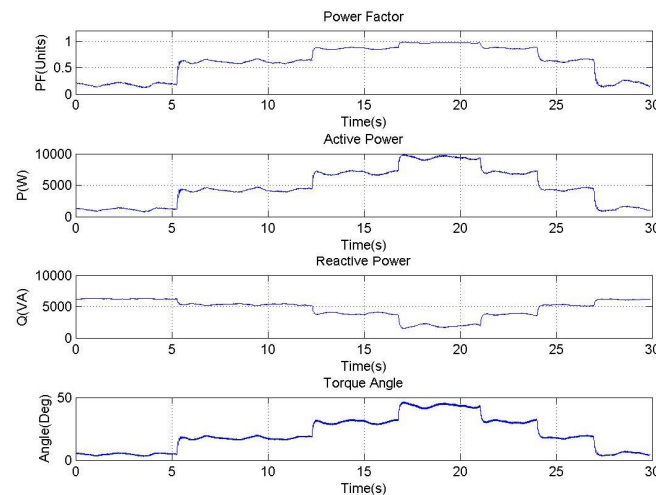


Fig 3.45 : (a)Power Factor (b)Active power (c)Reactive power (d)Power angle for constant excitation

Fig 3.45 shows the experimental results for a constant excitation voltage for the synchronous machine. The power (see Fig 3.45(b)) factor varies as discussed in Section 3.3.2.1. It follows the active power shown in Fig 3.45(b). However, the reactive power (Fig 3.45(c)) is roughly inverse in characteristics as the machine cycles through over-excitation, under-excitation and unity power factor. The torque angle also is shown to vary according to the operation modes shown in Fig 3.23.

3.4.1 Operation Modes – Lead and Lag

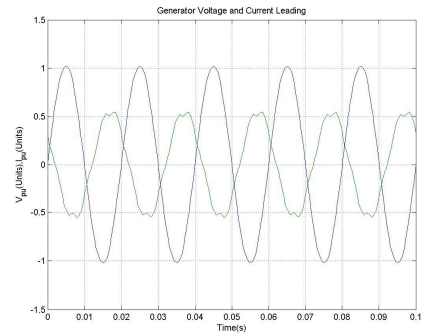
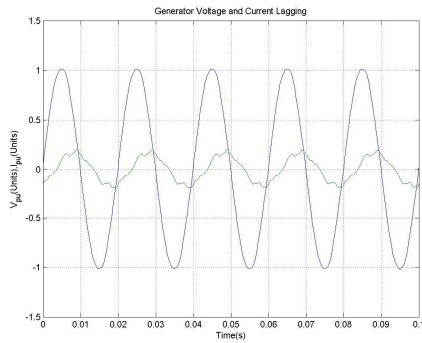


Fig 3.46 : Voltage and Current (a)Lagging PF (b)Leading PF

Fig 3.46 shows the operation mode of the synchronous generator.

In this section results obtained for various lead and lag operation modes of the SG are presented.

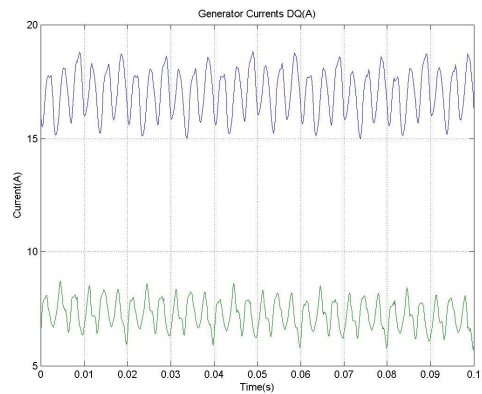
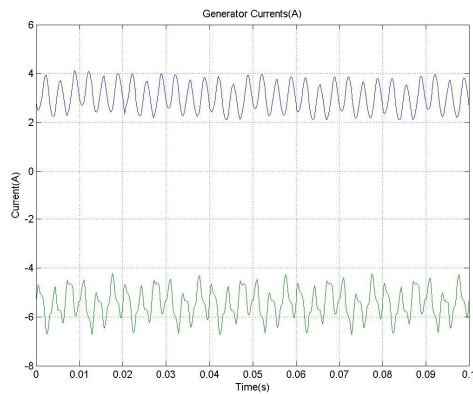


Fig 3.47 : I_d and I_q for (a)Lagging PF (b)Leading PF

Fig 3.47 shows the currents in dq reference frame. It is evident that the lagging power factor consists of a negative I_q component as the frame is oriented to the grid voltage vector. The ripple exist because of harmonics observed in the Fig 3.48

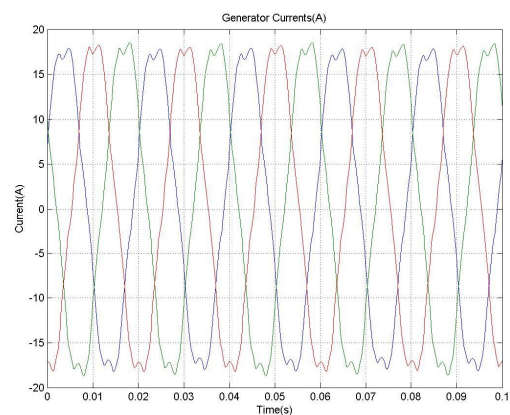
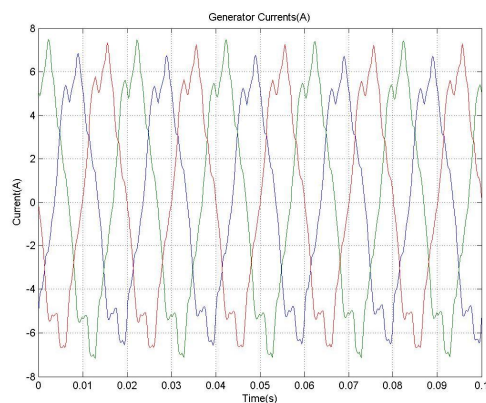
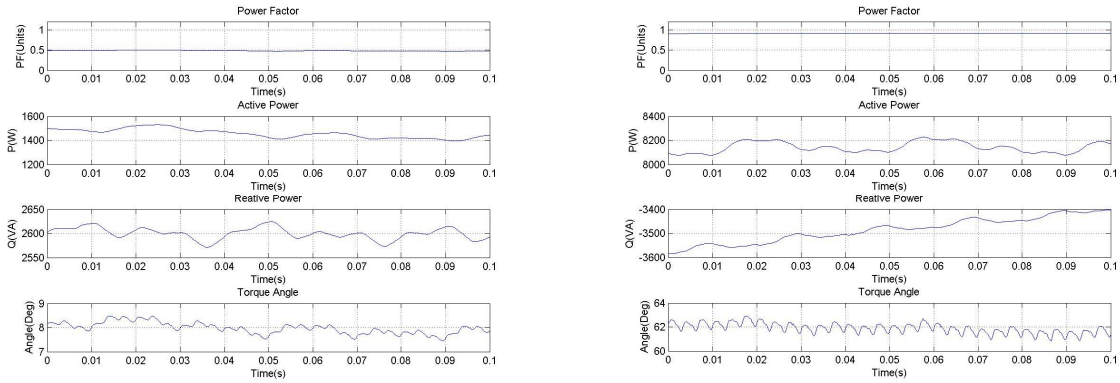


Fig 3.48 : Three phase currents (a)Lagging (b)Leading



Lag Lead

Fig 3.49 : (a)Power Factor (b)Active power (c)Reactive power (d)Power angle for lagging and leading

In Fig 3.49 it can be seen that the reactive power is injected if the PF is lagging and reactive power is consumed as expected. It can also be noted that during lagging operation the power angle is very low hence the system in over excited state is more stable compared to when it is under excited (lead) as seen from the power angles. This is illustrated in the stability of the induced voltage as shown in Fig 3.50. The inner circle represents the grid voltage in both cases.

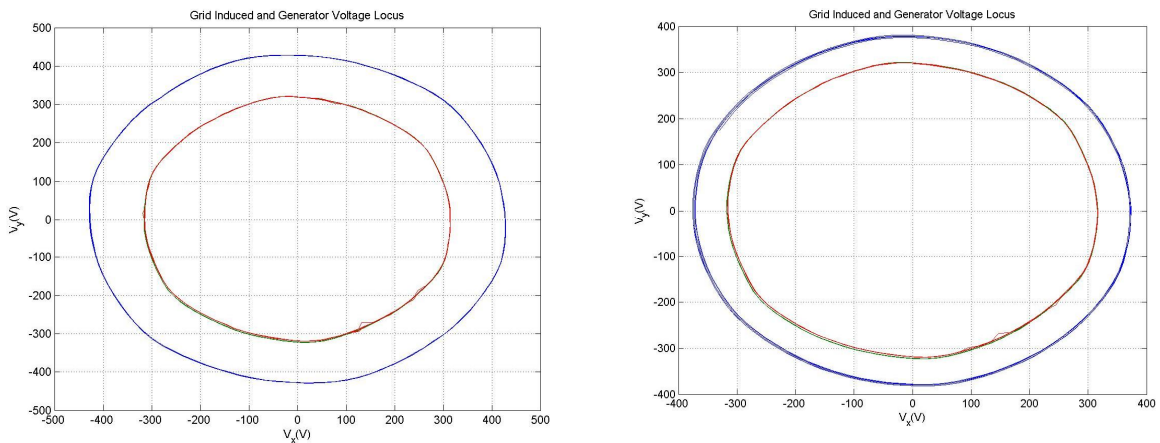


Fig 3.50: (a)Lagging PF (b)Leading PF

3.4.2 Operation Modes –Unity Power factor

The following results are obtained experimentally to ascertain the ability of the controller to maintain unity power factor under normal operating conditions.

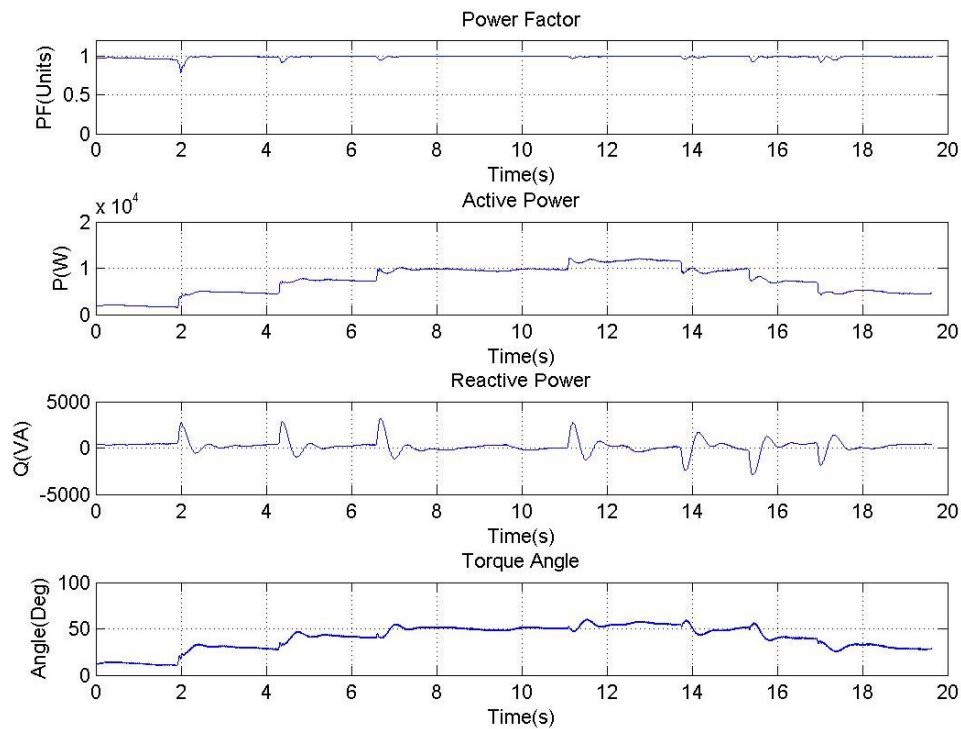


Fig 3.51: (a)Power Factor (b)Active power (c)Reactive power (d)Power angle for Unity PF

Fig 3.51(a) show that the machine is being operated at $PF=1$ for varying load represented by active power (see Fig 3.51(b)). The reactive power (see Fig 3.51(b)) is zero but transients appear when there is a step in load. This is satisfactory since in wind turbines the torque varies more smoothly due to mechanical filtering. The power angle is within $90[\text{deg}]$. Hence the system is stable.

3.5 Summary

The general theory about the synchronous generator was discussed to illustrate the behavior of the machine. This was done to develop a control scheme for the machine to operate at unity power factor. The control scheme is implemented both in laboratory and simulation. The results are used to explain the behavior of the machine.

4 Excitation converter

The chapter offers an overview of the exciter converters that are used to supply the rotor excitation. The chapter discusses some widely used technologies for this application. The buck converter used in the project is discussed and the design parameters are given.

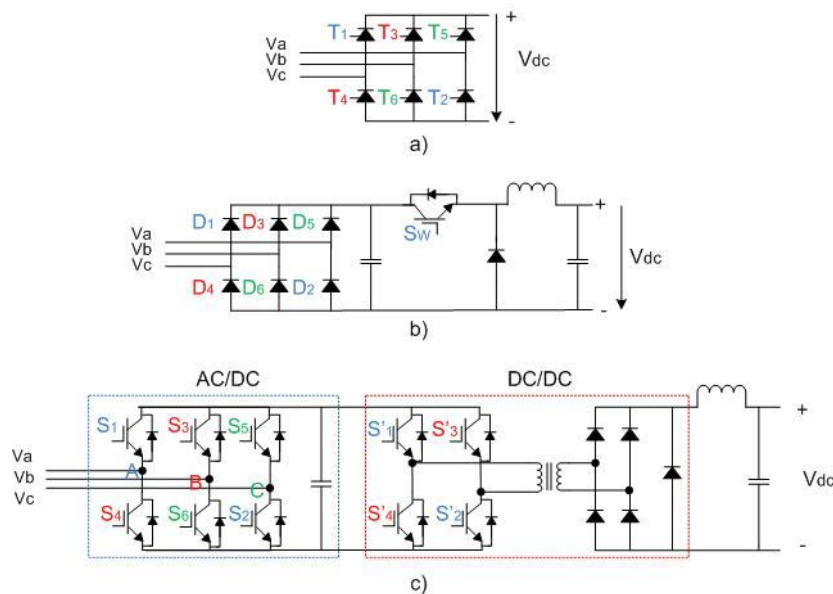


Fig 4.1: Converter topologies to supply brushless exciters

(a) Thyristor based converters (b) Passive rectifier and buck converter(c) Active rectifier and H-bridge with isolated transformer.

The different types are presented in Fig 4.1.[18]

4.1 Thyristor rectifier

The following section presents a simple 3-phase thyristor rectifier. The thyristor is a controlled diode, where the gate enables turn-on at a precise moment. The thyristor will conduct if the anode is positive and a positive impulse voltage is applied to the gate. However, it turns-off only when anode current falls to zero. Therefore, a thyristor converter can control the power flow by the phase control principle, which delays the firing angle of the gate. Synchronous generators usually have thyristor based rectifiers which is simple and robust, for rotor excitation. Three phase rectifier (see Fig 4.2) are usually used where the load is typically above 10kW. It balances the power flow in a three phase utility system.[19]

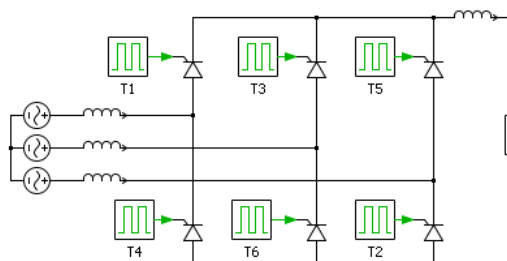


Fig 4.2:Three Phase Thyristor Rectifier

The rectifier modeled in PLECS™. The simulation results are plotted in Fig 4.3. The gate impulses are delayed by 60° . If the gate currents are applied continuously, the converter behaves like an average diode rectifier. The switching pattern is illustrated in Fig 4.3 along with the voltage and current output. The ripple is reduced by the output inductor. These rectifiers have poor dynamics compared to IGBT based converters.

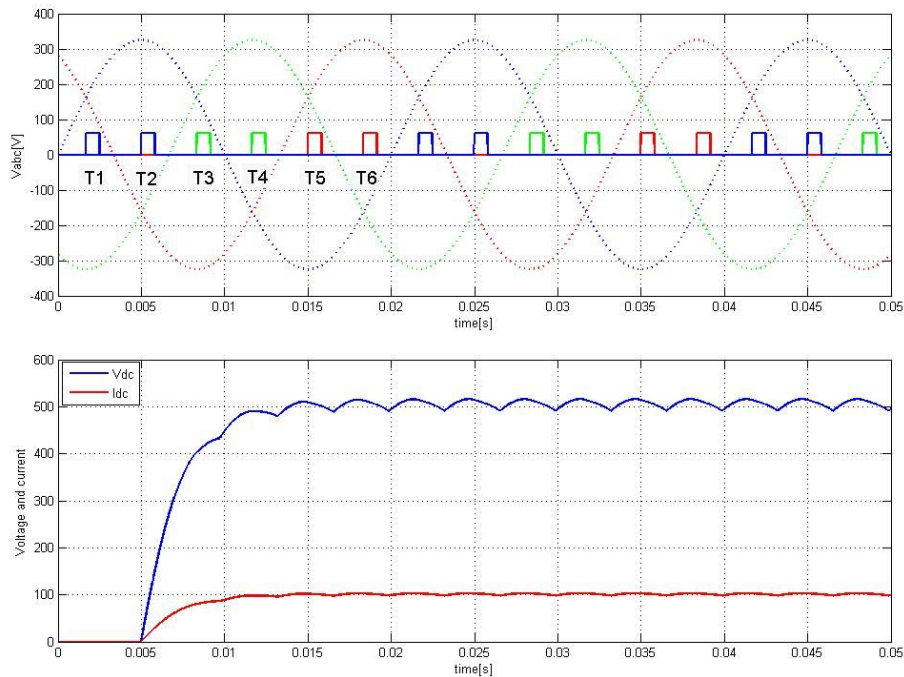


Fig 4.3: Three Phase Thyristor Rectifier – Simulation

4.2 Passive rectifier and buck converter

The passive rectifier consists of uncontrolled diodes which rectify the 3 phase ac supply to provide input to the buck converter (see Appendix E). The control is modeled based on Fig 3.34 in order to control the reactive power which is discussed in the next chapter. The PLECS™ implementation is shown below

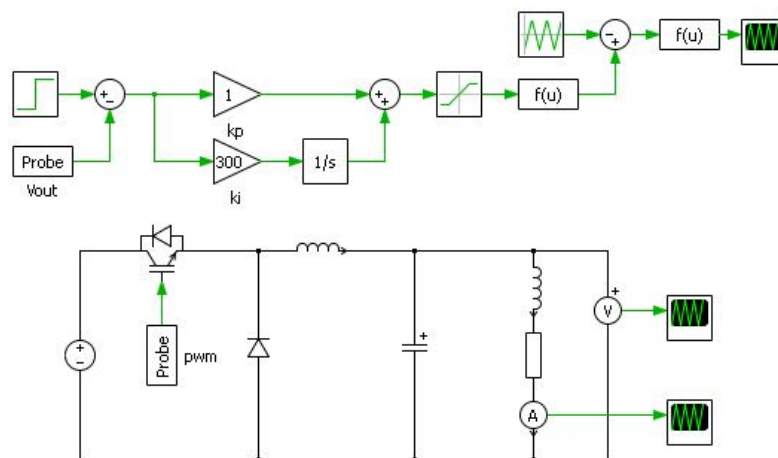


Fig 4.4: Buck converter

The control simulation uses pure DC source instead of the passive rectifier as shown in Fig 4.1(b).

The simulation for the system is presented in Fig 4.3. It shows the satisfactory performance of the PI controller when the reference is stepped up from 20[V] to 40[V], the settling time is 0.02[s] which translates to 1 cycle in 50Hz operation of a machine. Hence it conforms with the grid requirement.

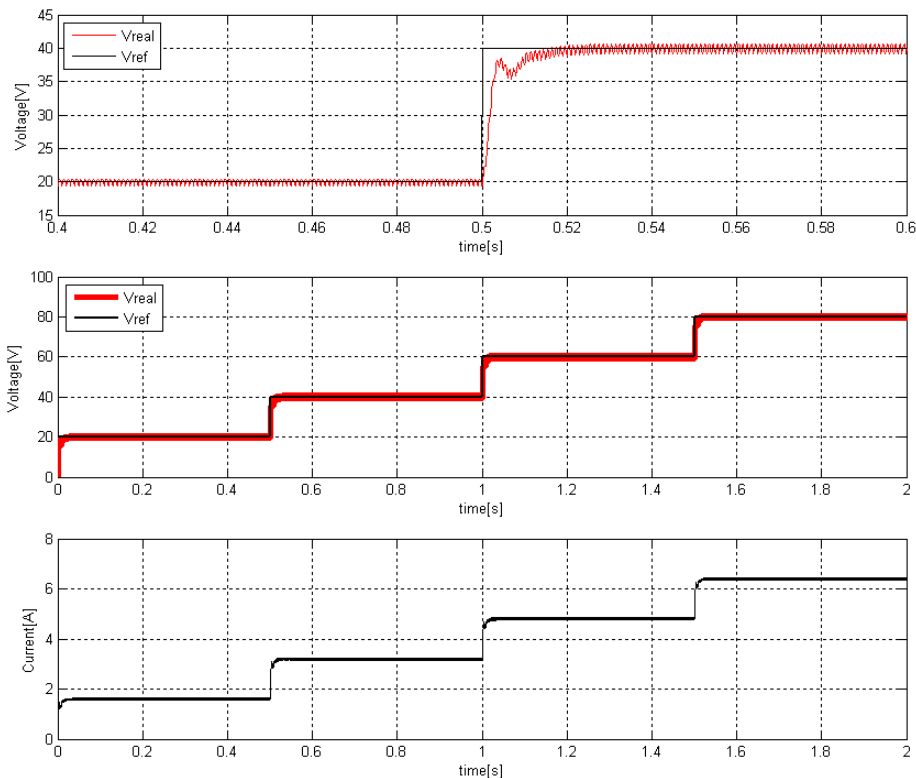


Fig 4.5: Buck converter simulation

4.3 AC/DC –DC/DC with PF control

The DC/DC converter consists of an H bridge IGBT converter seen in Fig 4.1(c). Output of the converter supplies a high frequency isolation transformer. Secondary of the transformer supplies a diode bridge rectifier to convert to DC output. Output filter stage consists of a LC filter. Output voltage is compared to a reference value and the error is fed through a PI controller. The output is the reference value of the duty cycle. Further on, it is compared to the carrier signal, to generate gate pulses to drive the IGBTs.

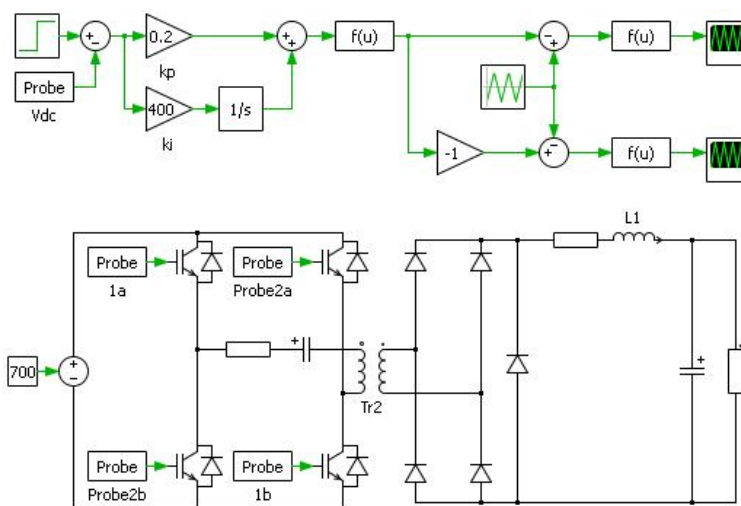


Fig 4.6: Control and Model of DC/DC H bridge

The simulations are presented in Fig 4.7

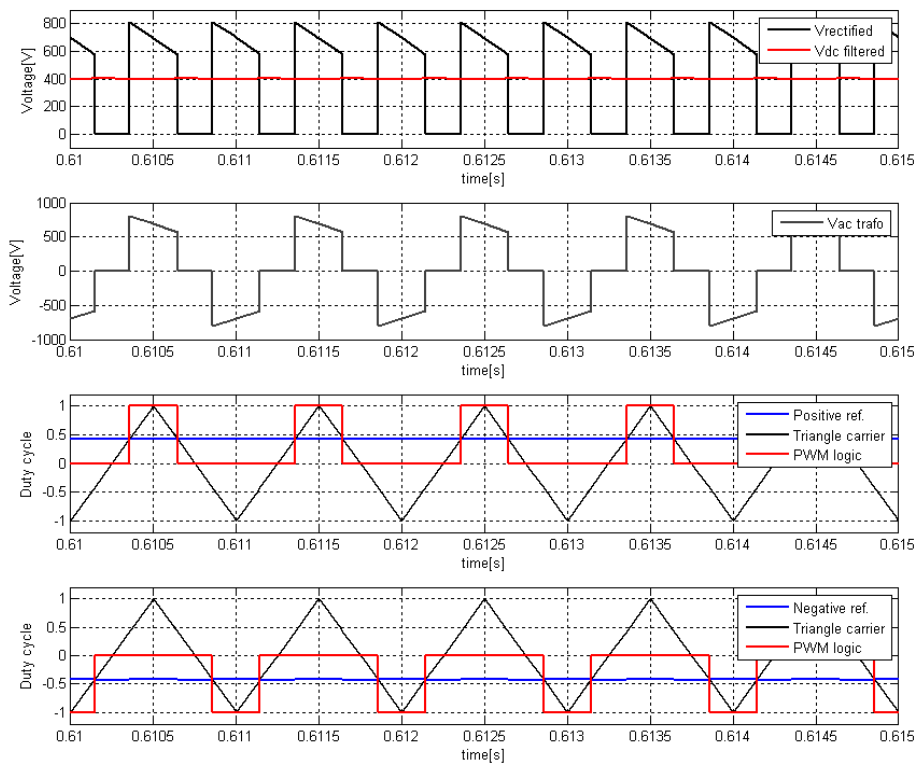


Fig 4.7: Voltage Output and Control Signals

The current and voltage output for steps in reference are shown in Fig 4.8

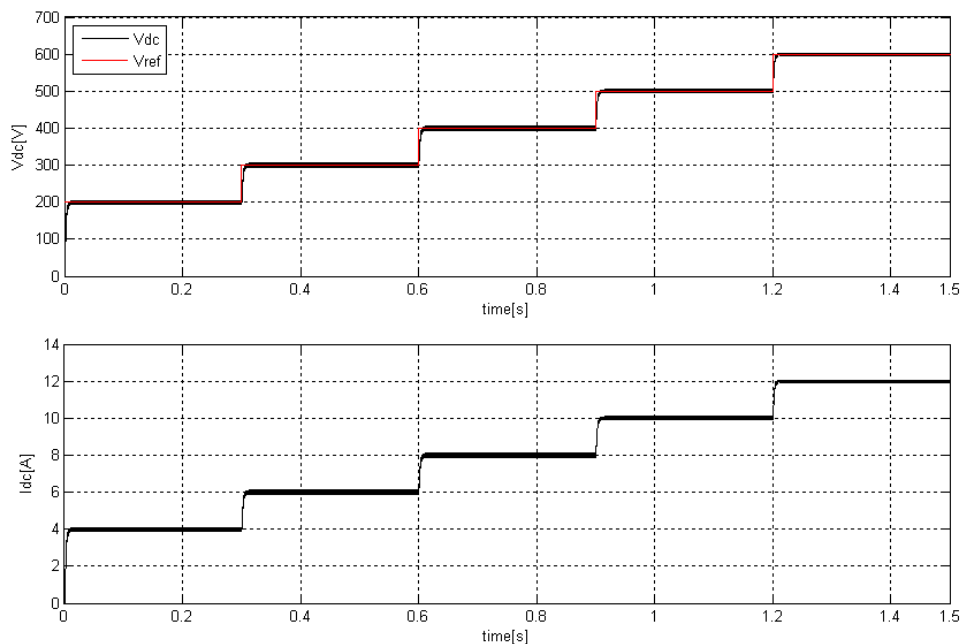


Fig 4.8: Voltage Output and Control Signals

The AC/DC converter rectifies 3 phase voltages and converts it to DC voltage. Further on, the DC/DC converter is supplied from the rectified voltage and controls the excitation of the brushless exciter according to the torque. The ac input currents are non pulsating, therefore very little EMI filtering is required. The converter is able of bidirectional power flow. A disadvantage is the requirement for six

active devices. If compared to a dc/dc converter with the same ratings, the utilization of semiconductors is low.[20]

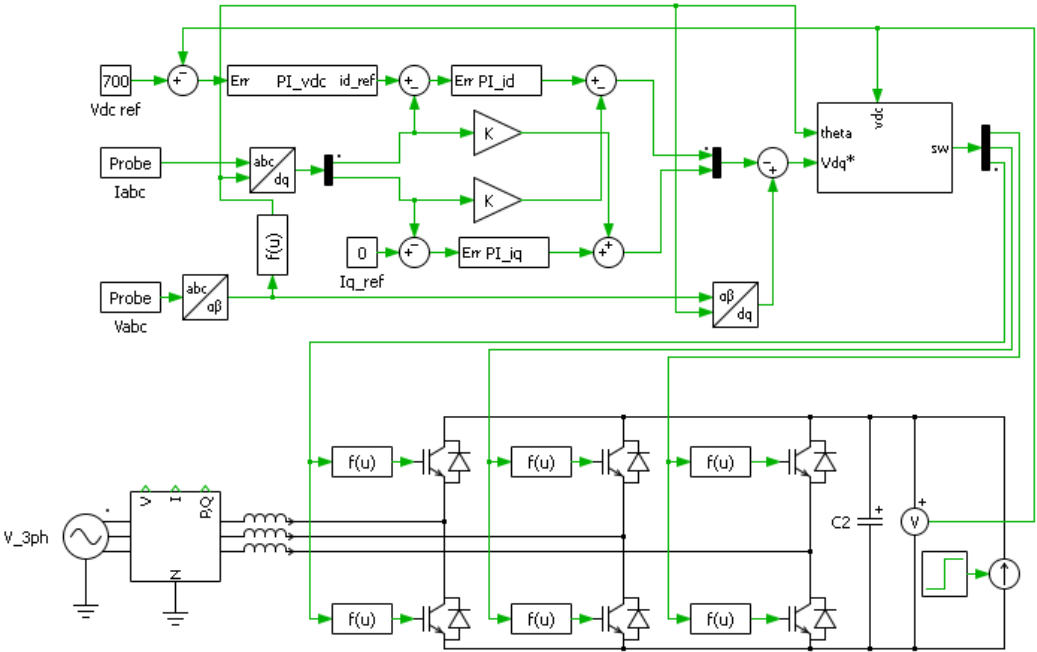


Fig 4.9: Model of AC/DC converter

The input 3 phase voltages pass through a filter and supply the 3 phase IGBT bridge. To obtain a power factor of 1, the current has to be in phase with the voltage. This can be achieved through SVPWM. Feedback control is achieved in the rotating reference frame, which is synchronized to the angle of the grid voltage. Measured currents I_a, I_b, I_c are converted to rotating dq axis using the theta angle of grid.

Reference I_q component of current is set to zero. Two PI controllers are used to adjust output voltage so real i_d and i_q follow the reference. In a simple manner, I_d controls active power and I_q is subjected to reactive power. Reference value of i_d is obtained from a third PI control loop, based on the difference between DC output voltage of the rectifier and the desired DC output voltage. Therefore, I_d is kept at a level where the DC bus is constant under varying load currents.

The simulation results are presented in Fig 4.10.

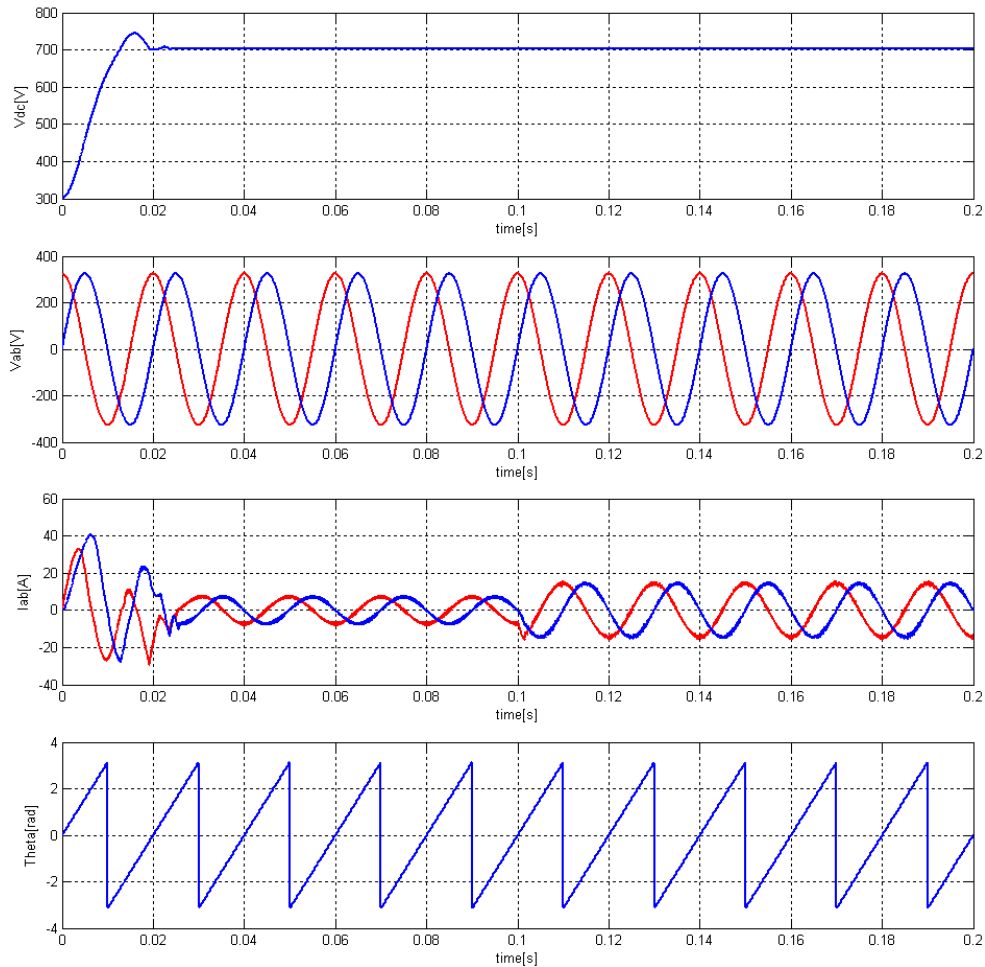


Fig 4.10: Simulation Output

A comparison of the various types of exciter circuits is presented in Table 4-1.

Table 4-1

Converter type	ADVANTAGES	DISADVANTAGES
AC-DC PF control	<ul style="list-style-type: none"> • Low harmonics • PF of 1 • Isolation from the supply • Ability to boost the DC voltage to higher values 	<ul style="list-style-type: none"> • Large number of semiconductors
DC-DC Buck Converter	<ul style="list-style-type: none"> • Good efficiency • Lesser number of semiconductor devices • Easy to fabricate 	<ul style="list-style-type: none"> • Suitable for low voltage
THYRISTOR RECTIFIER	<ul style="list-style-type: none"> • Simple, robust and inexpensive • Efficient for loads bigger the 10 kw 	<ul style="list-style-type: none"> • Bad dynamic response compared to transistor converters • Bad THD

In this project the buck converter is chosen because of the advantages mentioned above. Since the application range is low voltage this kind of converter is suitable.

It converts 24V (from the main supply, see Fig 4.12) to $\pm 15V$. Two large capacitors of $220\mu F$ (C44 and C45) are added in order to provide the necessary current. To avoid overvoltage on the gate drive, it is clamped by a Zener diode to 18V.

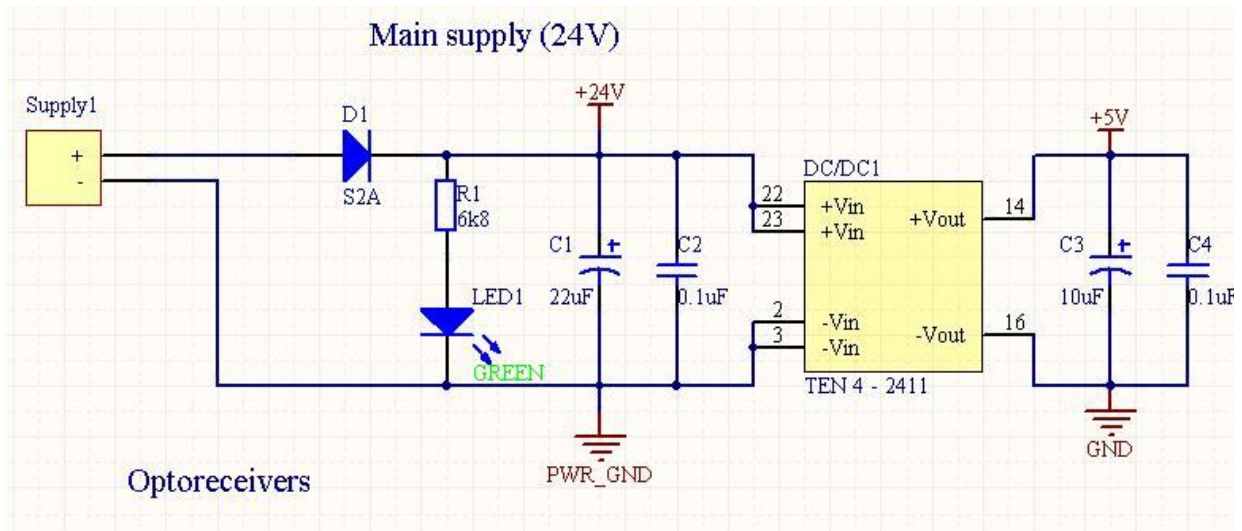


Fig 4.12 Main supply

The Altium layout for the design is shown below.

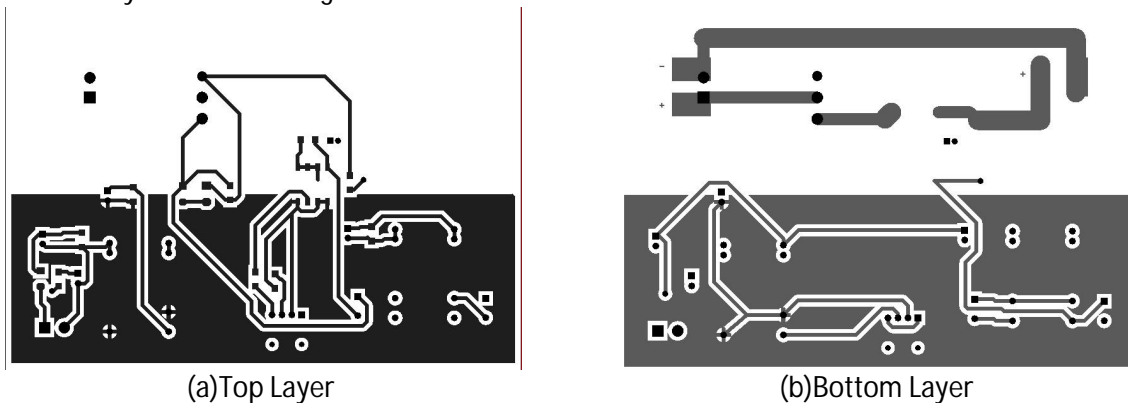


Fig 4.13 :PCB layout for buck converter

The response of the DC/DC converter along with the voltage induced in the machine is presented in Fig 4.14

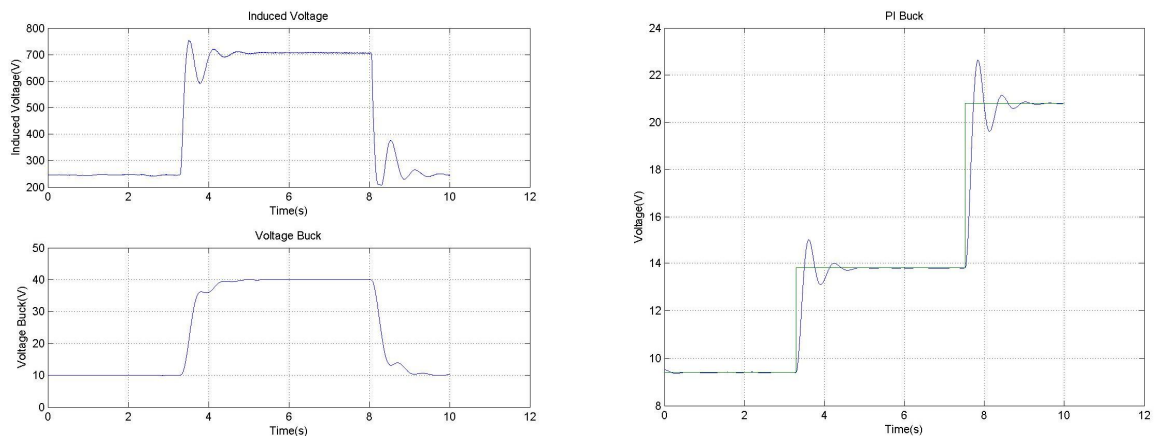


Fig 4.14 : Voltage in buck converter

4.6 Summary

Various converter technologies are described and implemented in simulation. The results are presented and compared. The DC/DC buck converter was chosen to be used in the project. The design specification was discussed with reference to Appendix E. The PCB was fabricated for the given specification. The schematic and layout designs are presented.

5 Grid Faults

This chapter introduced grid faults within the scope of the project. Various types of grid faults are discussed. Grid code requirement from various national codes are described. The faults are simulated and also implemented in the lab. The results are presented.

5.1 Introduction

Grid faults are defined as deviation from nominal grid operating conditions. This may occur because of short-circuit in the network grid passing or on another radial. Startup of large motors/load can also cause these faults. These result in Undervoltage or Voltage sags. Earth faults on another phase, and shut down of large loads can cause Voltage swelling/Overtvoltage. Non-linear loading, resonance phenomena and transformer saturation leads to harmonic distortion. Transient faults occur due to lighting strikes or switching events in power electronic devices. Voltage flicker or fluctuations are seen with arc furnaces or welding as loads. Short duration interruptions may occur due to direct short circuit and false tripping. Single phase loads lead to unbalanced disturbances.

Voltage sags are the short-duration reductions in voltage caused by faults in the electric supply system and the starting of large loads, such as motors. Voltage sags are widely recognized as one of the most important aspects of power quality [21]. This type of voltage fault is the main focus of the project.

5.2 Types of Grid Fault

A standard grid connection scheme is presented in Fig 5.1.

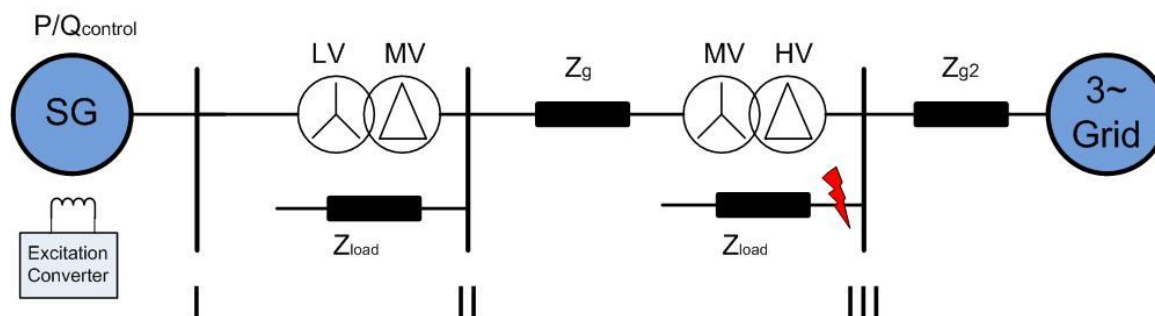


Fig 5.1: Grid Connection of SG with fault location and associated impedances

It is understood that only phase to ground faults and two-phase faults (A,B,C and E) can occur on the grid side. The transformers affect the character of three phase unbalanced voltage dips. The propagation of these fault through the system results in other type of faults (D,F and G) as seen in Table 5-1.

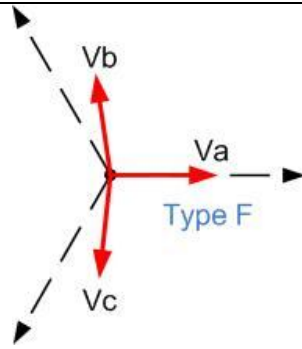
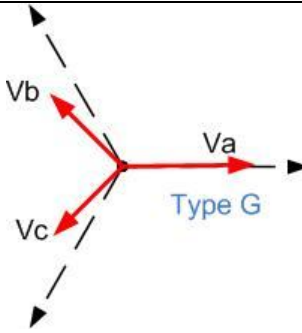
Table 5-1

Fault type	Measurement location		
	III	II	I
Three-phase	A	A	A
Single-phase-to-ground	B	C	D
Two-phase	C	D	C
Two Phase to Ground	E	F	G

The various voltage dips that can occur are shown in Table 5-2.[22]

Table 5-2

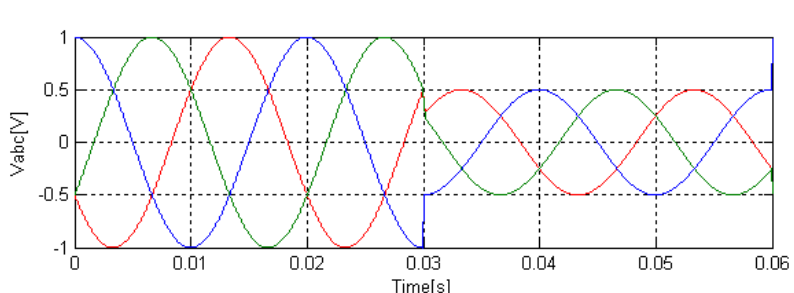
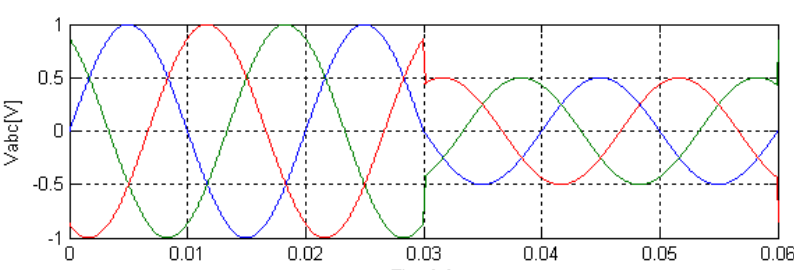
Type	Voltages	Phasor Representation	Notes
A	$V_a = V_f$ $V_b = -\frac{1}{2}V_f - \frac{1}{2}jV_f\sqrt{3}$ $V_c = -\frac{1}{2}V_f + \frac{1}{2}jV_f\sqrt{3}$	<p style="text-align: center;">Type A</p>	<p>The three phase symmetrical fault is considered the worst case scenario. This kind of fault occurs in less than 10% of the total faults. Synchronization is easy during the fault.</p>
B	$V_a = V_f$ $V_b = -\frac{1}{2}E - \frac{1}{2}jE\sqrt{3}$ $V_c = -\frac{1}{2}E + \frac{1}{2}jE\sqrt{3}$	<p style="text-align: center;">Type B</p>	<p>The single phase to ground fault occurs around 70% of the total faults. Voltage propagation depends on the grounding system.</p>
C	$V_a = E$ $V_b = -\frac{1}{2}E - \frac{1}{2}jV_f\sqrt{3}$ $V_c = -\frac{1}{2}E + \frac{1}{2}jV_f\sqrt{3}$	<p style="text-align: center;">Type C</p>	<p>Might be consequence of fault type B</p>
D	$V_a = V_f$ $V_b = -\frac{1}{2}V_f - \frac{1}{2}jE\sqrt{3}$ $V_c = -\frac{1}{2}V_f + \frac{1}{2}jE\sqrt{3}$	<p style="text-align: center;">Type D</p>	<p>This a very common fault. Consequence to fault type C.</p>
E	$V_a = E$ $V_b = -\frac{1}{2}V_f - \frac{1}{2}jV_f\sqrt{3}$ $V_c = -\frac{1}{2}V_f + \frac{1}{2}jV_f\sqrt{3}$	<p style="text-align: center;">Type E</p>	<p>Two phase to ground. Occurs around 20% of the total faults</p>

F	$V_a = V_f$ $V_b = -\frac{1}{2}V_f - \left(\frac{1}{3}E + \frac{1}{6}V_f\right)j\sqrt{3}$ $V_c = -\frac{1}{2}V_f + \left(\frac{1}{3}E + \frac{1}{6}V_f\right)j\sqrt{3}$		Consequence of fault type E.
G	$V_a = \frac{2}{3}E + \frac{1}{3}V_f$ $V_b = -\frac{1}{3}E - \frac{1}{6}V_f - \frac{1}{2}jV_f\sqrt{3}$ $V_c = -\frac{1}{3}E - \frac{1}{6}V_f + \frac{1}{2}jV_f\sqrt{3}$		Consequence of fault type E.

5.3 Simulation of grid fault propagation

Fig 5.2, Fig 5.3, Fig 5.4 and Fig 5.5 were generated through PLECS to confirm the propagation of faults as seen in Table 5-1.

CASE A: Three Phase faults

Node	Type	Fault Characteristic
III	A	
II	A	

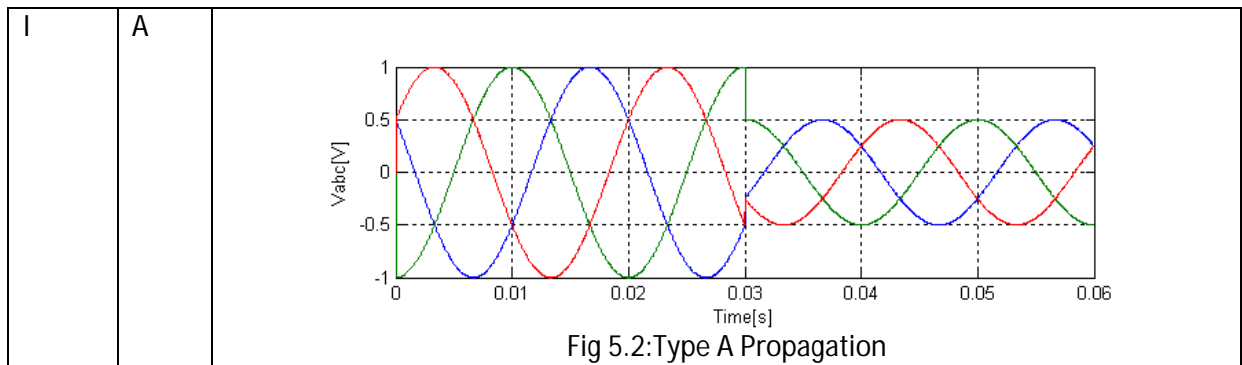


Fig 5.2 shows that the type A faults when measured at different nodes manifests as type A on all other nodes. It can be noted however there is a phase lag on each stage as the coupling transformers are seen as a reactance.

CASE B: Single-phase-to-ground

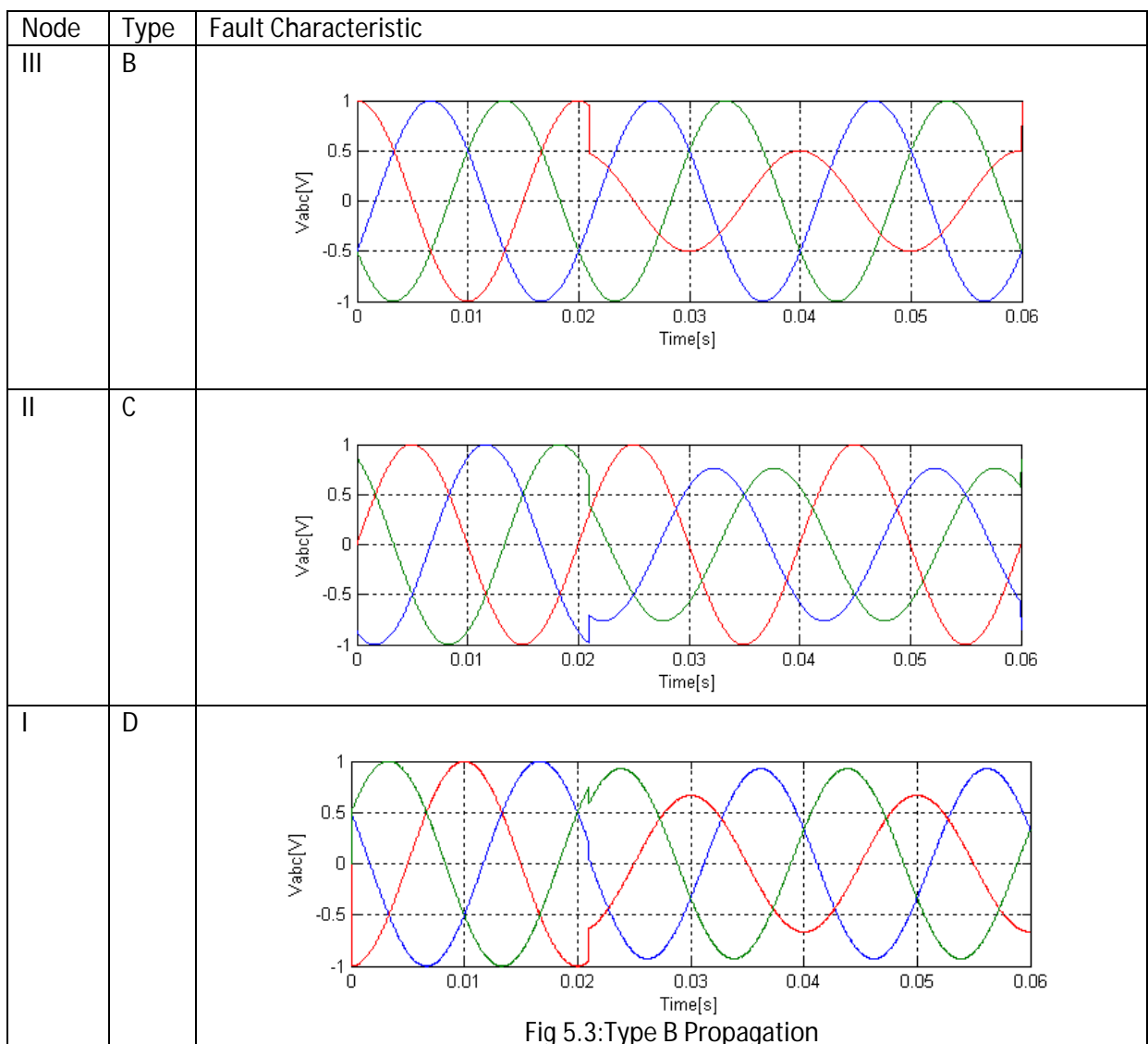


Fig 5.3 shows that the type B faults when measured at different nodes manifests as type C at node II and as type D at node I. Due to transformer coupling a single phase fault appears as two phase fault at node II .At node I all three phase are attenuated by different levels.

CASE C: Two-phase

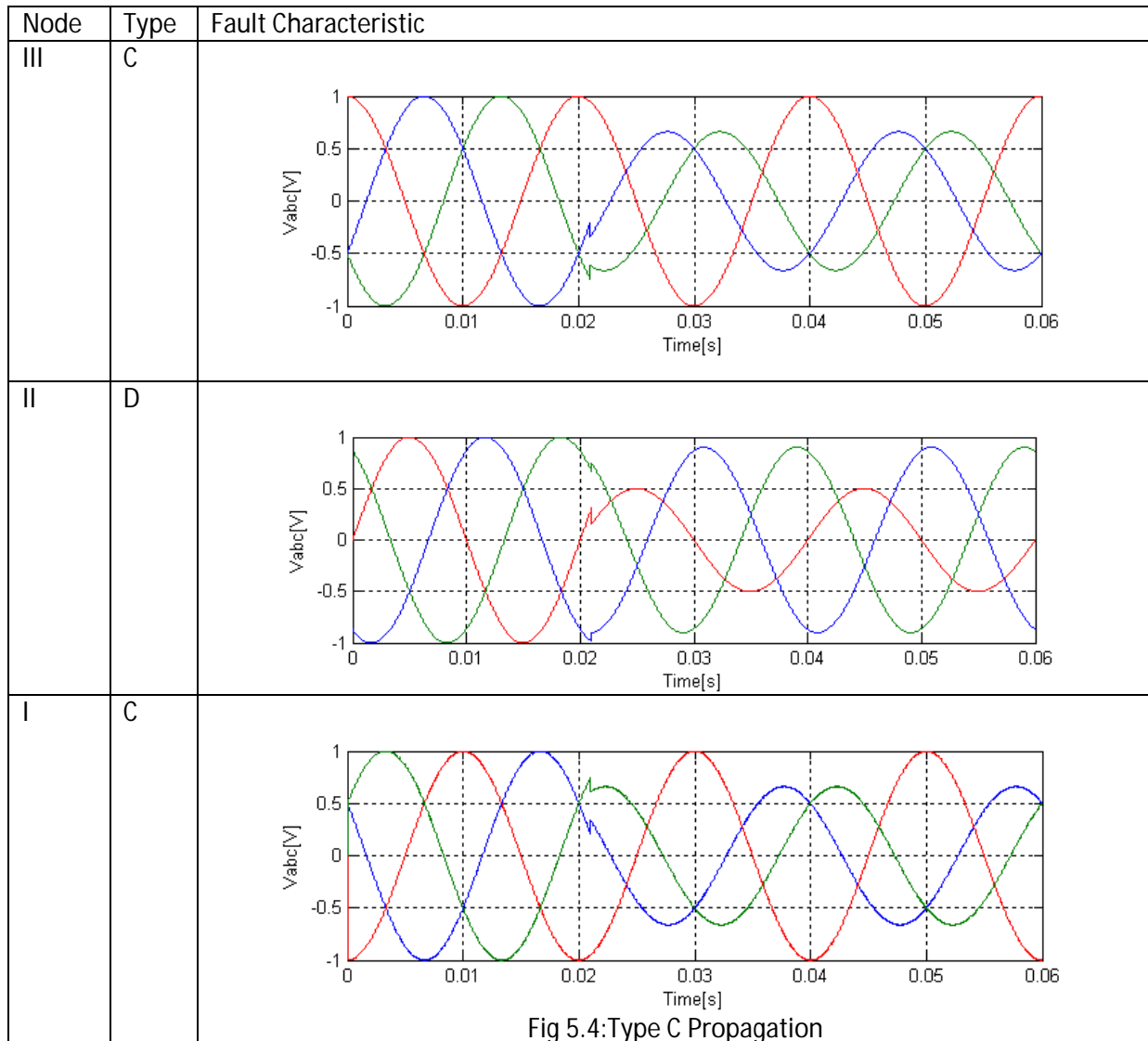


Fig 5.4 shows that the type C faults when measured at different nodes manifests as type D at node II and as type C at node I. As in previous case type D fault has magnitude attenuation of all three phases.

Fig 5.5 shows that the type E faults when measured at different nodes manifests as type F at node II and as type G at node I. Type F and Type G are characterized by attenuation in all three phases.

CASE E: Two-phase-to-ground

Node	Type	Fault Characteristic
III	E	
II	F	
I	G	<p style="text-align: center;">Fig 5.5: Type E Propagation</p>

5.4 Simulation of reactive power injection for different grid faults

Case I: Three Phase faults

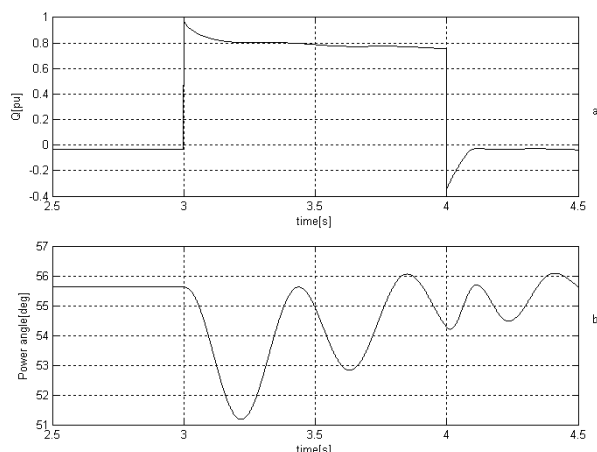


Fig 5.6: Type A at node I

It can be seen in Fig 5.6 that the reactive power is injected into the grid but not in compliance with the grid code. Since the power angle is below $90[\text{deg}]$ the machine does not lose synchronism.

Case II: Single-phase-to-ground

It can be seen in Fig 5.7 that the reactive power is injected into the grid but the ripple occurs due to unbalanced faults. Since the power angle is below $90[\text{deg}]$ the machine does not lose synchronism.

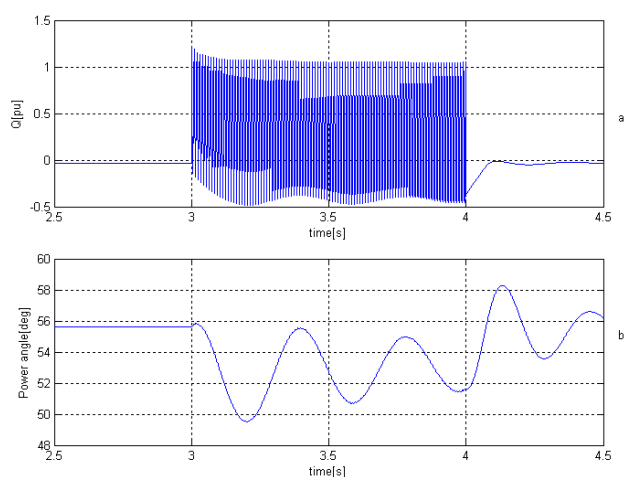


Fig 5.7: Type D at node I

Case III: Two-phase

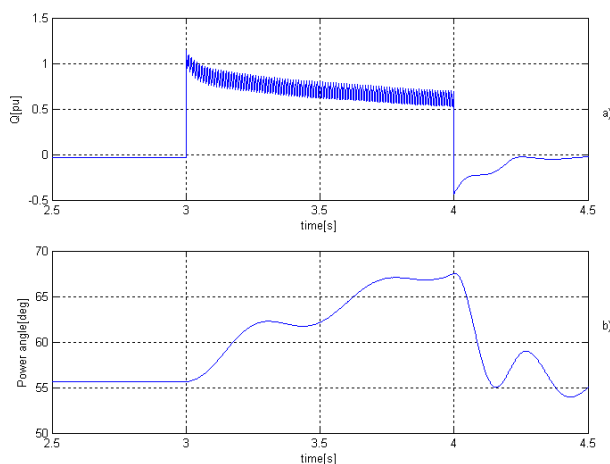


Fig 5.8: Type C at node I

It can be seen in Fig 5.8 that the reactive power is injected into the grid but the ripple occurs due to unbalanced faults but not as severe as in previous case. Since the power angle is below $90[\text{deg}]$ the machine does not lose synchronism.

Case IV: Two-phase-to-ground

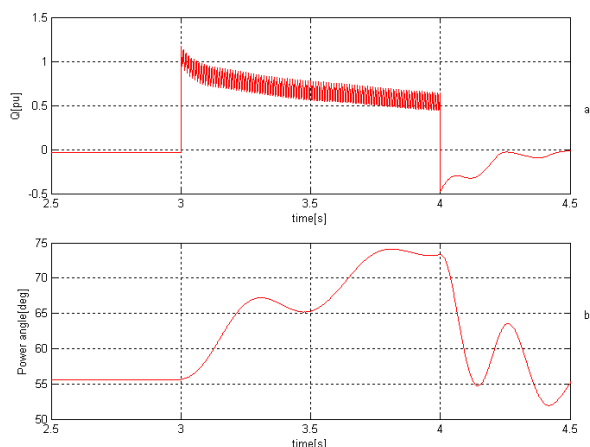


Fig 5.9: Type G at node I

It can be seen in Fig 5.8 that the reactive power is injected into the grid but the ripple occurs due to unbalanced faults but not as severe as in previous case. Since the power angle is below $90[\text{deg}]$ the machine does not lose synchronism. However the power angle is very high and close to losing synchronization.

5.5 Simulation of reactive power injection for 3~ grid fault

In these kinds of faults the short circuit is balanced. Hence no zero sequence component does not exist. Synchronization during these types of fault is easier.

The short circuit current has two components. One is an ac component, corresponding to the armature current required to oppose the time varying flux produced by the field winding as it rotates. The other component is dc, corresponding to the initial flux linkage which existed at the time of the short circuit[23]

5.5.1 No Control/Natural Response

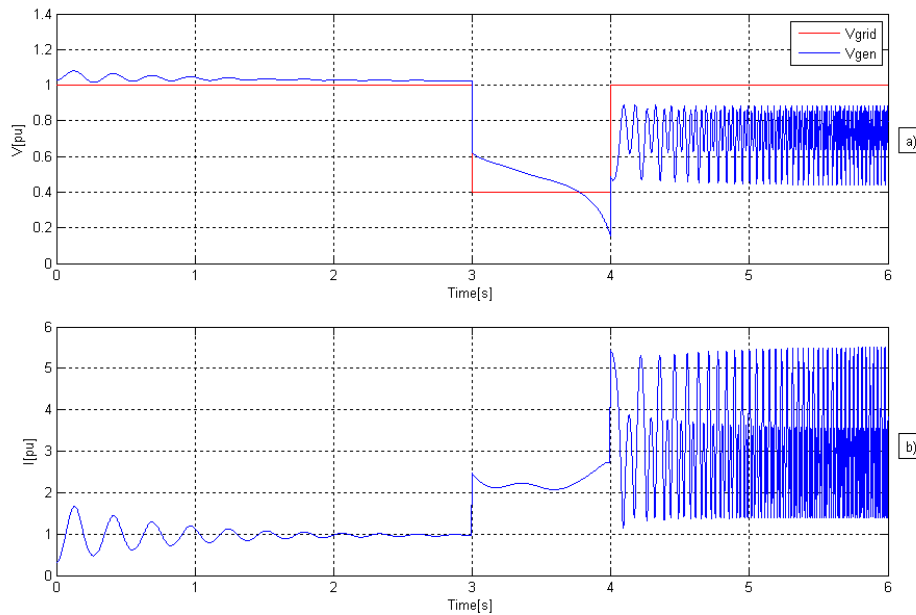


Fig 5.10 : (a) Voltage dip profile and generator voltage (b) Generator current

In Fig 5.10 a three phase fault to 0.4[p.u] occurs at $t=3[s]$ and is cleared at $t=4[s]$. The response of the generator current and voltage is also plotted. Fig 5.12 shows that the excitation voltage is 2[p.u], the SG is over excited at all times under normal operation.

The stator current (Fig 5.10(b)) is increases rapidly during the start of fault. For about 0.700[s], the terminal voltage of the SG (Fig 5.10(a)) is larger than the grid. The loss of synchronization results in oscillatory response with peaks at around 5 [p.u] in current and voltage as consequence of the speed and torque angle (see Fig 5.11(b) and Fig 5.11 (c)). This case represents grid disconnection and since the generator is still being supplied by active power the rotor accelerates at no load.

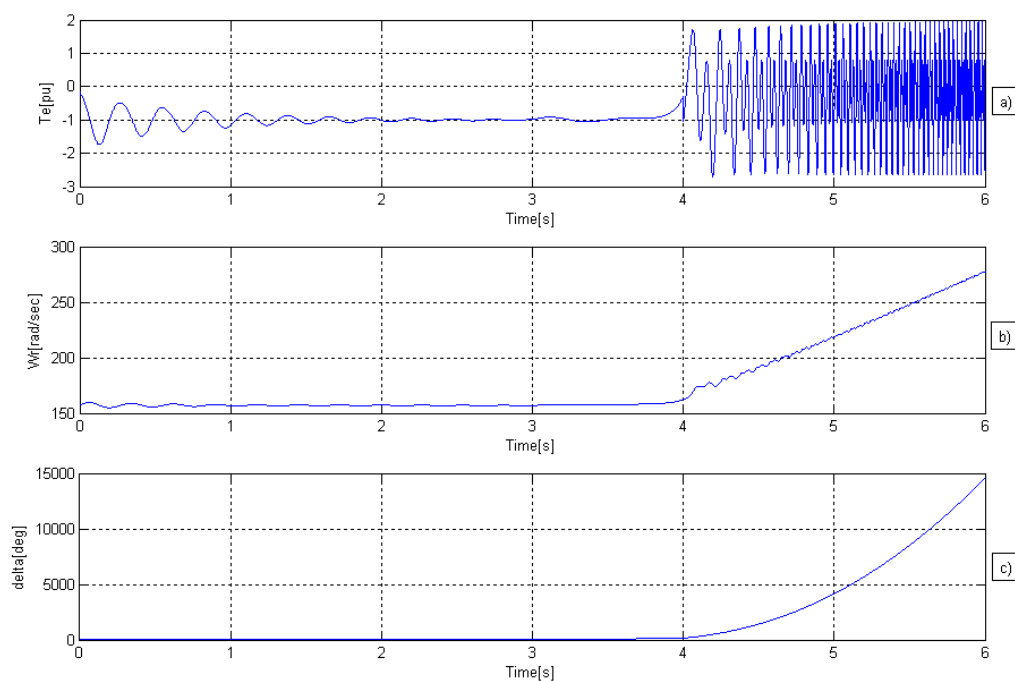


Fig 5.11 : (a) Voltage dip profile and generator voltage (b) Generator current

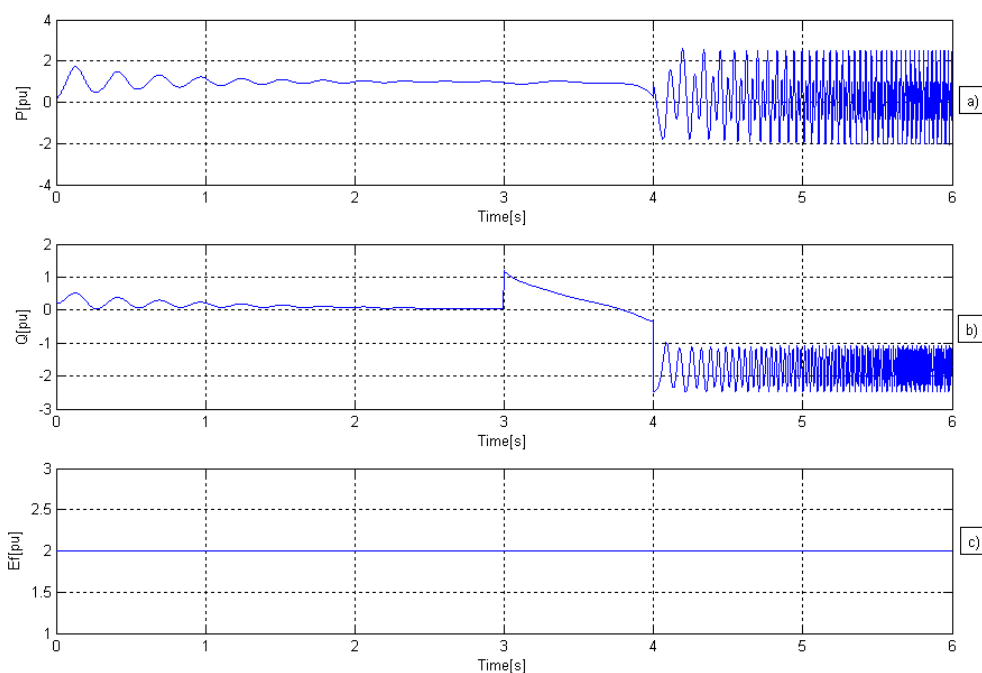


Fig 5.12 : (a) Active power (b) Reactive power (c) Excitation Voltage

Fig 5.12 shows the active, reactive and excitation in the machine. The instant the grid voltage drops the machine is in over-excitation operation as explained in section 3.3.2. Hence the SG naturally injects reactive power to the grid under fault condition. However simultaneously the power angle also increase due to torque on the shaft, hence effectively decreasing the amount of reactive power generate by the SG. When the power angle is over $90[\text{deg}]$ the machine loses synchronization.

Fig 5.12(a) shows that the active power injected to the grid is as per the torque (see Fig 5.11 (a)) on the shaft even during the fault.

5.5.2 Control

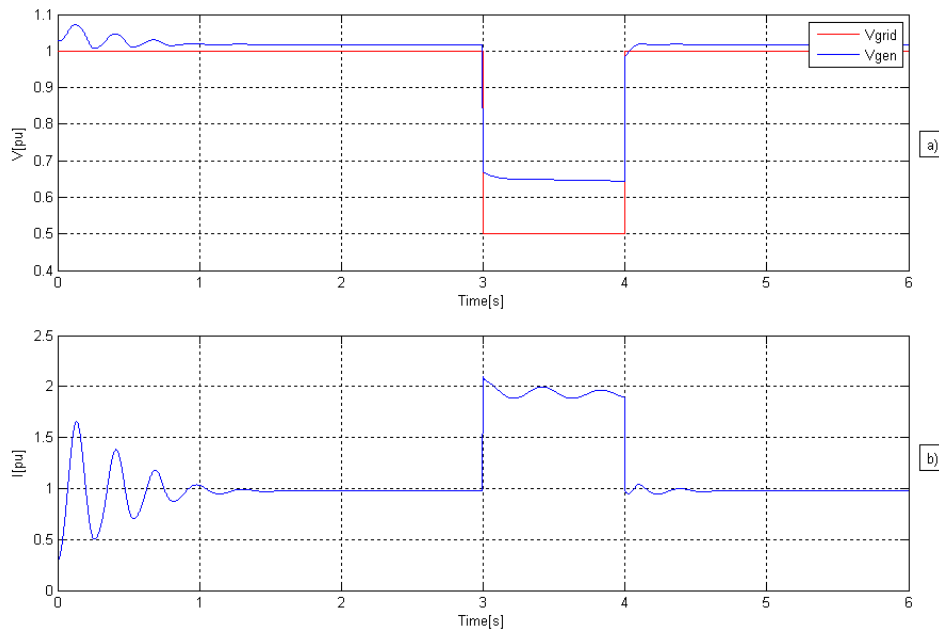


Fig 5.13 : (a) Voltage dip profile and generator voltage (b) Generator current

In Fig 5.13 a three phase fault of 0.5[p.u] occurs at $t=3[s]$ and is cleared at $t=4[s]$. The response of the generator current and voltage is also plotted. The current is greater during the fault due to reactive component. Fig 5.14 shows that the excitation voltage generated via controller which demand up to 4.0 [p.u]. This is not practical because of field winding saturation in the SG.

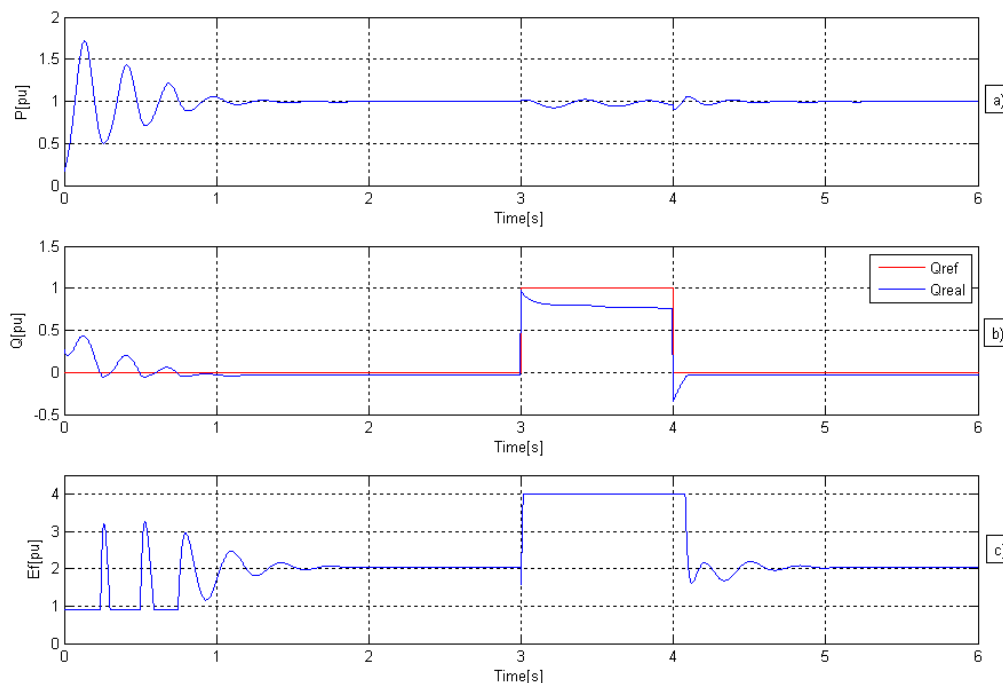


Fig 5.14 : (a) Voltage dip profile and generator voltage (b) Generator current

Fig 5.14(a) shows the active power correspond to the torque in Fig 5.15(a). Fig 5.14(b) shows the reactive power requirement (Q_{ref}) and the reactive power (Q_{real}). It is evident that the machine is not able to inject the required amount of reactive power into the grid. This is caused by the

saturation limit on the induced voltage of 4[p.u]. However the speed and power angle shown in Fig 5.15 illustrate that the machine is able to ride through the fault without disconnection.

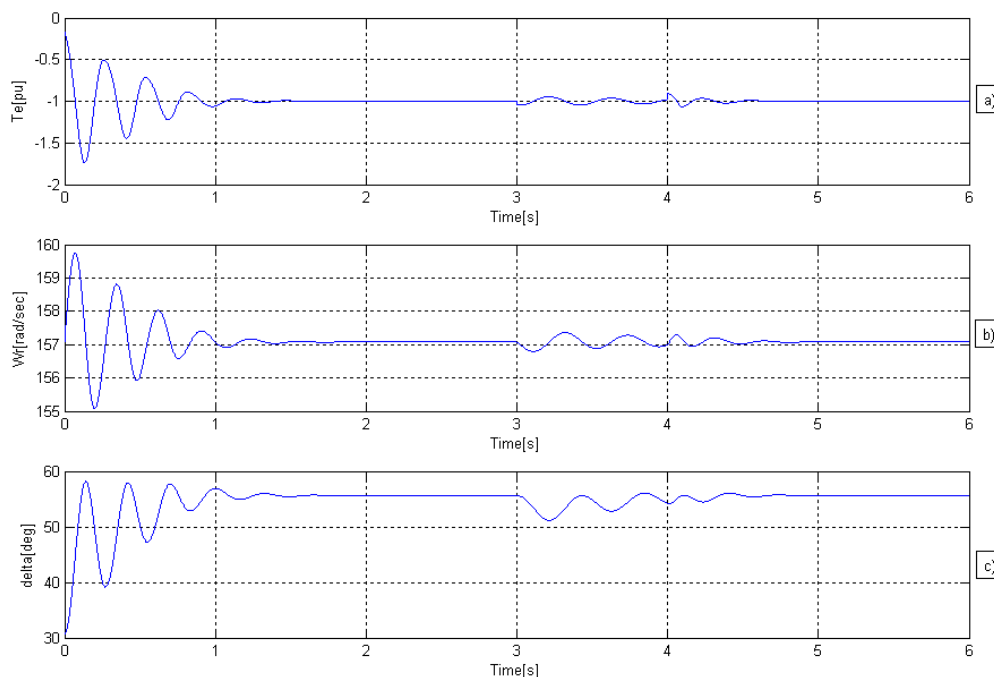


Fig 5.15 : (a) Voltage dip profile and generator voltage (b) Generator current

5.5.3 Grid code requirement

Grid codes are usually made by transmission system operators of countries with high wind energy penetration and incorporate the experience after several years of system operation. Faults and disturbances of the electrical network can never be completely avoided, despite the effort of system operators.

Some of the salient requirements are listed below:

- Network operators require wind turbines to be connected in case of severe disturbances.
- Wind turbines must have power system control(voltage and frequency)
- Wind turbines should have the ability to support the grid during voltage deeps.
- Provide reactive power to support grid stability
- Wind farms connected to HV grids must withstand voltage dips to a certain percentage of the nominal voltage and for a specified duration.
- Increase or decrease output power at the request of the system operator
- Automatically adjust power output in response to frequency changes on the network
- Ability to restart a system after a severe blackout
- Ability to ride through grid faults

This project focuses on the low-voltage ride through capability of a synchronous generator. Factors affecting fault ride through capability are:

- Shape of the voltage dip
- Absolute level of the voltage dip
- Fault type (1 phase, 2 phase, 3 phase)
- Fault clearance time

- Fault location
- Grid strength
- Grid architecture (mesh, radial)
- Active and reactive power conditions prior to the fault
- Active and reactive power requirements after fault clearance
- Load characteristics

Generator characteristics affecting fault ride capability are:

- Rotating inertia
- Generator reactance (Might change the impedance with a series compensator)
- Excitation system and AVR control

An electrical system is stable when the synchronous generator is operating in synchronism with it and there is a balance between demand and production of active and reactive power. Transient stability may be defined as the ability to keep synchronism while a severe fault. Three phase permanent faults are very rare. Most faults in electrical transmission systems involve only one or two phases and ground. One of the important aspects is to stay connected to the grid during faults the requirements or FRT curves by various operators is shown in Fig 5.16

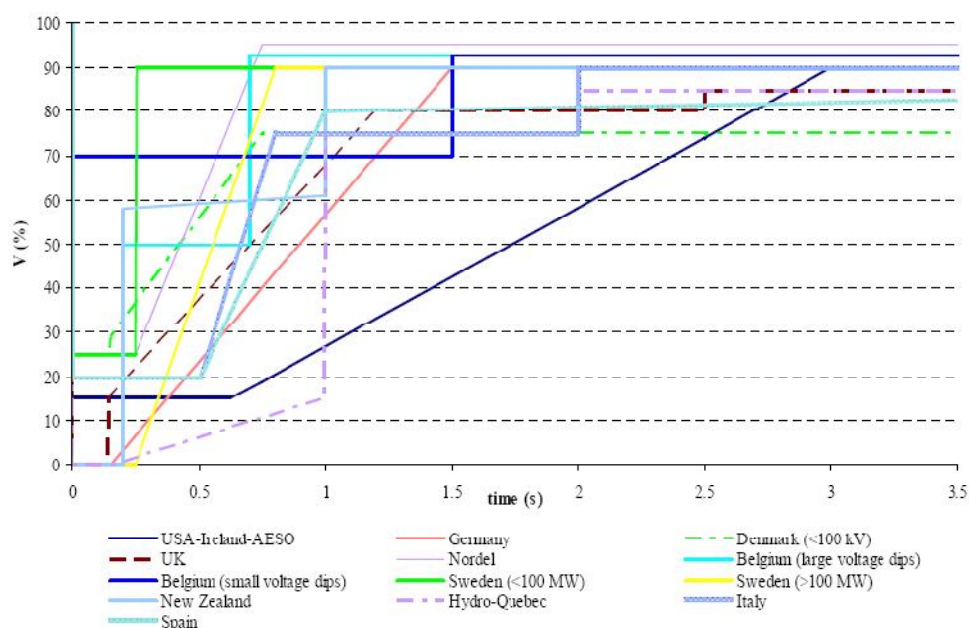


Fig 5.16 :Fault ride through requirement[24]

The following graph (Fig 5.17) presents the reactive power requirement for the wind turbine. E.ON requires wind farms to support grid voltage with additional reactive current during voltage dip, or increased reactive power consumption during voltage swell. Voltage control should take place after 20 ms after fault recognition. Injected current should be around 2 % for every 1 % of voltage drop. A reactive power of 100% should be available if necessary.

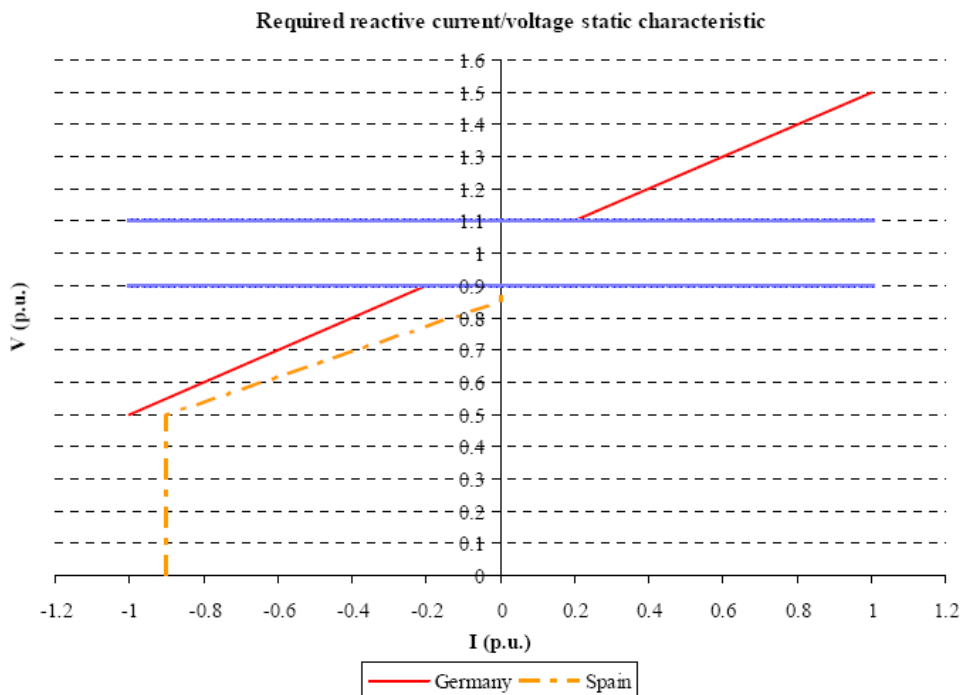


Fig 5.17 :Reactive power requirement

A comparison of reactive power requirements is shown in Fig 5.18 which includes several available active-reactive power curves imposed by national grid codes.

Situations in which a wind turbine must not trip (According to EKRAFT, ELTA, Regulations)
 The wind farm has to remain connected after the following types of faults:[24]

Three phase short circuit	Short circuit in 100 ms
Two phase short circuit with/without earth contact	Short circuit in 100 ms followed by a new short circuit 300...500 ms later, also with a duration of 100 ms
Single-phase short circuit to earth	Single-phase earth fault 300...500 ms later, also with a duration of 100 ms

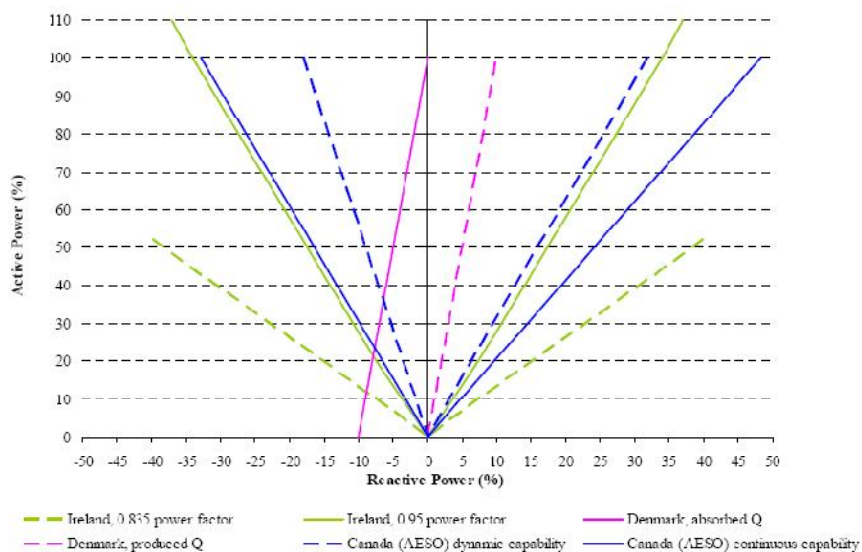


Fig 5.18 :Power power requirement[24]

Before connecting a wind farm to the electrical grid, simulation of stability at symmetric three-phase grid fault has to be simulated. The test has to indicate how the RMS value of current, active , reactive power and voltage vary at the connection terminals during the simulation.

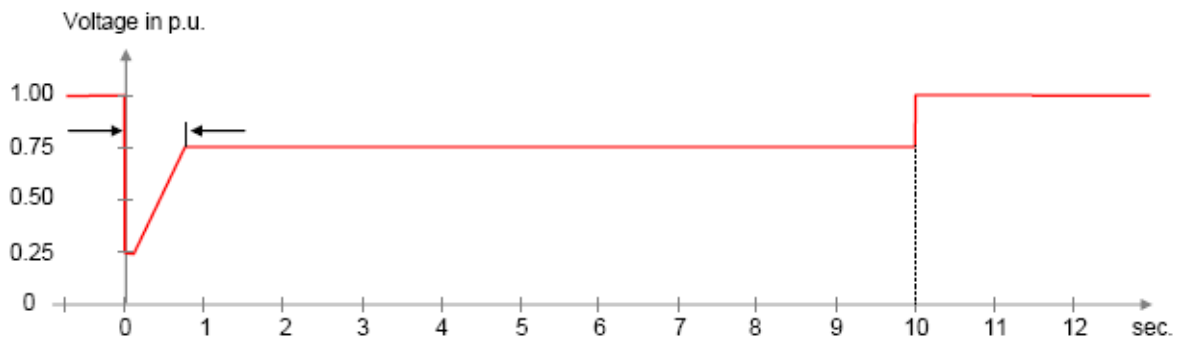


Fig 5.19 :Voltage profile for simulation of symmetric three-phase faults(Danish Code)

The wind farm meets the requirements when:

- The wind farm will produce the rated power no later than 10 seconds after the voltage is above 0.9 [p.u] again. During the voltage dip the active power in the connection has to meet the following conditions:

$$P_{current} \geq k_p * P_{t=0} \left(\frac{U_{current}}{U_{t=0}} \right)^2 \quad 5.1$$

Where:

- $P_{current}$: Current active power measured in the connection point
- $P_{t=0}$: Power measured in the connection point immediately before the voltage dip
- $U_{t=0}$: The voltage in the connection point immediately before the voltage dip
- $U_{current}$: Current voltage measured in the connection point
- $k_p = 0.4$: Reduction factor considering any voltage dips to the generator terminals
- During the voltage dip the reactive current has to be as a maximum 1.0 times the nominal current of the wind farm.
- During voltage dip the wind farm's regulation of the reactive power will change from normal regulation to maximum voltage support.

Fig 5.20 (a) shows the voltage fault profile as per the Danish grid code[24] and the voltage reflected on the terminals of the generator. Fig 5.20 (b) shows the reactive power requirement and the actual reactive power injected into the grid. It is evident that the reactive power requirement is not met. However the SG doesn't lose synchronism under the fault condition as illustrated by Fig 5.20 (c)

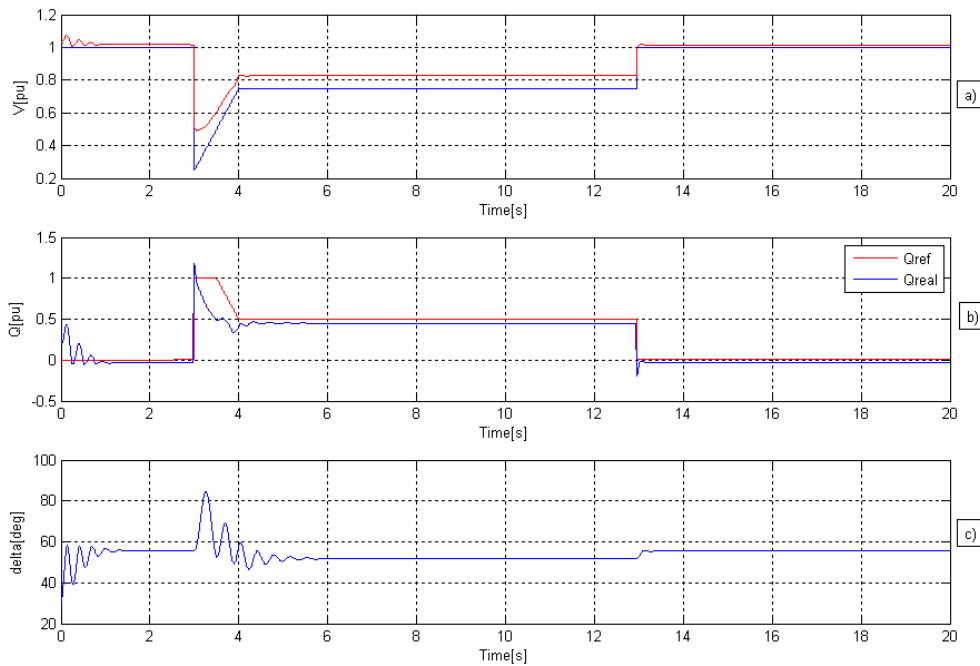


Fig 5.20 : (a)Voltage dip profile and generator voltage (b) Reactive power (c)Power angle

Fig 5.21 shows the operation upto 5kW.

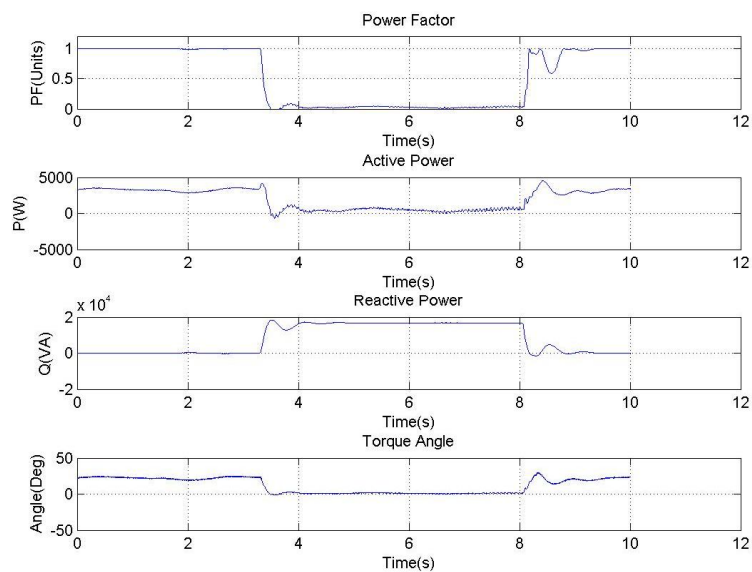


Fig 5.21:Characteristics of 5kW operation

5.6 Lab Implementation

The grid faults were emulated in the lab using inductor based voltage divider. The schematic is shown in Fig 5.22

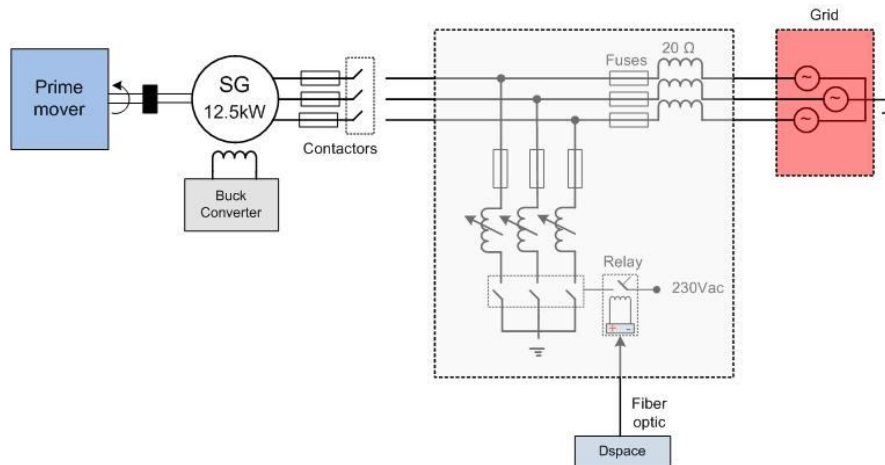


Fig 5.22: Schematic of grid fault generation

The fault level is controlled by adjusting the variable shunt inductors. The series reactance is chosen as 20Ω since for a 220V RMS, the current is 11 A. In accordance with Eqn 3.52 the power is limited to about $\frac{1}{3}$ of nominal power. In case of lower values of inductance the current through the inductor would be higher than the fuse rating of the system.

Table 5-3:

Fuses Location	Rating
Contactors	35 A
Inductor Fuses	25 A

The variable inductors are connected to the circuit using a switch which is controlled by a relay. Timing of the fault is predetermined by grid requirement and the relay is controlled from dSpace.

Type A, Type B, Type C and Type E faults as explained in previous sections, were used to test the synchronous machine.

5.6.1 Type A

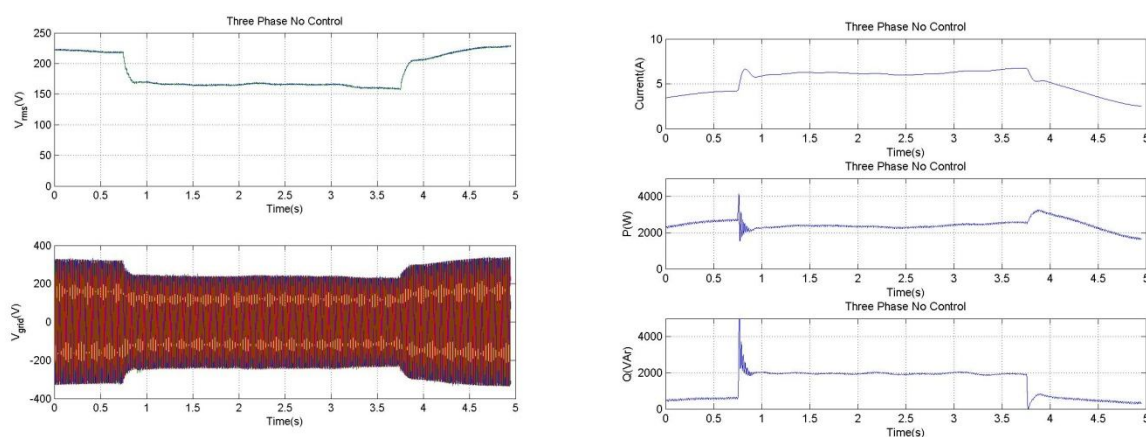


Fig 5.23: Type A fault to 0.75 [p.u] for 3 [s]

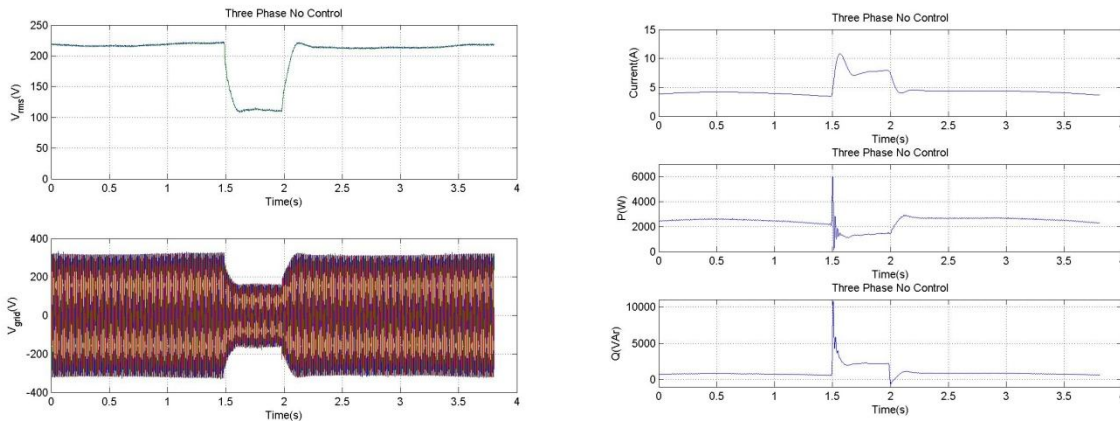


Fig 5.24: Type A fault to 0.5 [p.u] for 0.5 [s]

Fig 5.23 and Fig 5.24 shows the natural response of the machine when no control is implemented. This can be compared with Fig 5.12(b) where the SG injects reactive power naturally. But the faults tested in the lab are of lower magnitude than the simulation results. Hence in Fig 5.12(b) the machine loses synchronization. The comparison illustrates the natural response and not the reactive power capability of the machine.

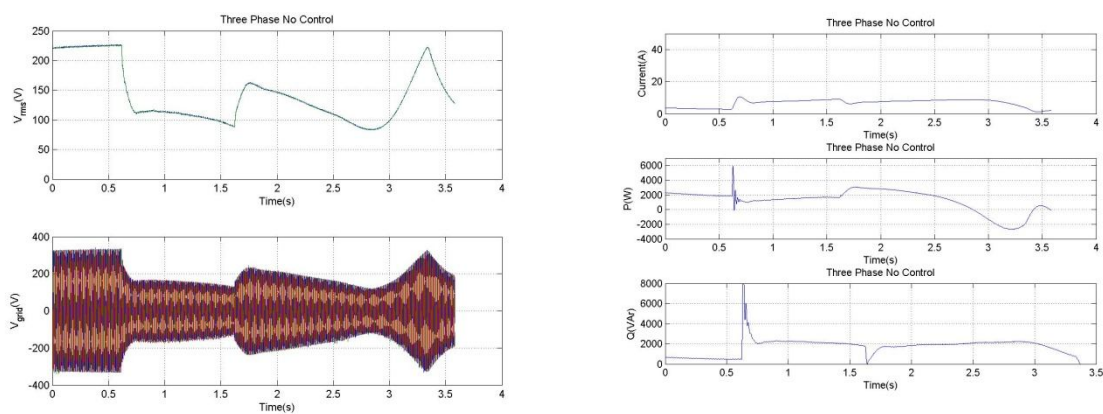


Fig 5.25: Type A fault to 0.5 [p.u] for 1 [s] without control

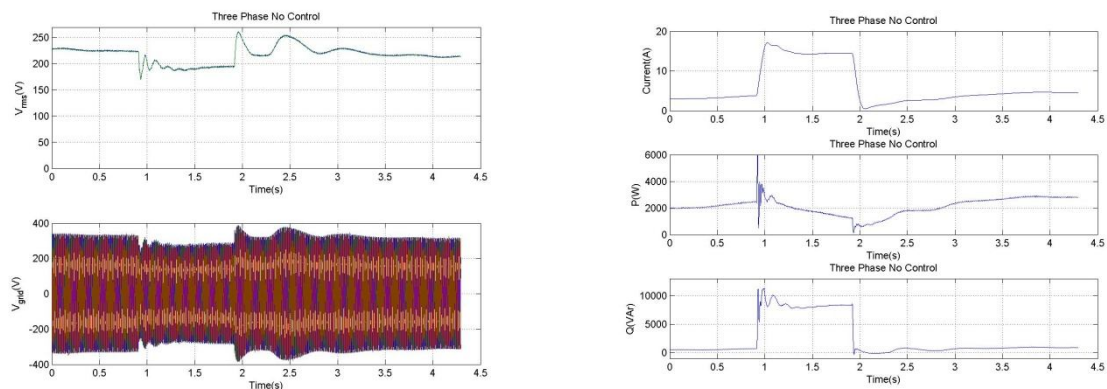


Fig 5.26: Type A fault to 0.5 [p.u] for 1 [s] with control(TYPO)

Fig 5.25 shows the response of the system without control. At the onset of the fault the SG injects reactive power but the magnetizing field cannot be sustained naturally and hence the machine loses synchronization and the active power is consumed by the system. This is seen in active power presented in Fig 5.25. However Fig 5.26 shows that when the controller is used the machine is able to

ride through the fault. A comparison of Fig 5.25 and Fig 5.26 reveals that the required reactive power is 4 times the naturally injected reactive power.

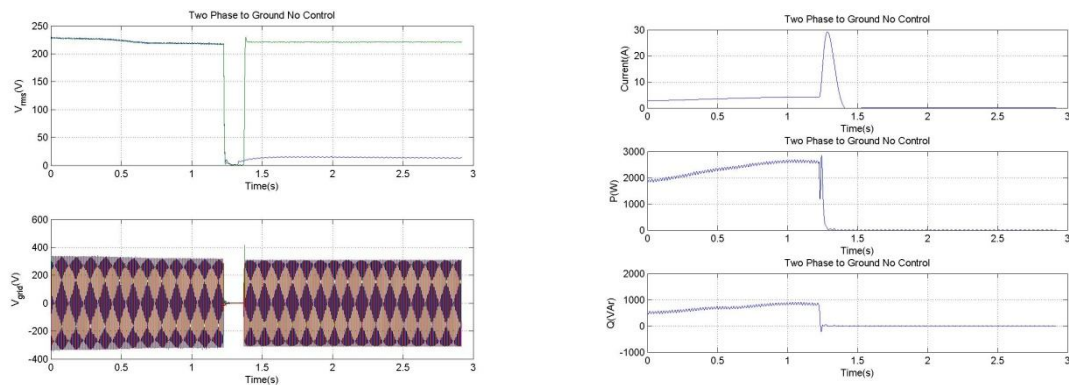


Fig 5.27: Type A fault to 0 [p.u] for 1 [s] without control(change name in graph)

Fig 5.27 shows the fault to 0 [p.u] and naturally the system cannot ride through a fault of this magnitude without control. However the control is also ineffective because of the power rating of the machine.

5.6.2 Type B

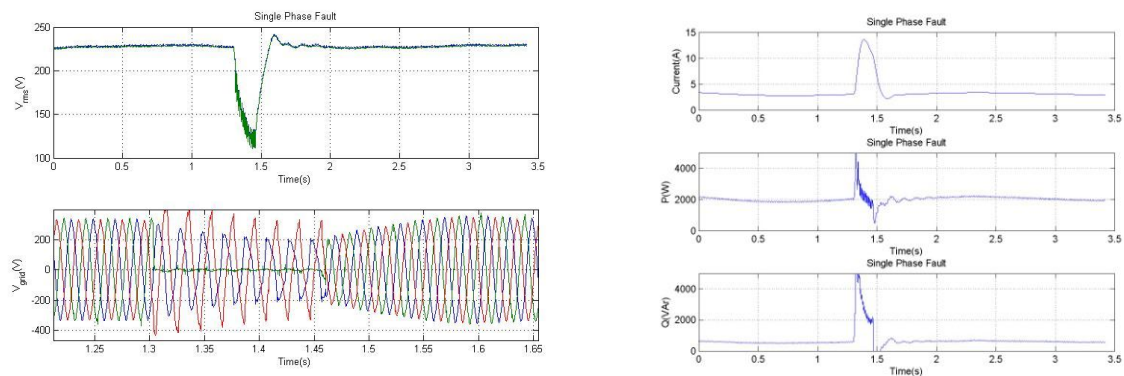


Fig 5.28: Type B to 0 [p.u] for .15 [s] without control

Fig. 5.28 shows that the SG is able to withstands fault of 0 [p.u] for relatively less duration of 0.15[s]. Reactive power is injected naturally. The current increases to 3 [p.u]. Note that the V_{rms} is calculated based on alpha beta components of three phase voltages, hence it is not the fault on the phase. Reactive power controller in lab is using V_{rms} to change the reference of injected reactive power.

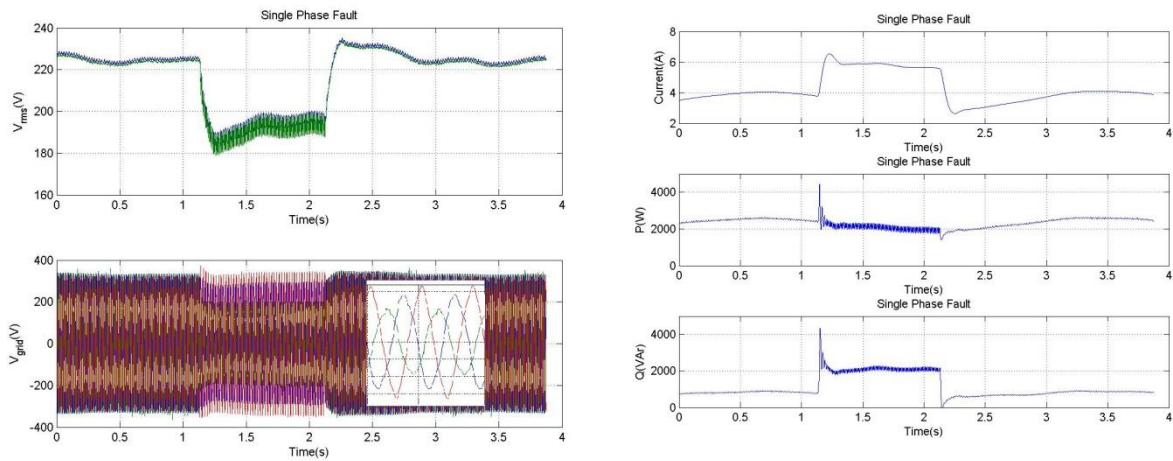


Fig 5.29: Type B fault to 0.5 [p.u] for 1 [s] without control

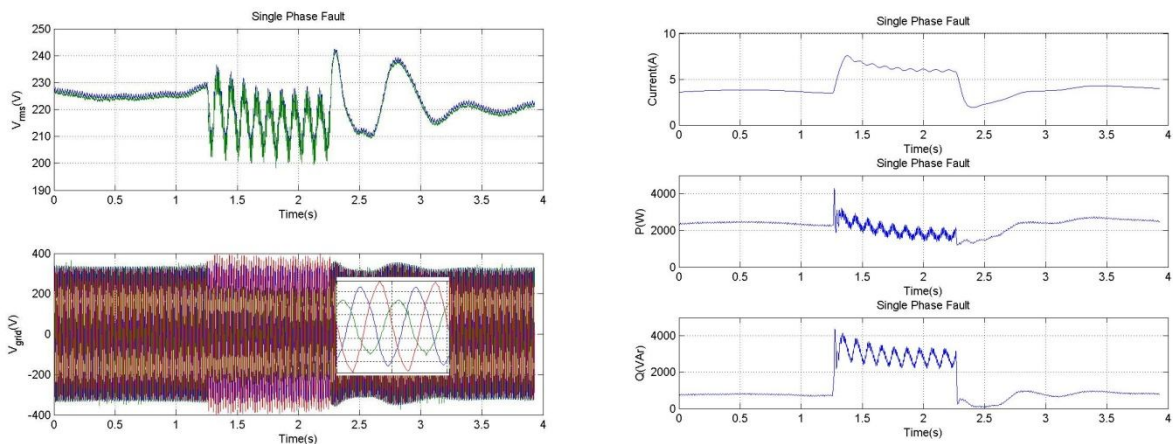


Fig 5.30: Type B fault to 0.5 [p.u] for 1 [s] with control

Fig 5.30 shows that V_{rms} is rippled and contains sags and swells. When the fault is cleared, the amplitude of V_{gen} is still larger the grid, because reactive power is still being injected. Injected power has a oscillating component since the system is not balanced and a larger current flows on one phase. This is seen in both Fig 5.29 and Fig 5.30.

5.6.3 TYPE C

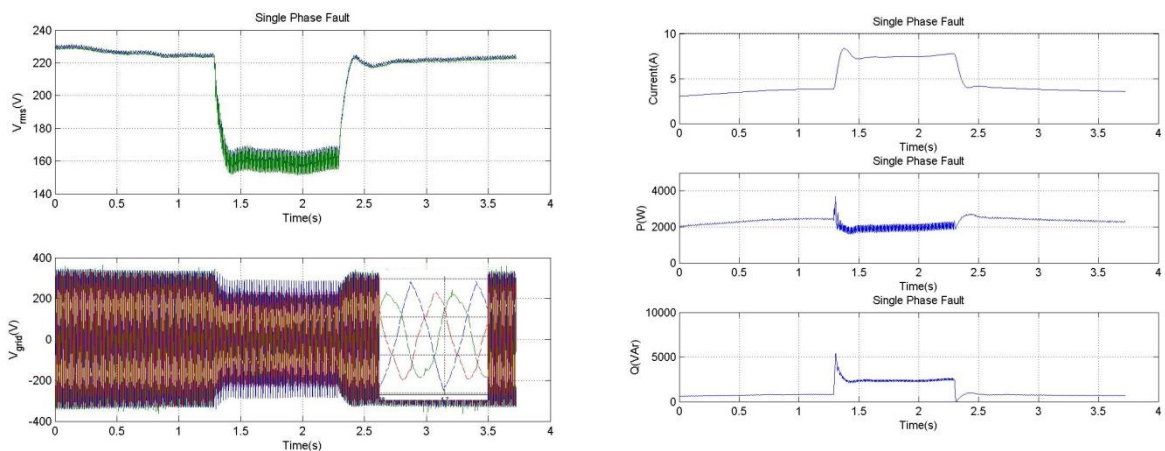


Fig 5.31: Type C fault to 0.5 [p.u] for 1 [s] without control

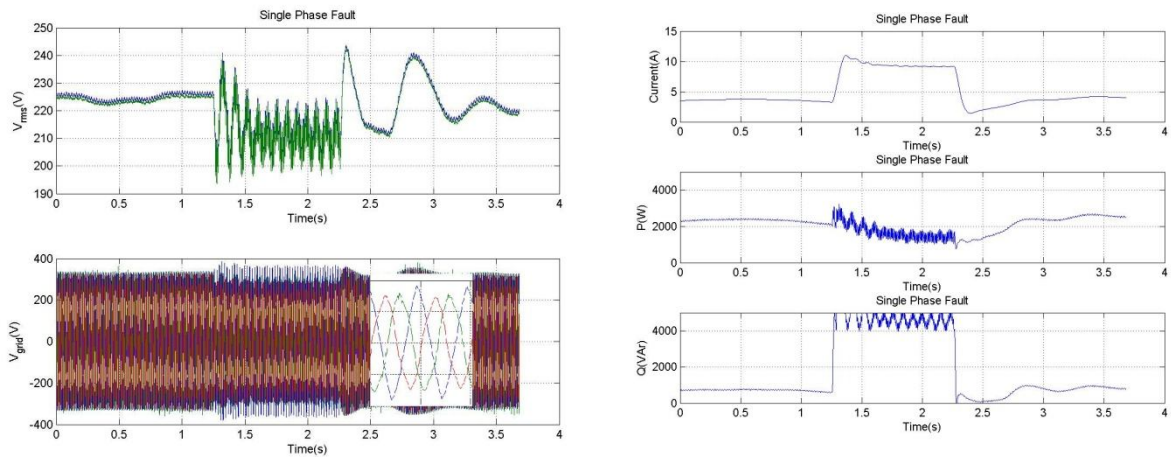


Fig 5.32: Type C fault to 0.5 [p.u] for 1 [s] with control

In uncontrolled mode, SG voltage has same behavior (sags and swell like in Fig 5.30). Reactive power injected is up to 3 times larger in excitation control compared to no control mode. This can also be seen in Fig 5.33 and Fig 5.34 which present the experimental results for the Type E faults.

5.6.4 TYPE E

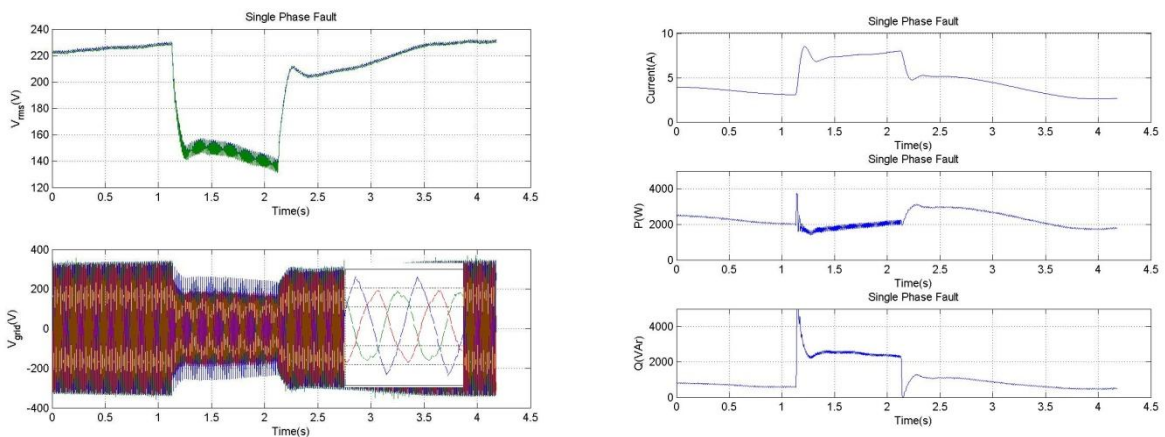


Fig 5.33: Type E fault to 0.5 [p.u] for 1 [s] without control

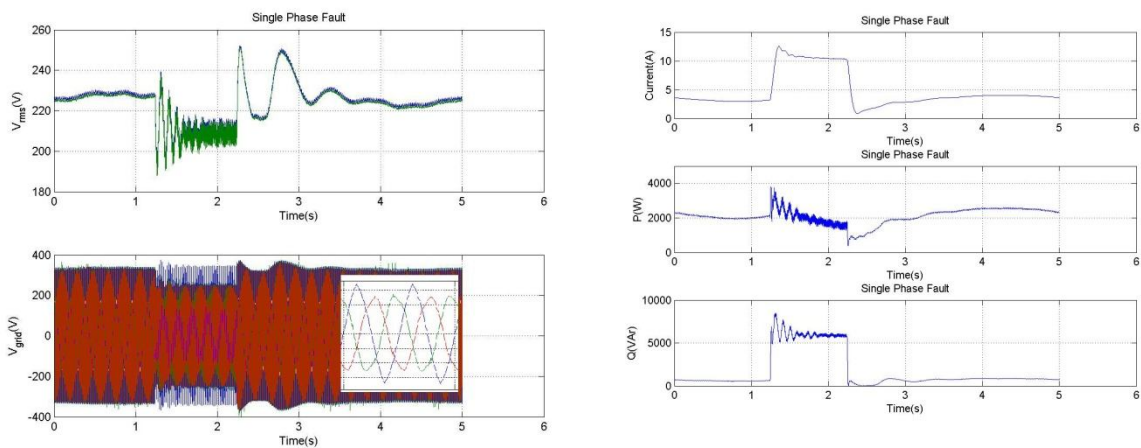


Fig 5.34: Type E fault to 0.5 [p.u] for 1 [s] with control

5.7 Summary

Various grid faults were analyzed based on the results produced from simulation. These results are used to explain the behavior of the machine during different grid fault. Finally the implemented control for reactive power control during the grid faults is tested in the laboratory and the results were presented along with the inferences.

6 Conclusion

The goal of the project was to investigate reactive power control and fault ride through capability of a brushless excited synchronous machine. In order to achieve this, simulations were developed and a laboratory setup was built. The project has been organized in seven chapters.

Chapter one discusses the background and motivation of the thesis. A short state of the art is being presented. The main objectives are being dawned: synchronize brushless synchronous generator to grid, maximize power factor while torque is varying and study the capability of the machine during grid faults. As prime mover in the lab, a three phase induction motor was chosen.

In the project the synchronous generator is driven by an induction motor. Indirect field oriented control is implemented both in MATLAB/Simulink based simulations and experimentally through dSpace. The motor is controlled in speed control for synchronization and in torque control after synchronization to emulate the wind characteristics. This is explained in chapter two.

Next chapter is introducing the theory and general behavior of the classical synchronous generators used in wind turbines.

The synchronous machine is modeled in MATLAB/Simulink to verify the performance of the reactive power control. In physical implementation a DC/DC converter is designed to control the brushless exciter voltage. PI controllers are employed to control the reactive power by controlling the excitation voltage.

The grid faults are prescribed by the national grid codes whose fulfillment is a prerequisite to commissioning of the generator in the wind turbine. Apart from the riding through the fault a synchronous generator is also required to support the network during the faults owing to the naturally ability to inject reactive power into the grid. This is done by controlling the reactive power through external excitation, which is also used to maintain unity power factor during normal operation.

Finally grid faults are created using variable inductors and a relay/switch circuit to control the duration of the fault. The results are presented and compared with the simulations. The observations are reported in the corresponding chapters along with their justifications.

Based on the observation the following inferences are presented. Simulation and laboratory test confirm that the synchronous machine is able to operate at unity power factor under normal load. The machine is able to ride through the faults as see in Chapter 5, but not always able to inject the required reactive power. Since during grid faults, the ability of the synchronous machine to inject reactive power is mainly governed by the following factors.

- **Rotor Inertia:** The inertia determines the speed with which the power angle changes during a grid fault. The input power available at the shaft translates as acceleration during grid faults. For a high value of inertia the acceleration is slower, hence most power is dissipated in accelerating the machine rotor but the speed doesn't increase appreciably. Hence a bigger machine can ride through faults more easily than a smaller machine.
- **Generator Reactance:** As per Eqn 3.52 during a grid fault the value of grid voltage decreases hence to balance the equation either of the two parameters – power angle or reactance. Hence

by dynamically changing reactance the machine can be prevented from losing synchronism. This factor is also related to the saturation of the machine, as the reactance varies when the machine is saturated.

- Excitation system: The speed of the excitation system determines the ability of the generator ability to produce the reactive power required. In case of brushless system, an increase in induced voltage is readily achieved whereas a decrease relies mostly on natural decay of current.
- Thermal Aspects: The reactive power capabilities curve, such as Fig 6.1, indicates the amount of reactive power that a SG is able to produce for a certain active power. When Q is increased, this leads to an increase in field current. Thus, rotor and stator losses will increase owing to heat losses. This limits the amount of reactive power given by the machine. Riding through a grid fault will impose for the generator to inject a level of Q to comply with grid codes. But this will be limited by heat losses. Therefore, a proper cooling system would raise the limit of reactive power.

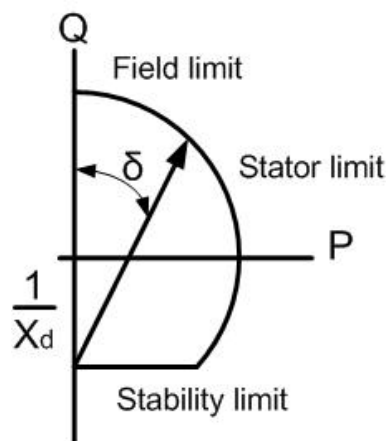


Fig 6.1 Reactive power capability curve

To circumvent these issues the machine maybe changed at design level:

- Hydrogen cooling
- Design synchronous reactance X_s to lie in linear region to avoid saturation
- Reduce load on wind farm by providing STATCOMS and Capacitor but of lesser rating than those used in DFIG's

7 Future Work

As saturation is described as an important factor in the ability of the machine, a detailed model of saturation effects can be implemented in simulation for further analysis.

The limitations of the project present scope for future work in employing more stable and flexible equipment like grid simulators to test grid faults.

Other type of generators like brushed synchronous machines can be coupled with the prime mover and grid fault test bench to investigate their performance.

The results of this project can be used to design a generator that complies with grid codes.

Appendix

A. Laboratory Setup

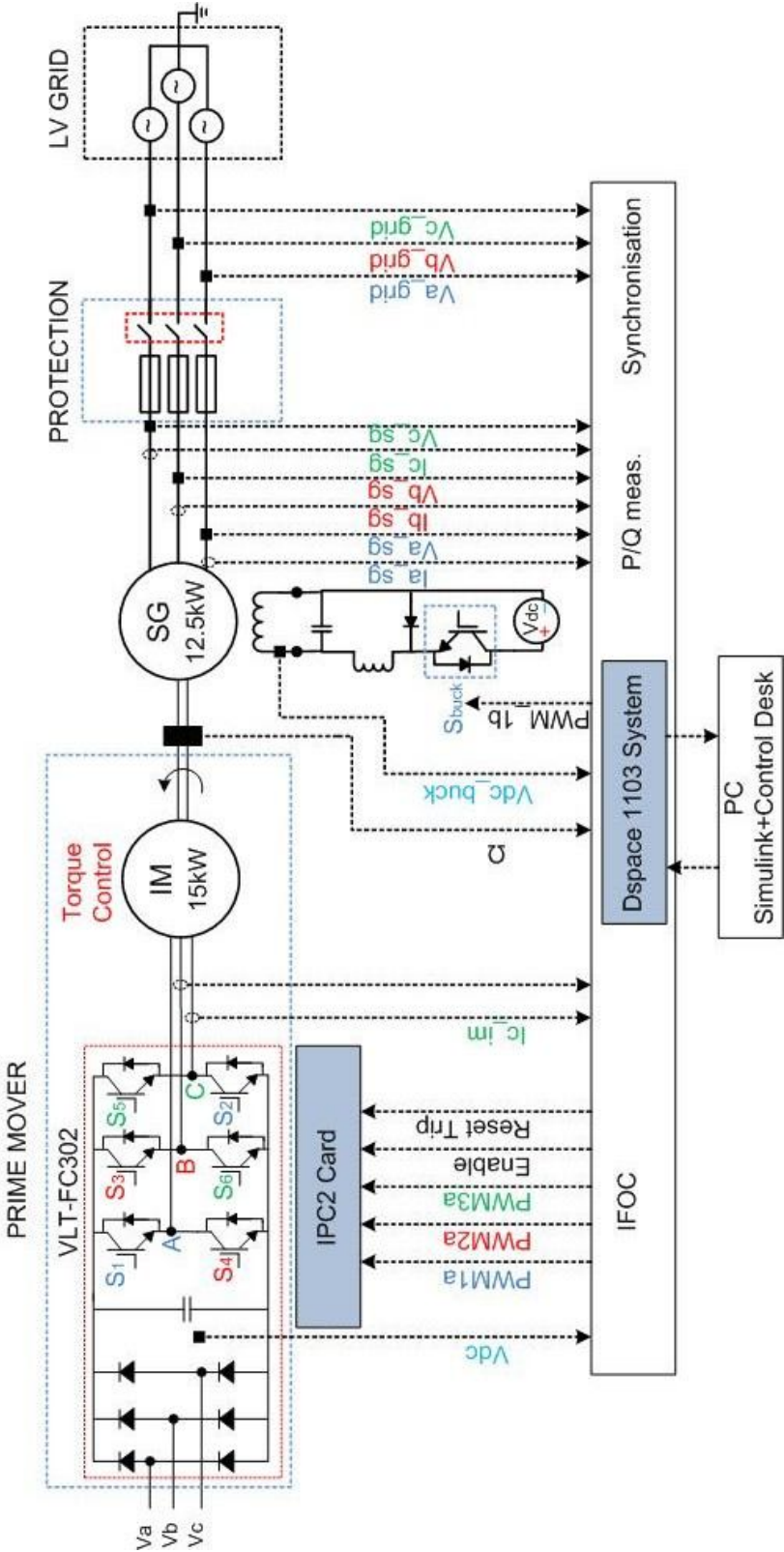


Fig A.1: Laboratory Setup

The setup implemented in the lab is shown in Fig A.1.

- Prime Mover

It consist of a induction machine controlled via a VLT FC302 whose ratings are given below

Induction Machine Rating:

Parameter	Value
Rated Power	15kW
Rated Speed	1453 rpm
Rated Torque	98.6 Nm
Rated Current	28.8 A
Rated PF	0.84
Rated Voltage	230 V Δ / 400 V Y
Pole Pairs	2

Inverter Rating:

Parameter	Value
Supply Voltage	380 – 500 V \pm 10% 525 – 600 V \pm 10% 525 - 690 V \pm 10%
Supply Frequency	50/60 Hz
Output Voltage	0 – 100% of supply
Output Frequency	0 – 1000 Hz
Power	15kW
Topology	2-Level

- Generator

A classic synchronous generator is used in the laboratory. The ratings are as follows

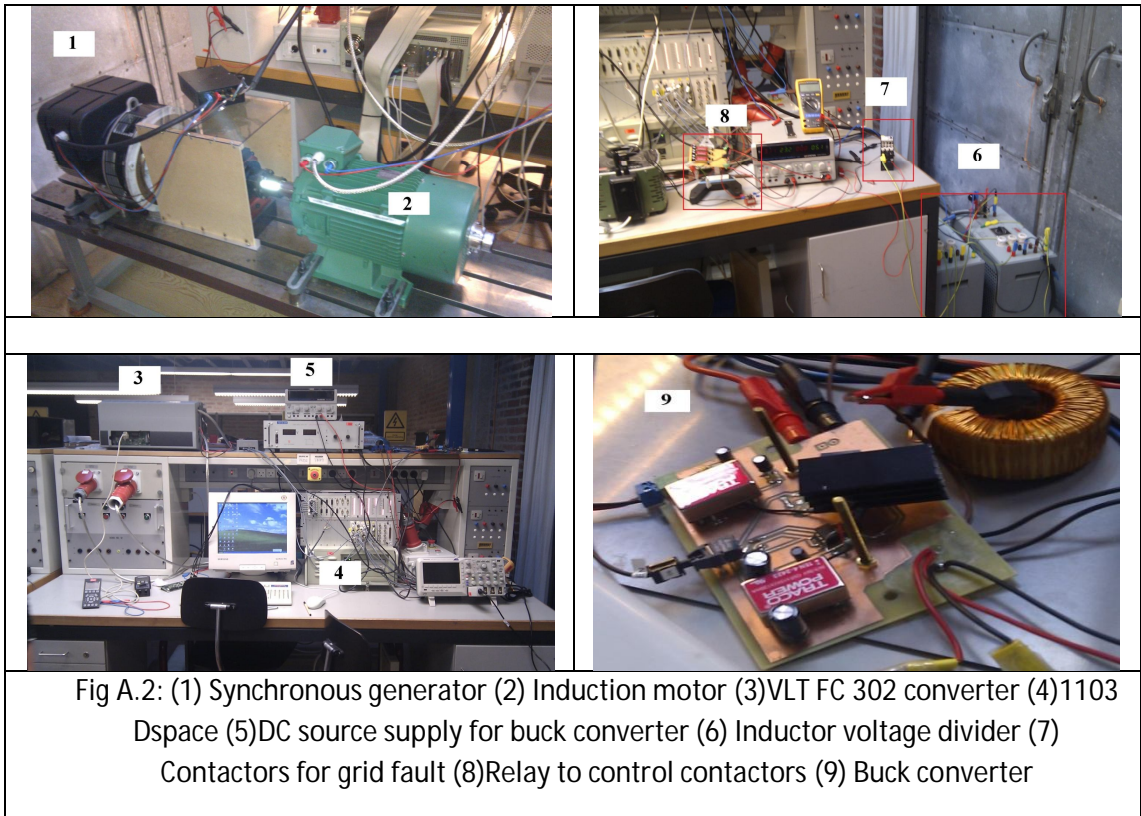
Parameter	Value
Rated Power	10kVA @40° Celsius 16kVA @27° Celsius
Rated Speed	1500 rpm
Rated Excitation Voltage	10V – No Load 24V – Rated Load
Rated Current	16 A @40° Celsius 24 A @27° Celsius
Rated PF	0.8
Rated Voltage	230 V Y
Pole Pairs	2

- Exciter Supply

The exciter is supplied by the buck whose parameters are

Parameter	Value
Inductance	4.16 mH
Capacitor	30 uF
Switching Frequency	5kHz

The photo of the equipment is shown here.



B. Parameters

Induction Machine Parameters

Parameter	Value
R_s	0.3679 Ohm
R_r	0.2319 Ohm
L_{ls}	0.0015 H
L_{lr}	0.0015 H
L_m	0.638 H
J	0.036 kg·m ²
B	0.0161 N.m.s

Synchronous Generator Parameters: 2.15 MW

Parameter	Units
Power	2.15 MW
Rated Frequency	50 Hz
PF	0.95
R_s	0.0064 Ohms
X_d	1.9 Ohms
X_q	0.6 Ohms
X_{ls}	0.026 Ohms
X'_d	0.12 Ohms
X''_d	0.078 Ohms
X'_q	0.12 Ohms
T_{do}	4.2 s
T_{qo}	0.1 s
T''_{do}	0.009 s
T''_{qo}	0.01 s
H	1 p.u

Synchronous Generator Parameters: 12.5 kW

Parameter	Units
Power	12.5 kW
Rated Frequency	50 Hz
PF	0.8
R_s	0.5 Ohms
X_d	16.7 Ohms
X_q	10 Ohms
X_{ls}	1.24 Ohms
X'_d	1.72 Ohms
X''_d	0.86 Ohms
X''_q	1.61 Ohms
T_{do}	0.78 s
T_d	0.074 s

Buck Parameters: 12.5 kW

Parameter	Units
Input Voltage	50 V
Input Power	200 W
Switching Frequency	5kHz
Output Voltage	25 V
Duty Cycle	0.5
Output Current	2 A
Current Ripple (30%)	0.6 A
Inductance	4.2 mH
Voltage Ripple (1%)	0.5 V
Capacitance	30 μ F
Boundary to discontinuous mode	0.3 A

C. m-Files

Synchronous Machine M-File

```

%%%%%%%%%%%%%%%%%%%%%%%%%%%%%%%%%%%%%%%%%%%%%%%%%%%%%%%%%%%%%%%%%%%%%%%%
Main generator parameters%%%%%%%%%%%%%%%%%%%%%%%%%%%%%%%%%%%%%%%%%%%%%%%%%%%%%%%%%%%%%%%%%%%%%%%%
clear all
close all
%%%%%%%%%%%%%%%%%%%%%%%%%%%%%%%%%%%%%%%%%%%%%%%%%%%%%%%%%%%%%%%%%%%%%%%%
%%%%%%%%%%%%%%%%%%%%%%%%%%%%%%%%%%%%%%%%%%%%%%%%%%%%%%%%%%%%%%%%%%%%%%%%
Perunit = 1 % parameters given in per unit of machine base
Frated = 50;
Poles = 4;
Pfrated= 0.95;
Vrated =850;
Prated=2150e3;
%%%%%%%%%%%%%%%%%%%%%%%%%%%%%%%%%%%%%%%%%%%%%%%%%%%%%%%%%%%%%%%%%%%%%%%%
%%%%%%%%%%%%%%%%%%%%%%%%%%%%%%%%%%%%%%%%%%%%%%%%%%%%%%%%%%%%%%%%%%%%%%%%
% Calculate base quantities
we = 2*pi*Frated;
wbase = 2*pi*Frated;
wbasem = wbase*(2/Poles);
Sbase = Prated/Pfrated;
Vbase = Vrated*sqrt(2/3); % Use peak values as base quantities
Ibase = sqrt(2)*(Sbase/(sqrt(3)*Vrated));
Zbase = Vbase/Ibase;
Tbase = Sbase/wbasem;
%%%%%%%%%%%%%%%%%%%%%%%%%%%%%%%%%%%%%%%%%%%%%%%%%%%%%%%%%%%%%%%%%%%%%%%%
%%%%%%%%%%%%%%%%%%%%%%%%%%%%%%%%%%%%%%%%%%%%%%%%%%%%%%%%%%%%%%%%%%%%%%%%
rs = 0.0064; % stator winding resistance
xd = 1.9; % d axis synchronous reactance
xq = 0.6; % q axis synchronous reactance
xls = 0.026; % stator winding leakage reactance
Xs=sqrt(xd*xd+xq*xq);
%%%%%%%%%%%%%%%%%%%%%%%%%%%%%%%%%%%%%%%%%%%%%%%%%%%%%%%%%%%%%%%%%%%%%%%%
%%%%%%%%%%%%%%%%%%%%%%%%%%%%%%%%%%%%%%%%%%%%%%%%%%%%%%%%%%%%%%%%%%%%%%%%
xpd = 0.12; % d axis transient reactance
xpq = 0; % q axis transient reactance
%%%%%%%%%%%%%%%%%%%%%%%%%%%%%%%%%%%%%%%%%%%%%%%%%%%%%%%%%%%%%%%%%%%%%%%%
%%%%%%%%%%%%%%%%%%%%%%%%%%%%%%%%%%%%%%%%%%%%%%%%%%%%%%%%%%%%%%%%%%%%%%%%
xppd = 0.078; % d axis sub transient reactance
xppq = 0.12; % q axis sub transient reactance
%%%%%%%%%%%%%%%%%%%%%%%%%%%%%%%%%%%%%%%%%%%%%%%%%%%%%%%%%%%%%%%%%%%%%%%%
%%%%%%%%%%%%%%%%%%%%%%%%%%%%%%%%%%%%%%%%%%%%%%%%%%%%%%%%%%%%%%%%%%%%%%%%
Tpdo = 4.2; % d axis transient time constant
Tpqo = 0.1; % q axis transient time constant
%%%%%%%%%%%%%%%%%%%%%%%%%%%%%%%%%%%%%%%%%%%%%%%%%%%%%%%%%%%%%%%%%%%%%%%%
%%%%%%%%%%%%%%%%%%%%%%%%%%%%%%%%%%%%%%%%%%%%%%%%%%%%%%%%%%%%%%%%%%%%%%%%
Tppdo = 0.009; % d axis sub transient time constant
Tppqo = 0.010; % q axis sub transient time constant
%%%%%%%%%%%%%%%%%%%%%%%%%%%%%%%%%%%%%%%%%%%%%%%%%%%%%%%%%%%%%%%%%%%%%%%%
%%%%%%%%%%%%%%%%%%%%%%%%%%%%%%%%%%%%%%%%%%%%%%%%%%%%%%%%%%%%%%%%%%%%%%%%
H = 1;
Omega = 0; % mechanical damping coeff
%%%%%%%%%%%%%%%%%%%%%%%%%%%%%%%%%%%%%%%%%%%%%%%%%%%%%%%%%%%%%%%%%%%%%%%%
%%%%%%%%%%%%%%%%%%%%%%%%%%%%%%%%%%%%%%%%%%%%%%%%%%%%%%%%%%%%%%%%%%%%%%%%
% Calculate dq0 equivalent circuit parameters

```

```

if(xls ==0) xls = x0 % assume leakage reactance = zero_sequence
end

xmq = xq - xls; % d axis stator magnetizing reactance
%xmq = c*Lmq;
xmd = xd - xls; % q axis stator magnetizing reactance
%xmd = c*Lmd;
xplf = xmd*(xpd - xls)/(xmd - (xpd-xls)); % field leakage reactance
%xplf = c*Llfd;
xplkd = xmd*xplf*(xppd-xls)/(xplf*xmd - ...
(xppd-xls)*(xmd+xplf)); % d axis damper leakage reactance
%xplkd = c*Llkd;
xplkq = xmq*(xppq - xls)/(xmq - (xppq-xls)); % q axis damper leakage
reactance
%xplkq = c*Llkq;
rpf = (xplf + xmd)/(wbase*Tpdo); % field resistance
%rpf = Rfd;
rpkd = (xplkd + xpd - xls)/(wbase*Tppdo); % d axis damper resistance
%rpkd = Rkd;
rpkq = (xplkq + xmq)/(wbase*Tppqo); % q axis damper resistance
%rpkq = Rkq;
%%%%%%%%%%%%%%%%%%%%%%%%%%%%%%%%%%%%%%%%%%%%%%%%%%%%%%%%%%%%%%%%%%%%%%%%
%%%%%%%%%%%%%%%%%%%%%%%%%%%%%%%%%%%%%%%%%%%%%%%%%%%%%%%%%%%%%%%%%%%%%%%%
% Convert to per unit dqo circuit parameters
if(Perunit == 0) % parameters given in Engineering units
fprintf('Dq0 circuit paramters in per unit\n')

H = 2;
rs = rs/Zbase;
xls = xls/Zbase;

xppd = xppd/Zbase;
xppq = xppq/Zbase;
xpd = xpd/Zbase;
xpq = xpq/Zbase;

xd = xd/Zbase;
xq = xq/Zbase;

xmd = xmd/Zbase;
xmq = xmq/Zbase;

rpf = rpf/Zbase;
rpkd = rpkd/Zbase;
rpkq = rpkq/Zbase;

xplf = xplf/Zbase;
xplkd = xplkd/Zbase;
xplkq = xplkq/Zbase;

end
%%%%%%%%%%%%%%%%%%%%%%%%%%%%%%%%%%%%%%%%%%%%%%%%%%%%%%%%%%%%%%%%%%%%%%%%
%%%%%%%%%%%%%%%%%%%%%%%%%%%%%%%%%%%%%%%%%%%%%%%%%%%%%%%%%%%%%%%%%%%%%%%%
%*****
% Establish initial conditions for starting simulation

wb=wbase;
xMQ = (1/xls + 1/xmq + 1/xplkq)^(-1);
xMD = (1/xls + 1/xmd + 1/xplf + 1/xplkd)^(-1);

```

```

% Specify desired operating condition lists

P = 1;% specify range and increment of real
Q = 0; % and reactive output power,
      % P is negative for motoring
Vt = 1 + 0*j; % specify terminal voltage
thetaeo = angle(Vt); % initial value of voltage angle
Vm = abs(Vt);
St = P+Q*j; % generated complex power

%%%%%%%%%%%%%%%%%%%%%%%%%%%%%%%%%%%%%%%%%%%%%%%%%%%%%%%%%%%%%%%%%%%%%%%%
%%%%%%%%%%%%%%%%%%%%%%%%%%%%%%%%%%%%%%%%%%%%%%%%%%%%%%%%%%%%%%%%%%%%%%%%
% Use steady-state phasor equations to determine
% steady-state values of fluxes, etc to establish good
% initial starting condition for simulation
% - or good estimates for the trim function
% It - phasor current of generator
% St - complex output power of generator
% Vt - terminal voltage phasor
% Eq - Voltage behind q-axis reactance
% I - d-q current with q axis align with Eq

It = conj(St/Vt);
Eq = Vt + (rs + j*xq)*It;
delt = angle(Eq); % angle Eq leads Vt

%%%%%%%%%%%%%%%%%%%%%%%%%%%%%%%%%%%%%%%%%%%%%%%%%%%%%%%%%%%%%%%%%%%%%%%%
%%%%%%%%%%%%%%%%%%%%%%%%%%%%%%%%%%%%%%%%%%%%%%%%%%%%%%%%%%%%%%%%%%%%%%%%
% compute q-d steady-state variables

Eqo = abs(Eq);
I = It*(cos(delt) - sin(delt)*j); % same as I = (conj(Eq)/Eqo)*It;
Iqo = real(I);
Ido = -imag(I); % when the d-axis lags the q-axis
Efo = Eqo + (xd-xq)*Ido;
Ifo = Efo/xmd;

Psiado = xmd*(-Ido + Ifo);
Psiaqo = xmq*(-Iqo);

Psiqo = xls*(-Iqo) + Psiaqo;
Psido = xls*(-Ido) + Psiado;
Psifo = xplf*Ifo + Psiado;
Psikqo = Psiaqo;
Psikdo = Psiado;

Vto = Vt*(cos(delt) - sin(delt)*j);
Vqo = real(Vto);
Vdo = -imag(Vto);
Sto = Vto*conj(I);
Eqpo = Vqo + xpd*Ido + rs*Iqo;
Edpo = Vdo - xpq*Iqo + rs*Ido;

delto = delt;% initial value of rotor angle
thetaro = delto+thetaeo;% thetar(0) in variable frequency oscillator
Pemo = real(Sto);
Qemo = imag(Sto);
Tmech = Pemo;

```

```
T2piy3 = 2*pi/3; % phase angle of bus phase voltages
```

Induction Machine M-File

```
clear all;
close all;
v =400*sqrt(2);
f = 50;
%%constants note vr_alpha=0 vr_beta=0
rs = 0.3679;
rr = 0.2319;
lm = 63.8e-3;%magnetising inductance
ls = lm + 0.0015;
lr = lm + 0.0015;
lm = 63.8e-3;%magnetising inductance
sigs = ls/lm-1;%stator leakage
sigr = lr/lm-1;%rotor leakage
sig = 1-lm^2/(ls*lr);%leakage factor
l_sigma = lr*ls - lm*lm;%inductance leakage
J = 0.036;
b = 0.0161;
ts = ls/rs;
tr = lr/rr;
p=4;
% Induction motor subsystem verification for steady state
w=2*pi*f;
Vth = i*w*lm/(rs+i*w*(ls))*v/sqrt(2);
Zth=i*w*lm*(rs+i*w*(ls-lm))/(rs+i*w*(ls));
slip=(1500-1400)/1500
Te=(3/2)*p/w*((abs(Vth)^2)*rr/slip)/((real(Zth)+rr/slip)^2+(imag(Zth)+w*(lr-lm))^2)%torque
Temax=3*p/4/w*(abs(Vth)^2)/(real(Zth)+sqrt(real(Zth)^2+((imag(Zth)+w*(lr-lm))^2)))%max torque
smax=rr/sqrt(real(Zth)^2+(imag(Zth)+ w*(lr-lm))^2)%max slip
%%plot
sl=1:-0.001:-1;
T=Temax*2./(sl/smax+smax./sl);
plot(-sl,T);
grid on;
xlabel('SLIP');
ylabel('TORQUE');
clc
```

Brushless Exciter M-File

```
close all;
P=2;%no:of poles
rs=0.121;%Stator resistance
rfd=4;%Field resistance
lmd=5e-3;%d-axis coupling inductance
lmq=5e-3;%q-axis coupling inductance
llfd = 2.5e-3;%d-axis field winding leakage(reflected to stator)
lls = 10e-4;
L=[-(lls + lmd) 0 lmd;
    0 -(lls+lmq) 0;
    -lmd 0 (llfd+lmd);]
A=L^-1;
Ibase=25
```

D. Symmetric Component

Any set of unbalanced three phase quantities can be expressed as the sum of three symmetrical sets of balanced phasors. Using this, unbalanced systems conditions can be analyzed.

Positive, negative and Zero Sequence Components

There are three sets of independent components in a three phase system: positive, negative and zero for both current and voltage.

- Positive sequence voltages are supplied by generators and have a clockwise rotation and are 120° apart (ABC).
- Negative sequence components are also 120° phase shifted but they have a counter-clockwise rotation (ACB).
- The zero sequence components are equal in magnitude, have the same phase, therefore there is no rotation.

The symmetrical components are used to determine any unbalanced current or voltage. Three phase voltages from symmetrical components are calculated as:

$$V_a = V_p + V_n + V_0 \quad D.1$$

$$V_b = a^2 V_p + a V_n + V_0 \quad D.2$$

$$V_c = a V_p + a^2 V_n + V_0 \quad D.3$$

The sequence voltages from 3 phase unbalanced voltages can be calculated with the following:

$$V_0 = \frac{1}{3}(V_a + V_b + V_c) \quad D.4$$

$$V_p = \frac{1}{3}(V_a + aV_b + a^2V_c) \quad D.5$$

$$V_n = \frac{1}{3}(V_a + a^2V_b + aV_c) \quad D.6$$

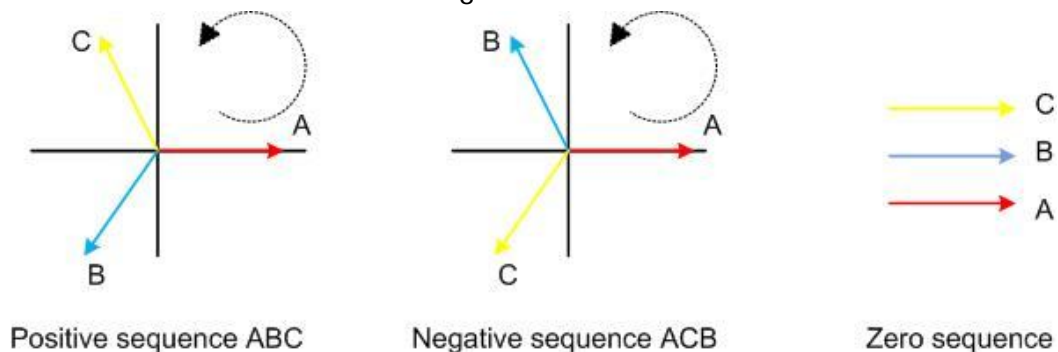


Fig D.3: Symmetrical components

E. Buck Converter

The buck converter produces a lower output voltage than the input voltage V_d . Output voltage is calculated based on the following equation:

$$V_o = \frac{1}{T_s} \int_0^{T_s} v_o(t) dt = \frac{1}{T_s} \left(\int_0^{T_{on}} V_d dt + \int_{T_{on}}^{T_s} 0 dt \right) = \frac{t_{on}}{T_s} V_d \quad \text{E.7}$$

$$V_o = DV_d \quad \text{E.8}$$

Basic circuit configuration is shown in Fig E.4(a). Output voltage is controlled by varying duty cycle t_{on}/T_s (Fig E.4b). Output voltage ripple is reduced by using a low pass filter. While the switch is on, the diode in Fig E.4a is reverse biased and input voltage is feeding the load through the inductor. When the switch is off, inductor current flows through the diode transferring some of the energy to the load.

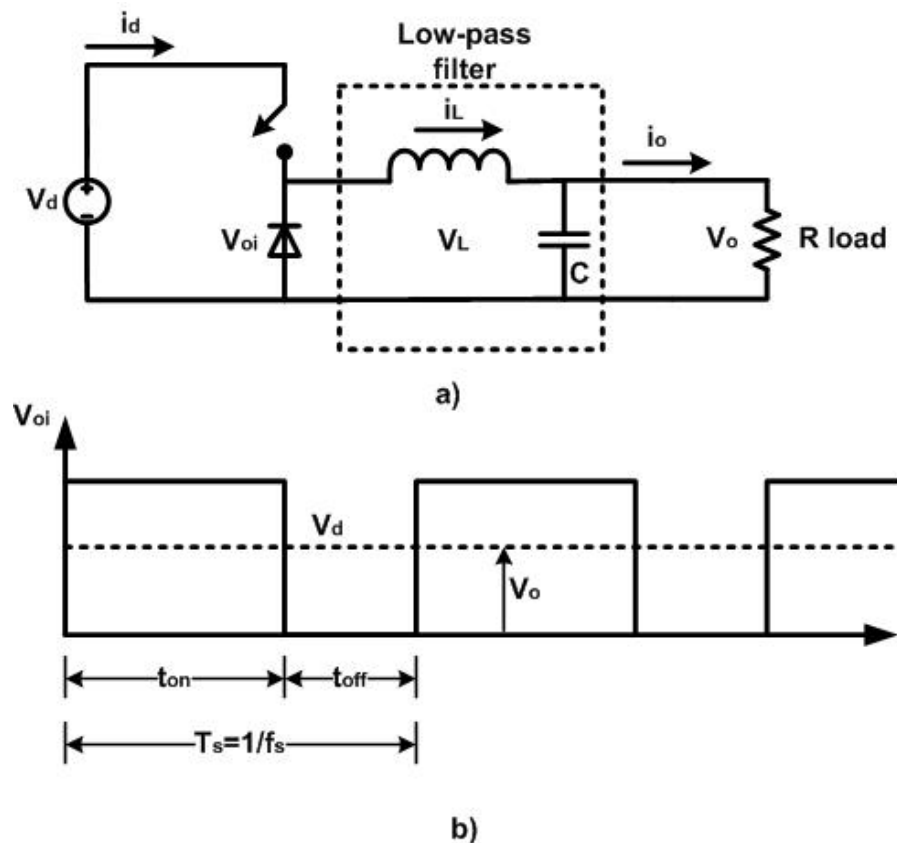


Fig E.4 Buck converter

Fig E.0.5 shows the waveform of the inductor current. During t_{on} , switch is conducting inductor current and diode is reverse biased. Voltage across the inductor is $V_L = V_d - V_o$. This will cause an increase in inductor current i_L . While the switch is off, $V_L = -V_o$. Current continues to flow due to inductive energy storage.

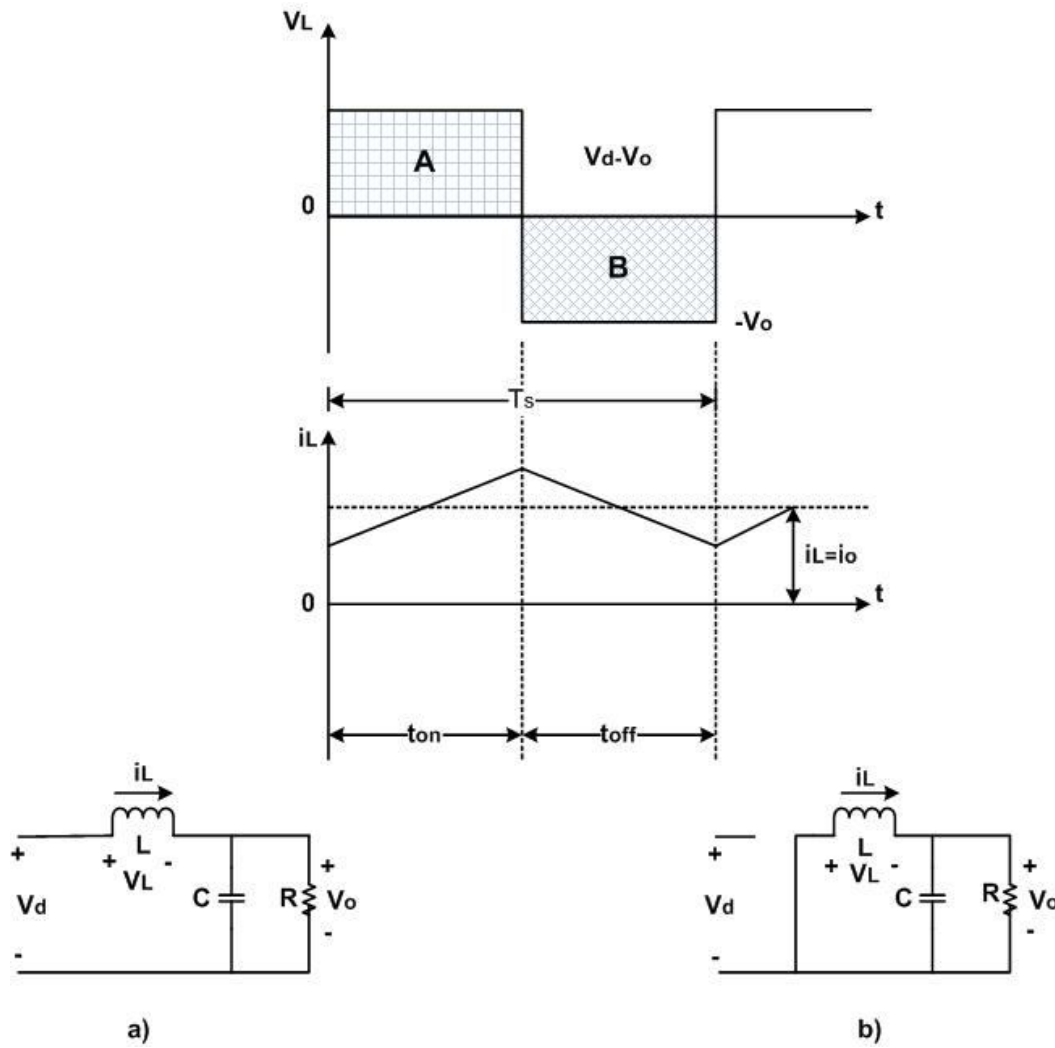


Fig E.0.5 Continuous-discontinuous state

The integral of the inductor voltage over one time period is zero.

$$\int_0^{T_s} V_L dt = \int_0^{t_{on}} V_L dt + \int_{t_{on}}^{T_s} V_L dt = 0 \quad \text{E.9}$$

This implies areas A and B are equal. Therefore,

$$(V_d - V_o)t_{on} = V_o(T_s - t_{on}) \quad \text{E.10}$$

And:

$$\frac{V_o}{V_d} = \frac{t_{on}}{T_s} = D \quad \text{E.11}$$

Knowing that the average voltage across the inductor in steady state is zero, foregoing equation can be derived as:

$$\frac{V_d t_{on} + 0 * t_{off}}{T_s} = V_o \quad \text{E.12}$$

$$\frac{V_o}{V_d} = \frac{t_{on}}{T_s} = D \quad \text{E.13}$$

Input power is equal to output power, if losses are neglected.

$$P_d = P_o \quad \text{E.14}$$

In continuous conduction mode, buck converter is similar to a dc transformer.

$$V_d I_d = V_o I_o \quad \text{E.15}$$

An appropriate filter at the input will required to eliminate effects of current harmonics.

$$\frac{I_o}{I_d} = \frac{V_d}{V_o} = \frac{1}{D} \quad \text{E.16}$$

Boundary between continuous and discontinuous conduction

Fig E.0.6a shows the waveform of inductor voltage and current at the limit between continuous conduction mode. Therefore, at every end of period, inductor current goes to zero.

At the limit, inductor current is calculated based on the formula:

$$I_{LB} = \frac{1}{2} i_{L,peak} = \frac{t_{on}}{2L} (V_d - V_o) = \frac{DT_s}{2L} (V_d - V_o) = I_{oB} \quad \text{E.17}$$

This means, if the average value of load current is smaller than I_{LB} , i_L will become discontinuous.

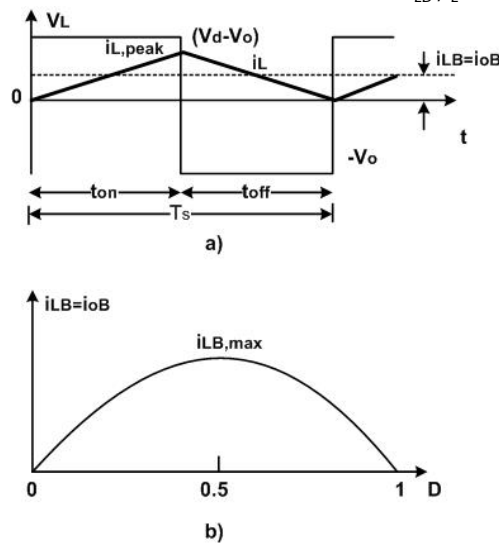


Fig E.0.5 Continuous-discontinuous state

Discontinuous conduction mode

The average inductor current at the edge of the continuous conduction mode is:

$$I_{LB} = \frac{T_s V_d}{2L} D(1 - D) \quad \text{E.18}$$

Fig E.0.5b shows how I_{LB} changes according to the duty cycle. Maximum value is reached at a duty cycle of 50%.

$$I_{LB,max} = \frac{T_s V_d}{8L} \quad \text{E.19}$$

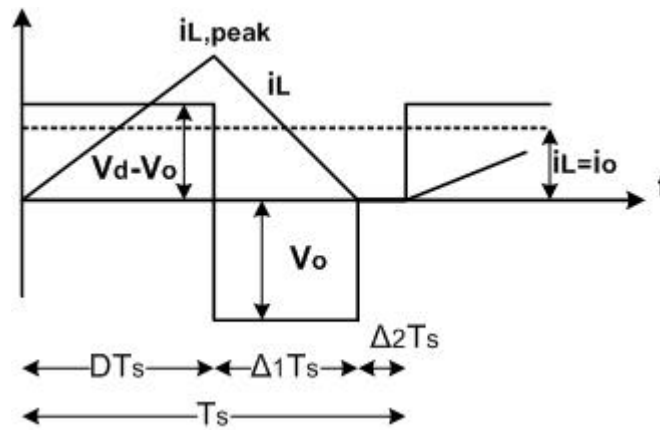


Fig E.0.6 Discontinuous mode

If output load power is decreased, then inductor current decreases. Fig E.0.6 shows how inductor voltage and current vary in discontinues mode. Following formula indicates output voltage during discontinuous mode.

$$\frac{V_o}{V_d} = \frac{D^2}{D^2 + \frac{1}{4} \left(\frac{I_o}{I_{LB,max}} \right)} \tag{E.20}$$

Fig E.0.7 presents buck characteristics for a constant input voltage. Voltage ratio V_o/V_d is plotted as a function of $I_o/I_{LB,MAX}$. Dashed curves represent boundary between continuous and discontinuous mode of operation. First graph shows characteristics for a constant V_d and second one for constant V_o .

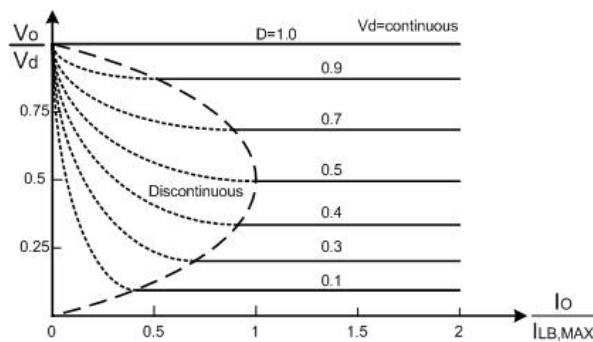


Fig E.0.7 Characteristic keeping V_d constant

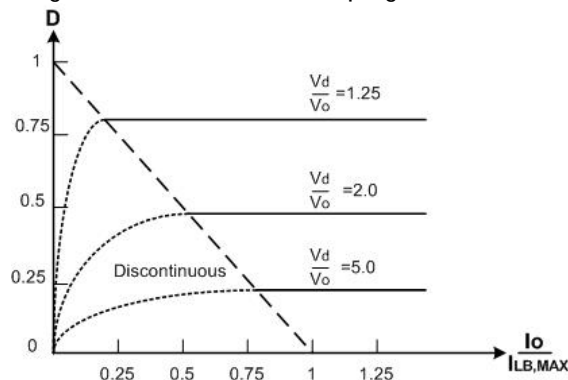


Fig E.0.8 Characteristic keeping V_o constant

Output voltage ripple

The ripple in output voltage can be calculated by considering the waveforms from Fig E.0.9. Peak to peak voltage ripple is :

$$\Delta V_o = \frac{\Delta Q}{C} \quad \text{E.21}$$

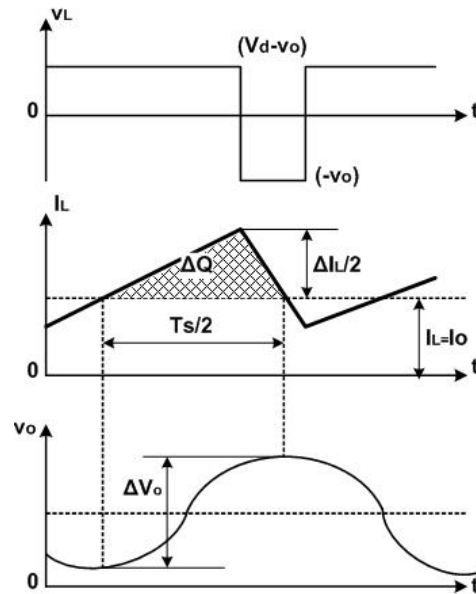


Fig E.0.9 Output voltage ripple

E.22 shows that the voltage ripple will be smaller if the low pass filter has a corner frequency smaller than the switching frequency. The ripple is also independent of the output load power, if the converter operated in the continuous mode of operation. [19]

$$\frac{\Delta V_o}{V_o} = \frac{\pi^2}{2} (1 - D) \left(\frac{f_c}{f_s}\right)^2 \quad \text{E.22}$$

$$f_c = \frac{1}{2\pi\sqrt{LC}} \quad \text{E.23}$$

F. Terminology of Synchronous Machine Parameters

Usually synchronous generator parameters are specified the manufacturers as reactance, time constants and resistances. The usual methods used to determine them are by open circuit and short circuit methods.

The definitions of the quantities and their methods of determination correspond to the accepted two-axis theory of synchronous machines, with representation of all circuits additional to the field winding and stationary circuits, by two equivalent circuits. One is along the direct axis and the other along the quadrature axis. Therefore, three reactance (synchronous, transient and sub-transient) and two time constants (transient and sub-transient) are considered along the direct axis, two reactances (synchronous and sub-transient) and one time constant (sub-transient) along the quadrature axis.

During the open circuit or no load saturation method, the generator is driven at the nominal speed with no load connected. During the test, excitation current, line voltage and frequency are measured in the same time. The excitation current is changed in gradual steps in order to induce voltage in the range from 0 to 130% of the nominal voltage U_N .

During the short circuit test, the three phases of the generator are short circuited. The excitation current is controlled so the armature current is in the range of 0 to 130% of the nominal current I_N .

During the short circuit test, the wave form of the current exhibits two distinctly different decay periods: sub transient and transient.

The synchronous machine quantities will vary with saturation of the magnetic circuits. In practical calculations both saturated and unsaturated values are used.[1]

Subtransient:

The sub-transient period characterized with a rapid decay of the current, attributable to the damper windings (larger resistance compared with field winding).

Changes in currents in the outer damping windings limit the stator –induced flux from penetrating the rotor.

Damper winding currents decay, transition period starts.

Transient:

The rate of the current decays in the transient period is slower and attributed to the changes in the currents of the rotor field winding.

Field winding reacts in the same manner, albeit slower. Flux is not penetrating the rotor. [9]

1. Synchronous inductance
2. Direct-axis synchronous reactance X_d

It is ratio between the armature voltage which is produced by the direct axis armature flux due to direct axis armature current, and the fundamental a.c. component of this current, when the machine is running at rated speed.

It is determined from the no load and sustained three phase short circuit characteristics.

$$X_d = \frac{U_{oc}}{I_{sc}} \quad \text{F.24}$$

Quadrature-axis synchronous reactance X_q :

It is the ration between the armature voltage which is produced by the quadrature axis armature flux due to quadrature axis armature current, and the fundamental a.c. component of this current, when the machine is running at rated speed.

It is determined through *negative excitation test*.

The test is conducted while machine is in parallel with the grid and is not loaded. The excitation current is decreased slowly to zero, then the polarity is reversed and increased up to the point where the machine slips one pole pitch. The value of the armature voltage, current and excitation are recorded.

$$X_q = \frac{U_r}{\sqrt{3}I_r} \quad \text{F.25}$$

- Inductance is ratio of flux linked to current.
- When mmf aligned with d-axis, ratio of stator flux linkage to stator current is L_d
- Aligned with q-axis, is L_q
- L_d is slightly bigger than L_q

$$\Delta\gamma_d = L_d \Delta i_d \quad \text{F.26}$$

$$\Delta\gamma_q = L_q \Delta i_q \quad \text{F.27}$$

$$\gamma_d^{st} = \gamma_d - \Delta\gamma_d = \gamma_d - L_d i_d = L_{md} i_f \quad \text{F.28}$$

$$\gamma_q^{st} = \gamma_q - \Delta\gamma_q = \gamma_q - L_q i_q = L_{mq} i_g \quad \text{F.29}$$

$$L_d = L_{ls} + L_{md} \quad \text{F.30}$$

- Change in current leads to a change in flux
- Flux linkage on both axes may be seen as consisting of two components

Transient inductance

Direct-axis transient reactance X'_d

It is the initial value of a sudden change in the armature voltage which is produced by the direct axis armature flux, and the value of the simultaneous change in the direct-axis armature current, while the machine is running at rated speed.

It can be determined through sudden three phase short circuit.

- Damper windings resistance is larger than the field winding. Induced currents in damper winding decay rapidly than those of field windings
- During transient period, the transients in the damper windings are over while the induced currents in the field windings are still changing to oppose the change in the flux linkage caused by the stator currents
- Ratio of ΔY to Δi is referred as *transient inductance*[1]

$$L'_d \cong \frac{\Delta \gamma_d}{\Delta i_d} = L_d - \frac{L_{md}^2}{L'_f} \quad \text{F.31}$$

$$L'_q \cong \frac{\Delta \gamma_q}{\Delta i_q} = L_q - \frac{L_{mq}^2}{L'_g} \quad \text{F.32}$$

$$L'_d = L_{ls} + \frac{L_{md}L_{lfd}}{L_{md}L_{lfd}} \quad \text{F.33}$$

$$L'_d = L_{ls} + \frac{L_{md}L_{lfd}}{L_{md}L_{lfd}} \quad \text{F.34}$$

Subtransient inductance

Direct-axis subtransient reactance X''_d

It has the same definition like the transient reactance and it's also determined through *sudden three phase short circuit method*.

Quadrature-axis subtransient reactance X''_q

It is the initial value of a sudden change in the armature voltage which is produced by the direct axis armature flux, and the value of the simultaneous change in the direct-axis armature current, while the machine is running at rated speed.

It is determined through the following methods:

- Applied voltage with the rotor in the direct and quadrature axis position with respect to the armature winding field axis*
- Applied voltage with the pole axis in any arbitrary position*

- *During sub-transient, transient currents induced in the rotor windings will keep the flux linkage initially constant*

$$L''_d = L_{ls} + \frac{L_{md} \frac{L'_{lkd}L'_{lf}}{L'_{lkd} + L'_{lf}}}{L_{md} + \frac{L'_{lkd}L'_{lf}}{L'_{lkd} + L'_{lf}}} \quad \text{F.35}$$

$$L''_q = L_{ls} + \frac{L_{mq} \frac{L'_{lkq}L'_{lg}}{L'_{lkq} + L'_{lg}}}{L_{mq} + \frac{L'_{lkq}L'_{lg}}{L'_{lkq} + L'_{lg}}} \quad \text{F.36}$$

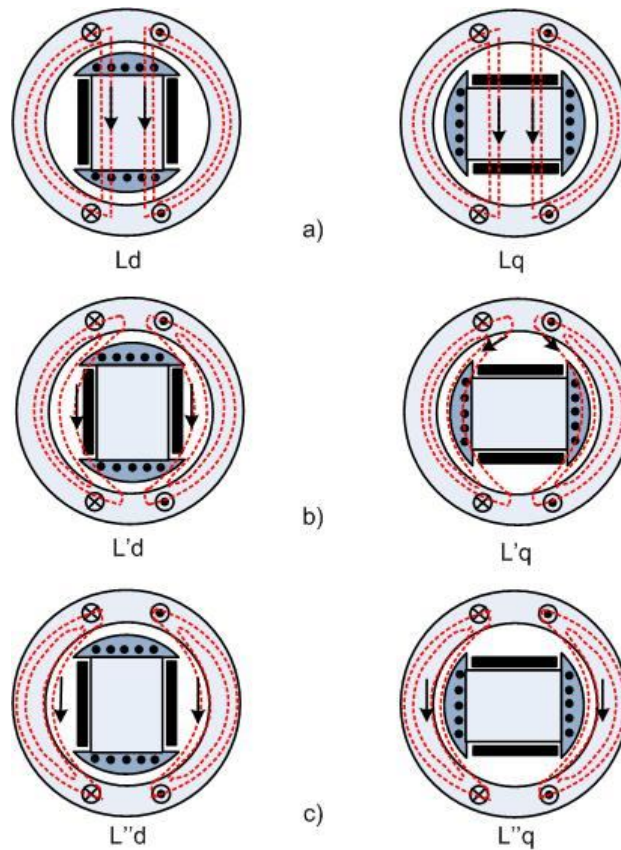


Fig F.10: Two axis reactance (a)Synchronous Reactance(b)Transient reactance(c)Sub-transient reactance.

Armature winding direct-current resistance R_s

Direct current winding resistance is determined directly through direct measurement through voltmeter and ammeter.

Time constants

Direct-axis transient open-circuit time constant τ'_{do}

It is indicating the rate of change of the open circuit armature voltage due to a change of the direct axis flux.

Direct-axis transient short-circuit time constant τ'_d

It is the time necessary for a change in the direct axis short circuit armature current due to a sudden change in operating conditions. It is determined through a *sudden three phase short circuit*.

Direct-axis subtransient short-circuit time constant τ''_d

Time required for a rapid change in the first few cycles in the direct-axis short circuit armature current. Is it determined in the same manner like the transient short circuit time constant.

Transient time constants:

- Transient time constants are larger than subtransient values
- Damper windings (larger resistance values) are associated with subtransient time constants
- When stator is open-circuited, the change in field currents in response to a change in excitation voltages is determined by the time constants :

$$T'_{do} = \frac{L_f}{r_f} \quad \text{F.37}$$

$$T'_{qo} = \frac{L_g}{r_g} \quad \text{F.38}$$

- T'_{do} is usually between 2 and 11
- When both the field winding and the stator windings are short-circuited, the apparent inductance of the field winding changes with external connection. The ratio of the time constants of the field winding with short-circuited stator winding to that with open circuit stator winding is equal to the ratio of apparent inductance seen by the stator current with field short-circuited to that with field open-circuited.

$$T'_{do} = \frac{1}{r_f} \left(\frac{(L_d - L_{ls})^2}{L_d - L'_d} \right) \quad \text{F.39}$$

Subtransient time constants

- T''_{do} is the time constant of the kd damper winding current when the terminals of the field winding are shorted and the stator windings are open-circuited.

$$T''_{do} = \frac{L''_{kdo}}{r'_{kd}} \quad \text{F.40}$$

D axis - Open circuit**Transient:**

$$T'_{do} = \frac{L_{lfd} + L_{md}}{r_{fd}} \quad \text{F.41}$$

Sub-transient:

$$T''_{do} = \frac{L_{lkd} + \frac{L_{md}L_{lfd}}{L_{md} + L_{lfd}}}{r_{kd}} \quad \text{F.42}$$

D axis - Short circuit**Transient:**

$$T'_d = \frac{L_{lfd} + \frac{L_{md}L_{ls}}{L_{md} + L_{ls}}}{r_{fd}} \quad \text{F.43}$$

Subtransient:

$$T''_d = \frac{L_{lkd} + \frac{L_{md}L_{ls}L_{lfd}}{L_{md}L_{lfd} + L_{md}L_{ls} + L_{lfd}L_{ls}}}{r_{kd}} \quad \text{F.44}$$

Q axis-Open circuit

Subtransient:

$$T''_{qo} = \frac{L_{lkq} + L_{mq}}{r_{kq}} \quad \text{F.45}$$

Q axis-Short circuit

Subtransient:

$$T''_{qo} = \frac{L_{lkq} + \frac{L_{mq}L_{ls}}{L_{mq} + L_{ls}}}{r_{kq}} \quad \text{F.46}$$

Transient reactance

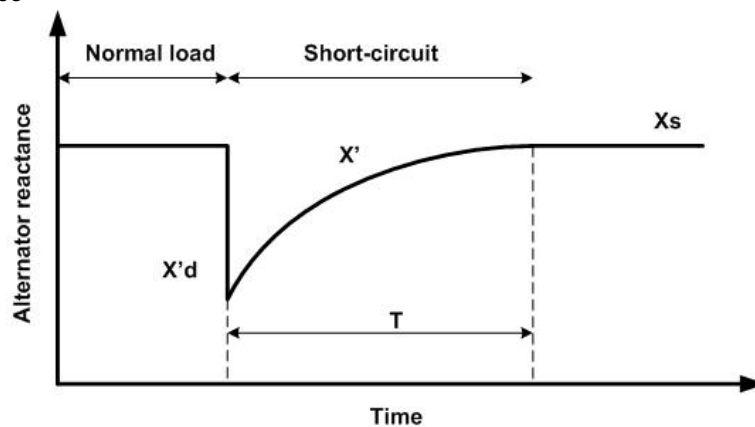


Fig F.0.11: Transient reactance

A synchronous generator connected to a power system can be the subject of rapidly changing loads or short circuit. In this case, the synchronous reactance cannot be used because it's reflecting only the steady state conditions.

For the above cases, X_s is replaced with X' , called the transient reactance. Fig F.0.11 indicates how X' varies with time when a generator is suddenly short-circuited. So, at the instance of short-circuit, the reactance falls to a lower value X'_d . It then increases gradually until it is again equal to X_s , after a time interval T . The duration of the interval depends upon the size of the generator. For machines below 100 kVA it only lasts a fraction of a second, but for machines in the 1000 MVA range it may last as long as 10 seconds.

X'_d may be as low as 15 % of the synchronous reactance. Therefore, the initial short-circuited current is much higher than that corresponding to X_s . Circuit breakers have to be chosen correspondingly. On the other hand, the low transient reactance simplifies the voltage regulation problem when the load on the generator increases rapidly. First the internal voltage drop due to X'_d is smaller than it would be for X_s . [4]

G. Simulink & dSpace Blocks

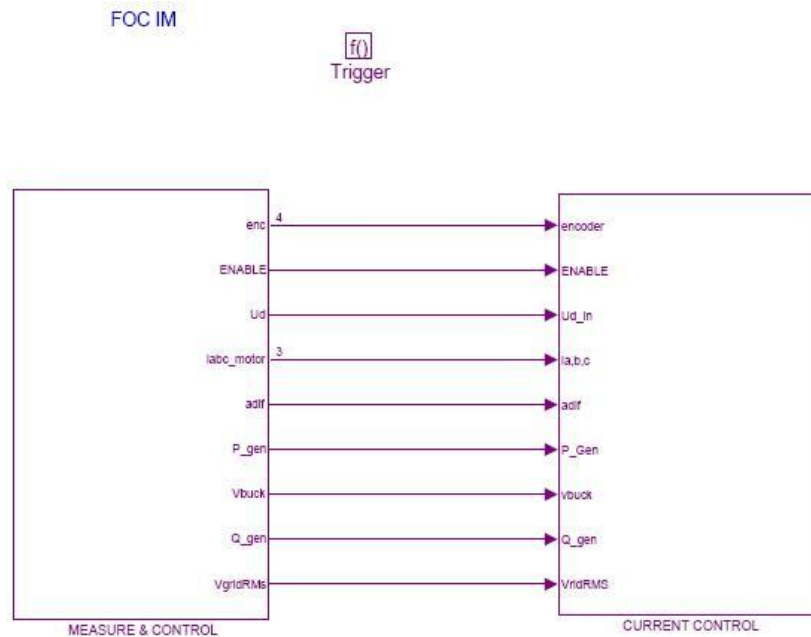


Fig G.12: Main block representing data flow

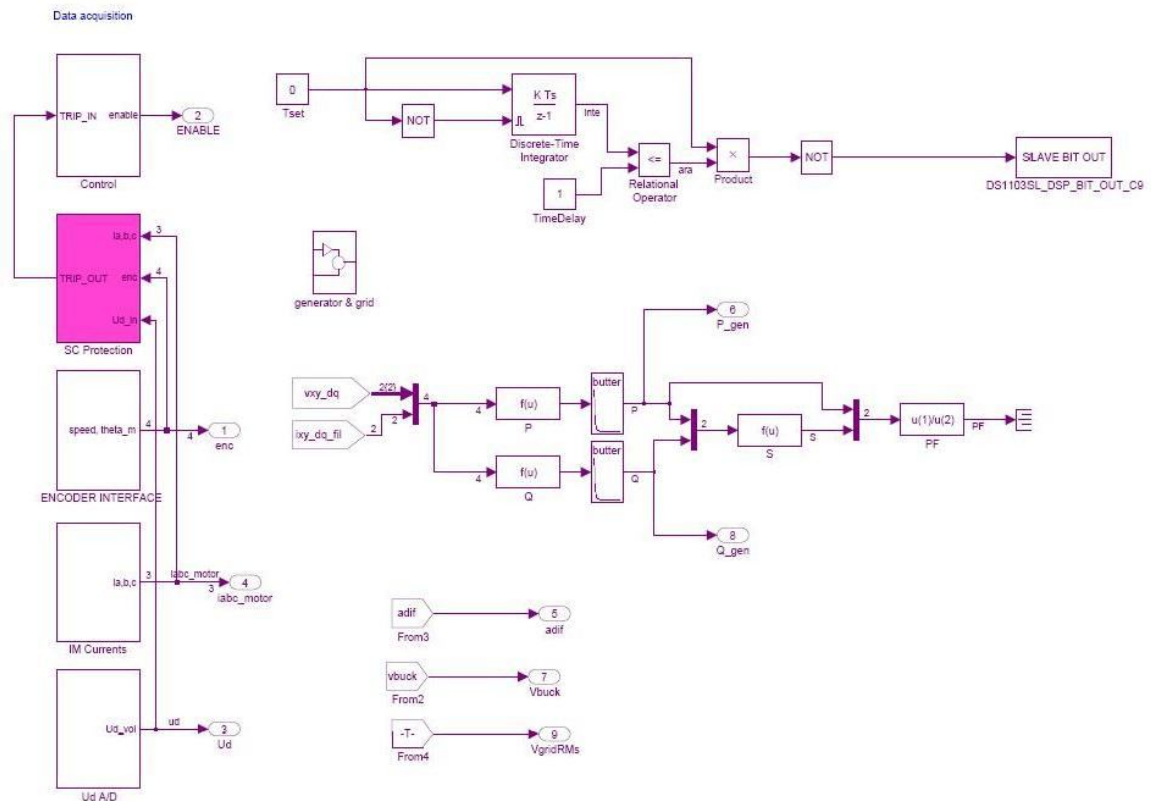


Fig G.13: Data acquisition and protections block.

H. P.U System

Using the per unit system when dealing with only one electrical machines offers no big advantages, other than the convenience of having the per unit system parameters of the machine already in terms of a set of base values that correspond to those of the rating of the machine.

The base power S_b is the rated KVA of the machine. The peak value of the line-to-line voltages is the base voltage V_b . Further on base value of the current is $2S_b/3V_b$.

The base values for the stator impedance and torque are given by:

$$\text{Base impedance: } Z_b = \frac{V_b}{I_b}$$

$$\text{Base torque: } T_b = \frac{S_b}{\omega_{bm}}$$

Where ω_{bm} is the mechanical angular frequency and it is equal to $2\omega_b/P$, and ω_b is the base electrical angular frequency and P is the number of pole pairs.

In per unit, the electromagnetic torque will become:

$$T_{em(pu)} = \frac{T_{em}}{T_b} = \frac{\frac{3}{2} \frac{P}{2\omega_b} (\psi_{d(pu)} i_{q(pu)} - \psi_{q(pu)} i_{d(pu)})}{\frac{3}{2} \left(\frac{V_b}{2} \frac{I_b}{\omega_b} \right)} \quad \text{H.47}$$

Because the base for the flux linkages, ψ_d and ψ_q , is the same as V_b for the stator voltage, the above expression reduces to

$$T_{em(pu)} = (\psi_{d(pu)} i_{q(pu)} - \psi_{q(pu)} i_{d(pu)}) \quad \text{H.48}$$

The mechanical equation of the rotor will become:

$$T_{em(pu)} + T_{mech(pu)} - T_{damp(pu)} = \left(\frac{1}{T_b} \right) \left(\frac{2J}{P} \right) \left(\frac{d\omega_r}{dt} \right) \quad \text{H.49}$$

In terms of the inertia constant, H , where is defined as $H = \frac{1}{2} J \frac{\omega_{bm}^2}{S_b}$, the equation will become:

$$T_{em(pu)} + T_{mech(pu)} - T_{damp(pu)} = 2H \frac{d\left(\frac{\omega_r}{\omega_b}\right)}{dt} = 2H \frac{d\left(\frac{\omega_r - \omega_e}{\omega_b}\right)}{dt} \quad \text{H.50}$$

Bibliography

- [1] Michael Durstewitz and Kurt Rohrig Berthold Hahn, "Reliability of Wind turbines," in *Reliability of Wind turbines*.: Springer, 2007, pp. 329-332.
- [2] Erich Hau, *Wind turbines: fundamentals, technologies, application, economics*.: Springer ISBN:9783540242406, 2006.
- [3] Frede Blaabjerg and Zhe Chen, *Power electronics for modern wind turbines*. Aalborg: Morgan and Claypool, 2006.
- [4] Theodore Wilde, *Electrical Machines Drives and Power Syhstems*, 5th ed.: Prentice- Hall, 2002.
- [5] Marcin Żelechowski, "DTC-SVM Inverter Fed Induction Machine," Institute of Control and Industrial Electronics, Warsaw University of Technology, Warsaw, Thesis 2005.
- [6] Bimal K Bose, *Modern Power Electronics and AC Drives*.: Prentice Hall, 2002.
- [7] Pavel Stopa, "High Speed Field Oriented Control," Aalborg, Master Thesis 2009.
- [8] M. Safiuddin J. W. Umland, "Magnitude and Symmetric Optimum Criterion," *IEEE Transaction on Industry Applications*, vol. 26, no. 3, pp. 489-497, may/june 1990.
- [9] Chee Mun Ong, *Dynamic Simulation of Electric Machinery*.: Prentice-Hall, 1998.
- [10] V.Hamata J.Cemus, *Transient Stability Analysis of Synchronous Motors*.: Elsevier Publisher, 1990.
- [11] Ivan Jadric, "Modelling and Control of a Synchronous Generator with Electronic Load," Virginia Polytechnic Institute and State University, Blacksburg, Virginia, Master Thesis 1998.
- [12] Ion Boldea, *Synchronous Generators*. Timiosara: CRC Press, 2006.
- [13] J.M. Vleeshouwers, "Derivation of a Model of the Exciter of a Brushless Synchronous Machine," 1992.
- [14] Western Power, "Generator Grid Connection Guide : An introduction to Power Systems and the Connection Process," 60025984, 2008.
- [15] David T. Johnsen Willi Christiansen, "Analysis of requirements in selected Grid Codes," Technical University of Denmark, Lyngby, Survey 2006.
- [16] C. R. Mummert, "Models for Var and Power Factor Controllers Added to IEEE 421.5," IEEE,.
- [17] Pedro Rodriguez, "STATCOM and Active Filtering, PERES Course," Technical University of Catalonia, Aalborg, 2011.
- [18] Manish Dalal, "High Voltage DC Converter System Modelling, Simulation and Analysis,".
- [19] Ned Mohan, *Power Electroncis : Converters, Application and Design*, 2nd ed.: John Wiley & Sons, 1996.
- [20] Dragan and Erikson, "Fundamentals of power electronics,".
- [21] Lars Helle, "Grid Codes for Wind Turbines," Universitat Politecnica De Catalunya, 2007.
- [22] L.D. Zhang M.H.J. Bollen, "Different methods for classification of three-phase unbalanced voltage dips due to faults," *Electric Power Systems Research*, pp. 59-69, 2003.
- [23] Fitzgerald,.
- [24] Ch. Patsiouras, S. Papathanassiou M. Tsili, "GRID CODE REQUIREMENTS FOR LARGE WIND FARMS: A REVIEW OF TECHNICAL REGULATIONS AND AVAILABLE WIND TURBINE TECHNOLOGIES," National Technical University of Athens (NTUA),.
- [25] H.W. Beaty, *Electric Motor Handbook*,. 1998.
- [26] M.E. El-Hawary, *Principles of Electrical Machines with Power Electronics Applications*,. 2002.
- [27] Harold W Gingrich, *Electric Machinery, Transformers and Control*,. 1979.

- [28] IEC standard, *Rotating Electrical Machines: Methods for determining synchronous machine quantities from test*.
- [29] T.A. Lipo, "Simulation of a Salient Pole Synchronous Machine with Both Field Pole and Stator Core Saturation,".